LIGNANS: INSIGHTS INTO THEIR BIOSYNTHESIS, METABOLIC ENGINEERING, ANALYTICAL METHODS AND HEALTH BENEFITS

EDITED BY: Christophe F. Hano, Albena Todorova Dinkova-Kostova, Norman George Lewis, John Robert Cort and Laurence B. Davin

PUBLISHED IN: Frontiers in Plant Science and Frontiers in Pharmacology

frontiers Research Topics

ISSN 1664-8714
ISBN 978-2-88966-491-7
DOI 10.3389/978-2-88966-491-7

About Frontiers

Frontiers is more than just an open-access publisher of scholarly articles: it is a pioneering approach to the world of academia, radically improving the way scholarly research is managed. The grand vision of Frontiers is a world where all people have an equal opportunity to seek, share and generate knowledge. Frontiers provides immediate and permanent online open access to all its publications, but this alone is not enough to realize our grand goals.

Frontiers Journal Series

The Frontiers Journal Series is a multi-tier and interdisciplinary set of open-access, online journals, promising a paradigm shift from the current review, selection and dissemination processes in academic publishing. All Frontiers journals are driven by researchers for researchers; therefore, they constitute a service to the scholarly community. At the same time, the Frontiers Journal Series operates on a revolutionary invention, the tiered publishing system, initially addressing specific communities of scholars, and gradually climbing up to broader public understanding, thus serving the interests of the lay society, too.

Dedication to Quality

Each Frontiers article is a landmark of the highest quality, thanks to genuinely collaborative interactions between authors and review editors, who include some of the world's best academicians. Research must be certified by peers before entering a stream of knowledge that may eventually reach the public - and shape society; therefore, Frontiers only applies the most rigorous and unbiased reviews.
Frontiers revolutionizes research publishing by freely delivering the most outstanding research, evaluated with no bias from both the academic and social point of view. By applying the most advanced information technologies, Frontiers is catapulting scholarly publishing into a new generation.

What are Frontiers Research Topics?

Frontiers Research Topics are very popular trademarks of the Frontiers Journals Series: they are collections of at least ten articles, all centered on a particular subject. With their unique mix of varied contributions from Original Research to Review Articles, Frontiers Research Topics unify the most influential researchers, the latest key findings and historical advances in a hot research area! Find out more on how to host your own Frontiers Research Topic or contribute to one as an author by contacting the Frontiers Editorial Office: frontiersin.org/about/contact

LIGNANS: INSIGHTS INTO THEIR BIOSYNTHESIS, METABOLIC ENGINEERING, ANALYTICAL METHODS AND HEALTH BENEFITS

Topic Editors:
Christophe F. Hano, INRA EA1207 Laboratoire de Biologie des Ligneux et des Grandes Cultures, France
Albena Todorova Dinkova-Kostova, University of Dundee, United Kingdom
Norman George Lewis, Washington State University, United States
John Robert Cort, Pacific Northwest National Laboratory (DOE), United States
Laurence B. Davin, Washington State University, United States

Citation: Hano, C. F., Dinkova-Kostova, A. T., Lewis, N. G., Cort, J. R., Davin, L. B., eds. (2021). Lignans: Insights into Their Biosynthesis, Metabolic Engineering, Analytical Methods and Health Benefits. Lausanne: Frontiers Media SA. doi: 10.3389/978-2-88966-491-7

Table of Contents

frontiers in Plant Science

EDITORIAL
published: 12 January 2021
doi: 10.3389/fpls.2020.630327

Editorial: Lignans: Insights Into Their Biosynthesis, Metabolic Engineering, Analytical Methods and Health Benefits

Christophe F. Hano[1,2]*, *Albena T. Dinkova-Kostova*[3,4,5]*, *Laurence B. Davin*[6]*, *John R. Cort*[6,7]* and *Norman G. Lewis*[6]*

[1] Laboratoire de Biologie des Ligneux et des Grandes Cultures, INRAE USC1328, Université d'Orléans, Chartres, France, [2] COSM'ACTIFS, CNRS GDR3711, Chartres, France, [3] Division of Cellular Medicine, Jacqui Wood Cancer Centre, Ninewells Hospital and Medical School, University of Dundee, Dundee, United Kingdom, [4] Department of Pharmacology and Molecular Sciences, Johns Hopkins University School of Medicine, Baltimore, MD, United States, [5] Department of Medicine, Johns Hopkins University School of Medicine, Baltimore, MD, United States, [6] Institute of Biological Chemistry, Washington State University, Pullman, WA, United States, [7] Earth and Biological Sciences Directorate, Pacific Northwest National Laboratory, Richland, WA, United States

Keywords: lignans, metabolic engineering, analytical method, biological activity, lignans metabolism

OPEN ACCESS

Edited and reviewed by:
Wanchai De-Eknamkul, Chulalongkorn University, Thailand

***Correspondence:**
Christophe F. Hano
hano@univ-orleans.fr
Albena T. Dinkova-Kostova
a.dinkovakostova@dundee.ac.uk
Laurence B. Davin
davin@wsu.edu
John R. Cort
john.cort@pnnl.gov
Norman G. Lewis
lewisn@wsu.edu

Specialty section:
This article was submitted to Plant Metabolism and Chemodiversity, a section of the journal Frontiers in Plant Science

Received: *17 November 2020*
Accepted: *08 December 2020*
Published: *12 January 2021*

Citation:
Hano CF, Dinkova-Kostova AT, Davin LB, Cort JR and Lewis NG (2021) Editorial: Lignans: Insights Into Their Biosynthesis, Metabolic Engineering, Analytical Methods and Health Benefits. Front. Plant Sci. 11:630327. doi: 10.3389/fpls.2020.630327

Editorial on the Research Topic

Lignans: Insights Into Their Biosynthesis, Metabolic Engineering, Analytical Methods and Health Benefits

Lignans constitute a multifaceted group of phytochemicals widely distributed in terrestrial plant lineages (Ayres and Loike, 1990; Vassão et al., 2010). Lignans have important roles in plant physiology, development, and ecology (i.e., interactions and adaptations to ever-changing environments) (Burlat et al., 2001; Markulin et al., 2019). As their specialized metabolite nature might suggest, lignans have been implicated in plant defense protection against a variety of herbivores and microorganisms (Gang et al., 1999; Vassão et al., 2010; Seneviratne et al., 2015).

Reputable studies in the fields of human diet and/or nutritional care were initiated with the discovery of mammalian lignan (ML) formation from lignan-rich diets over the last decades (Axelson et al., 1982). Indeed, some lignans, aka "phytoestrogen" lignans, are converted into the MLs, enterodiol and enterolactone, by human gut microbiota upon their ingestion. These MLs have extensively described and discussed chemopreventive properties against various tumors (such as breast, colon, and prostate cancers) and/or cardiovascular disorders (Rietjens et al., 2017).

Critical analysis of the lignan research literature by Yeung et al. also revealed important features about trends in lignan research. Significantly, around 80% of lignan-related papers were published since 2000, of which about half of these were in 2010 or later; this clearly demonstrates a significant growth in interest over the last 20 years for this natural product family. Furthermore, the overall importance of flax (*Linum usitatissimum*), Schisandra (*Schisandra chinensis*), and Forsythia (*Forsythia x. intermedia*) is clearly evident in the literature analysis of lignans. Far from being limited solely to plant biology (around 20% of publications), many papers were centered on pharmacology (around one fourth) and chemistry (around one fourth). It should be noted that, in line with this observation, the current Research Topic herein includes studies on plant biology [i.e., biosynthesis of lignans and neolignans in flax (Bose et al.), chemistry] [e.g., extraction of sesame oil lignans (Michailidis et al.)], and pharmacology [e.g., pharmacological value of nordihydroguaiaretic acid (NDGA) and its (semi-)synthetic derivatives (Manda et al.)]. Yeung et al.

also indicated a significant increase, in the most recently published publications, for studies based on the pharmacological importance of ingestion of lignans (e.g., secoisolariciresinol, lariciresinol, matairesinol, pinoresinol, medioresinol, and syringaresinol) in the diet, with particular emphasis on their cancer, cardiovascular disease, and diabetes prevention or antioxidant properties. However, the authors of this critical analysis also pointed out the need for more clinical trials to support beneficial effects and to establish optimal doses of lignan intake in humans, as such trials are estimated to contribute to only 0.2–1.1% of the literature reviewed.

Many lignans are formed by the oxidative coupling of E-coniferyl alcohol moieties. Lignans can share the same precursors as for lignins, the complex biopolymers that provide rigidity and support to vascular plants (Davin and Lewis, 2003). Understanding regulation of lignan biosynthesis is of particular importance for many applications. For instance, the use of plant tissue culture in cosmetics has gained renewed impetus in the last few decades, and the cosmetics industry is expected to expand to a turnover of several hundred billion US dollars per year. Interestingly, Bose et al. focused on *in vitro* culture of flax (*Linum usitatissimum*), a well-known rich source of lignans and neolignans, for its potent cosmetic properties. In-depth phytochemical study using UPLC-HRMS confirmed the high lignan and neolignan accumulation potential of this species, including 7 neolignans newly described, and their potential use in cosmetic applications. In particular, the study confirmed the importance of optimizing conditions of *in vitro* culture for a specific application.

Designing effective analytical methods for lignans also helps to gain new insights into natural lignan chemodiversity, evolution across the plant kingdom, as well as into the mechanism(s) of certain biological activities that remain elusive, and which require purified compounds for further study (Teponno et al., 2016). Moreover, extraction and purification steps are well-known limitations for the potential industrial use of certain lignans. Accordingly, due to their broad biological importance, a range of studies reported herein address isolation and purification of the lignans sesamin and sesamolin from sesame (*Sesamum indicum*), including their sourcing from sesame seed and sesame seed-derived products. Just a few previous works have reported producing both of these two lignans in high quantity and purity using a low cost, fast, methodology. That is, Michailidis et al. describe an integrated method for the recovery of sesame and sesamolin from sesame oil, with a purity of more than 95%, using centrifugal partition extraction. These purified compounds were then further tested for their tyrosinase, elastase, collagenase, and inhibition function of hyaluronidase in order to assess their cosmetic properties.

The path to the market of a natural product can often be lengthy and sometimes involves the removal of significant disadvantages, such as low solubility or adverse toxicity (Cragg and Newman, 2001). The most commonly known lignan example is podophyllotoxin, which is medicinally used worldwide as a starting compound for semi-synthesis of potent anticancer drugs that inhibit topoisomerase II (Cragg and Newman, 2001). Moreover, the review paper herein by Manda et al. sheds light on nordihydroguaiaretic acid (NDGA), another lead lignan medicinal compound, and a clear example of all these considerations. NDGA is a phenolic lignan from the creosote bush (*Larrea tridentata*), found in deserts of Mexico and the United States. It has long been used in traditional medicine for treating various diseases, including cancer, renal, cardiovascular, immunological, and neurological disorders, and even aging. The review encompasses current knowledge of NDGA uses, including its targets and side-effects and its synthetic analogs as potential therapeutic agents. In particular, preclinical studies in cell culture and rodents suggest that NDGA is a promising drug for the prevention or treatment of many chronic diseases and cancers, largely due to its direct (scavenging of reactive oxygen species) and indirect (activation of endogenous antioxidant responses mediated by transcription factor Nrf2) antioxidant effects. However, high concentrations of NDGA can also be cytotoxic. In recent years, production of NDGA analogs, some being more potent and target-selective, and exhibiting lower toxicity due to the prevention of the conversion of the catechol functionality to a quinone, has given new impetus to this area. These efforts have culminated in the development of tetra-*O*-methyl nordihydroguaiaretic acid (Terameprocol), currently used in several cancer clinical trials. Interestingly, some NDGA analogs are also promising in treatment of neurodegenerative disorders and metabolic syndrome.

In summary, *in planta* lignan biosynthesis and functions, together with their improved extraction procedures and/or health benefits, provide exciting new frontiers for scientists from numerous fields of expertise for further research. It is anticipated that the papers herein on this Research Topic have the benefit of shedding new light on this family of natural products, the interest in which has been increasing over the last 20 years, whether in plant science, chemistry or pharmacology.

AUTHOR CONTRIBUTIONS

All authors wrote, revised, and approved the final version of the manuscript.

REFERENCES

Axelson, M., Sjövall, J., Gustafsson, B. E., and Setchell, K. D. R. (1982). Origin of lignans in mammals and identification of a precursor from plants. *Nature* 298, 659–660.

Ayres, D. C., and Loike, J. D. (1990). *Lignans: Chemical, Biological and Clinical Properties*. Cambridge: Cambridge University Press.

Burlat, V., Kwon, M., Davin, L. B., and Lewis, N. G. (2001). Dirigent proteins and dirigent sites in lignifying tissues. *Phytochemistry* 57, 883–897. doi: 10.1016/S0031-9422(01)00117-0

Cragg, G. M., and Newman, D. J. (2001). Natural product drug discovery in the next millennium. *Pharm. Biol.* 39, 8–17. doi: 10.1076/phbi.39.s1.8.0009

Davin, L. B., and Lewis, N. G. (2003). An historical perspective on lignan biosynthesis: monolignol, allylphenol and hydroxycinnamic acid

coupling and downstream metabolism. *Phytochem. Rev.* 2, 257–288. doi: 10.1023/B:PHYT.0000046175.83729.b5

Gang, D. R., Kasahara, H., Xia, Z. Q., Vander Mijnsbrugge, K., Bauw, G., Boerjan, W., et al. (1999). Evolution of plant defense mechanisms relationships of phenylcoumaran benzylic ether reductases to pinoresinol-lariciresinol and isoflavone reductases. *J. Biol. Chem.* 274, 7516–7527.

Markulin, L., Corbin, C., Renouard, S., Drouet, S., Gutierrez, L., Mateljak, I., et al. (2019). Pinoresinol-lariciresinol reductases, key to the lignan synthesis in plants. *Planta* 249, 1695–1714. doi: 10.1007/s00425-019-03137-y

Rietjens, I. M., Louisse, J., and Beekmann, K. (2017). The potential health effects of dietary phytoestrogens. *Br. J. Pharmacol.* 174, 1263–1280. doi: 10.1111/bph.13622

Seneviratne, H. K., Dalisay, D. S., Kim, K. W., Moinuddin, S. G. A., Yang, H., Hartshorn, C. M., et al. (2015). Non-host disease resistance response in pea (*Pisum sativum*) pods: biochemical function of DRR206 and phytoalexin pathway localization. *Phytochemistry* 113, 140–148. doi: 10.1016/j.phytochem.2014.10.013

Teponno, R. B., Kusari, S., and Spiteller, M. (2016). Recent advances in research on lignans and neolignans. *Nat. Prod. Rep.* 33, 1044–1092. doi: 10.1039/C6NP00021E

Vassão, D. G., Kim, K.-W., Davin, L. B., and Lewis, N. G. (2010). "Lignans (neolignans) and allyl/propenyl phenols: biogenesis, structural biology, and biological/human health considerations," in *Comprehensive Natural Products II Chemistry and Biology*, eds L. Mander and H.-W. Liu (Oxford: Elsevier), 815–928.

Conflict of Interest: The authors declare that the research was conducted in the absence of any commercial or financial relationships that could be construed as a potential conflict of interest.

frontiers in Pharmacology

ORIGINAL RESEARCH
published: 28 June 2019
doi: 10.3389/fphar.2019.00723

Recovery of Sesamin, Sesamolin, and Minor Lignans From Sesame Oil Using Solid Support-Free Liquid–Liquid Extraction and Chromatography Techniques and Evaluation of Their Enzymatic Inhibition Properties

*Dimitris Michailidis, Apostolis Angelis, Nektarios Aligiannis, Sofia Mitakou, and Léandros Skaltsounis**

Faculty of Pharmacy, Department of Pharmacognosy and Natural Products Chemistry, University of Athens, Athens, Greece

OPEN ACCESS

Edited by:
Salvatore Salomone, University of Catania, Italy

Reviewed by:
Chul Young Kim, Hanyang University, South Korea
Gianluigi Lauro, University of Salerno, Italy

***Correspondence:**
Léandros Skaltsounis
skaltsounis@pharm.uoa.gr

Specialty section:
This article was submitted to Experimental Pharmacology and Drug Discovery, a section of the journal Frontiers in Pharmacology

Received: *13 February 2019*
Accepted: *05 June 2019*
Published: *28 June 2019*

Citation:
Michailidis D, Angelis A, Aligiannis N, Mitakou S and Skaltsounis L (2019) Recovery of Sesamin, Sesamolin and Minor Lignans From Sesame Oil Using Solid Support Free Liquid–Liquid Extraction and Chromatography Techniques and Evaluation of Their Enzymatic Inhibition Properties. Front. Pharmacol. 10:723. doi: 10.3389/fphar.2019.00723

In this study, an integrated process for the recovery of sesamin and sesamolin, two high added-value lignans of sesame oil (SO) was developed, using synchronous extraction and chromatography techniques. The extraction of SO phenolic content was studied using two different extraction techniques: Annular centrifugal extraction (ACE) and centrifugal partition extraction (CPE). The derived data of each experiment were compared in terms of revealing the yields, time, and solvents consumption showing that CPE is the most effective technique, concerning the solvent consumption. The isolation of lignans was achieved using centrifugal partition chromatography (CPC) both on semi-preparative and preparative scale. The biphasic system used for this purpose consisted of the following solvents: n-Hex/EtOAc/EtOH/H_2O in proportion 2:3:3:2 (v/v/v/v) and direct recovery of the two major lignans sesamin and sesamolin was achieved. In parallel the CPC analysis resulted in the isolation of four minor lignans of sesame oil, i.e., samin, sesamol, sesaminol, and episesaminol. Structure elucidation of isolated lignans was based on HRMS/MS and NMR experiments. High-performance liquid chromatography (HPLC) was employed for quantitative analysis of the obtained extracts to determine the purity of the isolated compounds as well. The results of this study demonstrated that sesamin and sesamolin were recovered in purity higher than 95%, verifying the effectiveness of the purposed separation methodology. Finally, due to the general application of sesame oil in cosmetic industry, all the pure compounds were evaluated for their tyrosinase, elastase, collagenase, and hyaluronidase inhibition activity.

Keywords: sesame oil, sesamin, sesamolin, liquid–liquid extraction, centrifugal partition extraction, annular centrifugal extraction, centrifugal partition chromatography, collagenase inhibition activity

INTRODUCTION

Sesame oil is a product of high importance, obtained from the seeds of *Sesamum indicum* (Pedaliaceae) and is directly linked to the traditional nutrition of Asian and African people for more than 5,000 years (Zhang et al., 2013; Sarkis et al., 2014). According to Food and Agriculture Organization of the United Nations (FAO) in 2014 the global production of SO exceeded the amount of one and a half million tonne to meet market needs (Food and Agriculture Organization of the United Nations (FAO), 2017). These numbers have attracted scientific interest, leading to the study of the chemical content and bioactivity of SO secondary metabolites (Barbosa et al., 2017; Dossa et al., 2017). Many scientific researches have proved that phenolic compounds of SO have numerous biological activities. Especially sesamin and sesamolin (**Figure 1**), the two major lignans of SO extract, have been tested *in vitro*, *in vivo*, and in clinical studies for numerous activities.

Particularly, *in vivo* experiments have proved the hypocholesterolemic activity of sesamin (Nakai et al., 2003), whereas a clinical study demonstrated positive results against total and LDL-cholesterol on humans, probably synergistic with vitamin E (Penalvo et al., 2006). In addition, this molecule promotes the reduction of fat ratio on human body obviating atherosclerosis and corpulence (Dar and Arumugam, 2013), whereas experiments on gerbils and mice have demonstrated the neuroprotective role of sesamin against cerebral ischemia (Chung et al., 2010; Dar and Arumugam, 2013). Another important activity of this lignan is the anti-inflammatory, *via* the inhibition of delta 5-desaturase (Ohnmacht et al., 2008), an enzyme that is connected with the pro-inflammatory mediators (Obukowicz et al., 1998). When the organism lacks glucose, ketone bodies are used to cover the energy demands. Sesamin is able to increase the ketone body concentration (Anilakumar et al., 2010). This furanofuran lignan also decreases the metabolism of γ-tocopherol and as a result, elevates the concentration of tocopherol (Wu et al., 2009). The antioxidant activity of sesamin and its protective role against damages of alcohol and carbon tetrachloride on liver have been proven as well (Nakai et al., 2003).

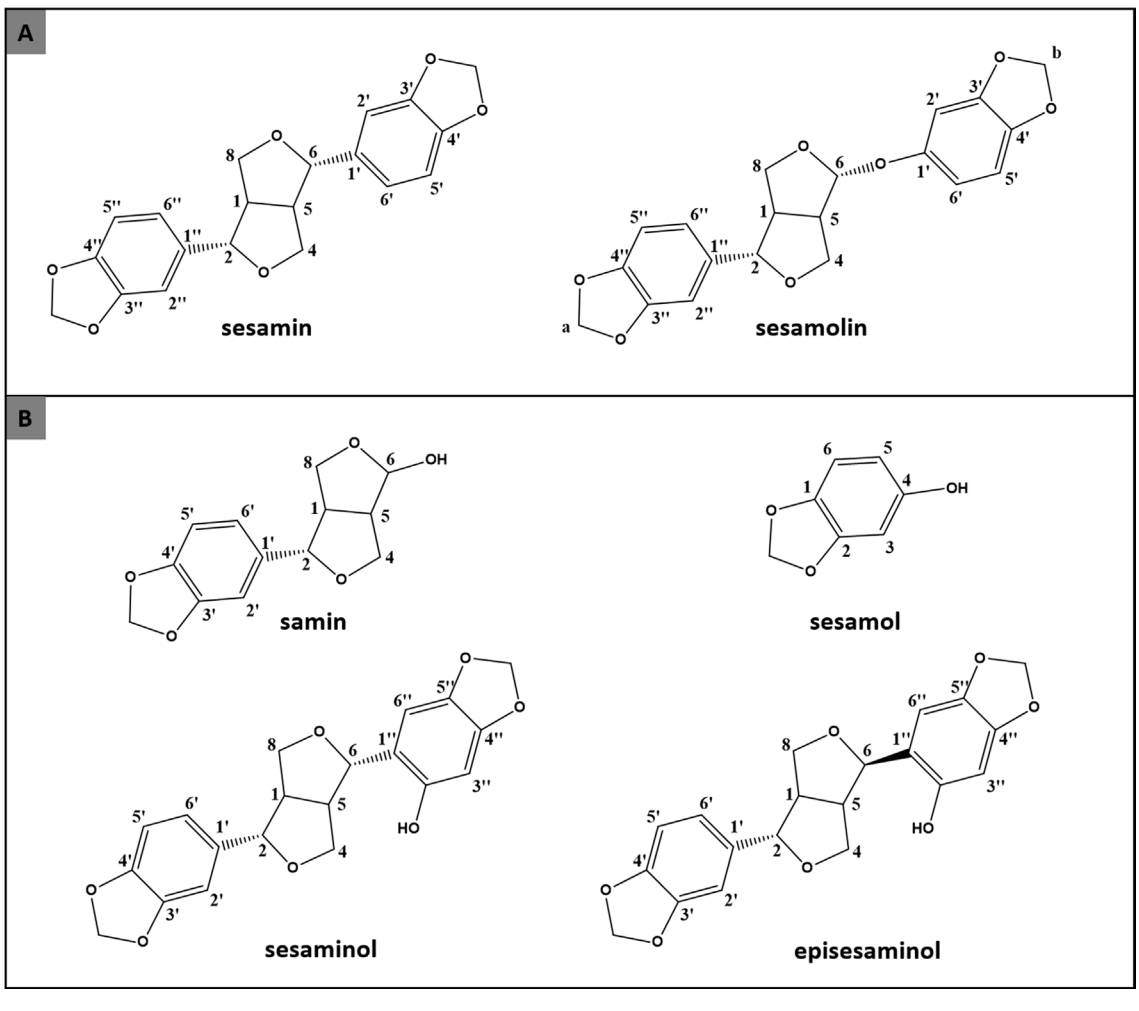

FIGURE 1 | Chemical structures of major (**A**: sesamin and sesamolin) and minor (**B**: samin, sesamol, sesaminol, and episesaminol) lignans isolated from sesame oil.

Sesamolin, the second major lignan of SO, has also a significant number of biological activities. It induces apoptosis of human lymphoid leukemia Molt 4B cells, inhibits the growth of those cells (Miyahara et al., 2001), and prevents from mutagenic activity of H_2O_2 (Grougnet et al., 2012). Sesamolin has also free radical scavenging activity and provides protection against neuronal hypoxia (Park et al., 2010).

Due to the high pharmacological interest of sesamin and sesamolin, there are several works regarding the isolation and purification of these lignans from *Sesamum indicum* materials like sesame seeds, sesame meal, and SO (Lee and Choe, 2006; Wang et al., 2009; Reshma et al., 2010; Dar et al., 2015; Hammann et al., 2015; Jeon et al., 2016). In the literature, silica gel column is referred as separation technique of SO extract, which is mostly applied for laboratory purposes (Lee and Choe, 2006). Moreover, crystallization method is carried out, providing mixture of lignans (Reshma et al., 2010). Another study is based on semi-preparative high-performance liquid chromatography (HPLC), which has limited capacity of sample treatment (Dar et al., 2015). Considering counter-current chromatography, two studies are reported, whereas one of them provide a mixture of sesamin and sesamolin, and the other one is characterized by reduced yield of pure compounds (Wang et al., 2009; Hammann et al., 2015). Only in one study was the centrifugal partition chromatography (CPC) technique applied, but because raw material sesame seed meal was used, while the procedure was more time-consuming, and the results gave lower recovery and lower purity (Jeon et al., 2016). However, there is no previous work for producing these two lignans in high amounts and purity using a low cost and fast methodology. Following this need, our research targeted to develop a novel approach, which could meet the abovementioned parameters.

The following experimental procedure is based on liquid–liquid techniques. Centrifugal partition extraction (CPE) is a solid support-free liquid–liquid extraction technique which is based on the immiscible nature of two phases and the partition of compounds in the formed biphasic system (Berthod et al., 2009; Michel et al., 2011; Ungureanu et al., 2013). This technique is mainly used for rapid fractionations of mixtures, pH zone refining separations as well as for the extraction of liquid nature raw materials, such as edible oils (Ungureanu et al., 2013; Angelis et al., 2017). Low experimental time and solvent consumption rendered it suitable for analytical, preparative, pilot, and industrial scale as well (Hamzaoui et al., 2011; Kumar et al., 2014). Two common extraction methods of CPE are co-current elution and multi-dual mode. In the first method, the biphasic system passes through the column and is separated out of the apparatus. At the second method, column is fed with the stationary phase, and the mobile phase passes through the first. The kinetic nature of the two phases can be changed by the rotation of valve ascending/descending, which sets the inlet of solvents in column. Another extraction technique that was used in this study was annular centrifugal extraction (ACE). This technique can rapidly separate the biphasic systems and is characterized by high mass transfer efficiency per time unit (Jing et al., 2017). The centrifugal force is used, first, to mix the two phases and then to separate them (Duan et al., 2015).

CPC is governed by the same principles of CPE with a difference in the number and the volume of column cells (Hamzaoui et al., 2011). The CPE and CPC columns are metallic cylinders with a number of cells that are proportionally related with theoretical plates. Chromatography column cells are higher in number but smaller in volume than extraction column cells (Goll et al., 2015). One phase (stationary phase) is immobilized by strong centrifugal forces into the column, whereas the other phase (mobile phase) is pumped through the column, separating thus the mixture compounds, on the basis of their partition coefficient (K_D) (Roullier et al., 2009; Ning et al., 2018). The nature of this technique gives the ability of obtainment the maximum amount of the extract and handling high amounts of sample (Jeon and Kim, 2013; Agalou et al., 2018). Also, this technique permits the use of various polarity solvent systems which result in widening the chromatographic performances (Toribio et al., 2011). Another advantage of CPC is the ability of alternation the mobile phase to stationary during a run, accelerating the recovery of compounds (Sutherland, 2007).

The aim of this study was the development of an effective and capable scaling up process for the treatment of sesame oil and isolation of sesamin and sesamolin in high purity. The primary step was the extraction of phenolic compounds from SO. Two extraction techniques were compared to choose the most advantageous concerning experimental time and extract productivity. The second step was the isolation of sesamin and sesamolin in semi-preparative and preparative scale. The last part of the study was the quantification of the obtained lignans using HPLC-DAD. Also, NMR experiments were used for the identification of the targeted molecules. TLC analysis and HPLC experiments were conducted for the qualification of SO extracts. In parallel, sesamin, sesamolin, and minor compounds isolated from SO were evaluated with enzymatic assays (tyrosinase, elastase, collagenase, and hyaluronidase) for their inhibition activity.

MATERIALS AND METHODS

Reagents

The standards of lignans that were used for the quantitative analysis were purchased from Sigma-Aldrich (Missouri, USA). Also, all the reagents were purchased from Sigma-Aldrich. In detail, for the enzymatic assays mushroom tyrosinase (lyophilized powder, ≥1000 units/mg solid, EC Number: 1.14.18.1), 3,4-dihydroxy-L-phenylalanine, sodium phosphate monobasic, sodium phosphate dibasic, kojic acid, elastase type IV from porcine pancreas (EC Number 254-453-6), N-Succinyl-Ala-Ala-Ala-p-nitroanilide (EC Number 257-823-5), Trizma base reagent grade, elastatinal, collagenase from *Clostridium histolyticum* (released from physiologically active rat pancreatic islets Type V, ≥1 FALGPA units/mg solid, > 125 CDU/mg solid, EC Number: 232-582-9), MMP 2 substrate fluorogenic, chlorexidine, bovine serum albumin (BSA), acetic acid glacial, p-(dimethylamino) benzaldehyde, sodium tetraborate, hyaluronidase (released from bovine testes Type I-S, lyophilized powder, 400–1,000 units/mg solid, EC Number: 3.2.1.35), hyaluronic acid, and tanic acid

were purchased also from Sigma-Aldrich. The used solvents for the extraction and separation processes were of analytical grade while those used for UPLC-HRMS analysis were of LC-MS grade. All solvents were supplied from Fisher Scientific (Pennsylvania, USA). TLC analysis was performed on Silica gel 60 F_{254} 20 × 20 cm plates purchased from Merck Millipore (Massachusetts, USA). Sesame oil was provided from HAITOGLOU BROS S.A.

Apparatus

The extraction of SO phenolic fraction was performed using two different liquid–liquid techniques: CPE and ACE. The CPE experiments were performed on an A-CPC apparatus (Rousselet-Robatel Kromaton, Anonay, France) equipped with a 300-ml capacity extraction column (FCPE300®) while solvents pumped with preparative Lab Alliance Series III P300 pumps (Pennsylvania, USA). ACE experiments were performed using laboratory scale BXP012 apparatus (Rousselet-Robatel Kromaton, Anonay, France) with 2.2 ml bowl volume. Basic Verderflex pumps (Castleford, United Kingdom) were used for pumping the solvents through the annular extractor.

Semi-preparative and preparative fractionations of SO phenolic fraction were carried out on an FCPC apparatus (Kromaton, Anonay, France) equipped with a 200-ml capacity chromatographic column (FCPC200®) and 1,000-ml capacity chromatographic column (FCPC1000®), respectively. Solvents were pumped with preparative Ecom ECP2000 pumps (Prague, Czech Republic). Chromatograms were recorded with a detector UV Flash 14 DAD UV of Ecom (Prague, Czech Republic) and the fractions were collected with a C6-60 Buchi collector (Flawil, Switzerland).

HPLC analysis was performed on a Thermo Finnigan HPLC system (Ontario, Canada) equipped with a SpectraSystem P4000 pump, a SpectraSystem 1000 degasser, a SpectraSystem AS3000 automated injector, and a UV SpectraSystem UV6000LP detector. Data acquisition was controlled by the ChromQuest™ 5.0 software (ThermoScientific™).

Nuclear magnetic resonance spectra were registered on 600 MHz of Bruker AvanceAVIII-600 spectrometer (Karlsruhe, Germany) and was supported by TopSpin software (Bruker). UPLC-HRMS and HRMS/MS analysis was performed on an AQUITY system (Waters) connected with an LTQ Orbitrap Discovery hybrid mass spectrometer (Thermo Scientific) equipped with an ESI source, in negative and positive mode.

For all the enzymatic assays the reader Infinite 200 PRO series (Tecan, Zürich, Switzerland) was used, supported by software Magellan™ (Tecan, Zürich, Switzerland).

Liquid–Liquid Extraction of SOs' Lignans

Extraction of Lignans Using Laboratory Scale Annular Centrifugal Extractor (BXP012)

Two different experiments were performed using for the extraction the biphasic system SO/Acetonitrile (AcN). In both experiments the rotor speed was set at 3,900 rpm and 200 ml of SO were extracted by using 600 ml of acetonitrile. For the first experiment, the extraction was performed on three successive cycles using 200 ml of AcN in each run (total 600 ml of AcN). AcN (upper phase) and SO (lower phase) were pumped through the apparatus at a flow rate of 8 ml/min for each phase (1/1 ratio of the two phases). The total experiment lasted approximately 1 h and 15 min (~25 min for each cycle). In the second experiment, the flow rate of AcN was increased at 24 ml/min while the flow rate of SO remained stable at 8 ml/min giving thus a ratio of 1/3 SO/AcN into the extraction bowl. The procedure was accomplished on one single run after 25 min. Samples were collected from each experiment and were analyzed for quantification of the two targeted lignans *via* HPLC technique.

Extraction of Lignans Using FCPE300®

Three extraction runs took place with CPE using multi-dual mode method (Angelis et al., 2017). CPE column was filled with SO (stationary phase) in descending mode, whereas the flow rate and the rotation were set at 20 ml/min and 200 rpm, respectively. Then, AcN was pumped in ascending mode at 10 ml/min and 800 rpm to equilibrate the biphasic system (SO/AcN) inside the column. Stationary phase retention volume was 200 ml and Sf was calculated at 66.6%. Afterward, 240 ml of AcN were collected in 12 fractions of 20 ml. Then, the pumping mode switched to descending and 200 ml of untreated SO replaced the extracted SO with a flow rate of 10 ml/min. The above extraction-recovery cycle was repeated three times of 44 min per run. The extraction solvent (AcN) was evaporated under vacuum at 40°C to dryness to obtain the SO extract.

Fractionation of SO Extract Using Semi-Preparative FCPC200® and Preparative FCPC1000® Apparatus

Solvent System Selection

Seventeen biphasic solvent systems (**Supplementary Table 1**) were created and studied to select the appropriate systems for the CPC separation process. All systems were initially tested regarding the solubility of the extract and settling time and then the suitability of biphasic systems was evaluated by TLC and HPLC-DAD. The procedure was as follows: 10 mg of SO extract were weighed into a 10-ml glass tube, 3 ml of each phase of the pre-equilibrated biphasic solvent systems were added to the sample and shaken vigorously. After equilibration of the biphasic system (t < 1 min), 1 ml of each layer was evaporated to dryness, the residues were diluted in 1 ml of acetonitrile, and analyzed by TLC and HPLC-DAD. The K_D values of the target compounds were expressed as the ratio between the peak area in the stationary phase and the peak area in the mobile phase.

Semi-Preparative CPC Analysis

The CPC experiment was carried out in elution extrusion mode by using the biphasic system n-Hex/EtOAc/EtOH/H_2O in proportion 2:3:3:2 (v/v/v/v). Initially, the column was filled with the stationary phase (the upper phase) on descending mode at a flow rate of 10 ml/min and setting the rotation speed at 200 rpm. Then, the rotation speed was maximized at 900 rpm, and the mobile phase was pumped through the column with a flow rate of 5 ml/min on descending mode. After the system equilibration, the retention volume of the stationary phase was calculated at 105 ml giving a high Sf value of 52.5%. Crude SO extract (110 mg) were dissolved in 10 ml of biphasic system and injected into column. In the elution step 350 ml of mobile phase were passed through the stationary phase at

a flow rate of 5 ml/min on descending mode. The experiment was completed by passing 200 ml of the stationary phase on descending mode and extruding the column content. All procedures were monitored by UV detector at 255, 275, 280, and 320 nm while the automatic fraction collector was set to collect fractions every 2 min. The total analysis time was 110 min, and finally, 55 fractions of 10 ml were collected.

Preparative CPC Analysis

The semi-preparative method was scaled up to preparative column (1,000 ml rotor) adjusting all the experimental parameters to the larger scale. After filling the column with the upper stationary phase (500 rpm and 25 ml/min), the rotation speed was increased to 750 rpm, and the lower phase of the same system (mobile phase) was pumped at 15 ml/min in descending mode to equilibrate the two phases into the column (Sf was calculated at 65%). Then, 900 mg of the extract were diluted in a mixture of the two phases (ratio 7/3 upper phase/lower phase) and injected *via* a 30-ml injection loop. The volume of mobile phase used for the elution step was 1,600 ml while the experiment completed by passing 1,000 ml of the stationary phase in descending mode (extrusion step). The rotation speed and flow rate were kept stable at 750 rpm and 15 ml/min, respectively, during the whole experiment. The total analysis time lasted approximately 170 min, and finally, 130 fractions of 20 ml were collected.

Quantitative Analyses of Sesamin and Sesamolin in Crude Extracts and CPC Fractions

For the quantitative analysis of the two lignans, the construction of standard calibration curves on HPLC-DAD was necessary. For the separation, a Supelco Analytical (Sigma-Aldrich) HS C18 column, with dimensions 25 × 4.6 mm, 5 μm was used, heated at 40°C. As mobile phase was used in a gradient system consisted of AcN (A) and water (B). The elusion started with 54% of A and reached 79% in 5 min. Then, in 5 min, A reached 83% and during the next 3 min was increased to 95%. The gradient continued for 2 min with A reaching 100%. In 1 min, the solvent system returned to initial conditions and maintained for 4 min. The total running time was 20 min, and the flow rate was set at 1 ml/min. The injection volume was 10 μl. For sesamin, six concentrations were used: 50, 75, 100, 125, 150, and 175 μg/ml. Also, for sesamolin were used: 25, 50, 75, 100, 125, and 150 μg/ml. As internal standard (IS) vanillin was used in a concentration of 10 μg/ml. For the construction of the calibration curves the ratio area of analyte/IS was used. Linearity was evaluated by coefficient of determination, which was over 0.99 for both analytes (**Supplementary Diagrams 1** and **2**).

Thin Layer Chromatography (TLC), Ultra High-Performance Liquid Chromatography-High Resolution MS/MS (UHPLC-HRMS/MS), and NMR Analysis

TLC plates were developed in dichloromethane (DCM). Plates were observed at 254 nm, 366 nm, and at visible after treatment with a sulfuric vanillin solution (5% w/v in methanol)—H_2SO_4 (5% v/v in methanol) and heated at 100°C to 120°C for 1 min.

The phenolic fraction and selected CPC fractions were analyzed using UPLC-HRMS technique. The separation was run in a Fortis C-18 (1.7 μm, 150 × 2.1 mm) column at 40°C. The elution system consisted of water acidified with 0.1% formic acid (A) and acetonitrile (B) in the following gradient mode: 0–2 min 2% B, 2 to 18 min from 2% to 100% B, 18 to 20 min 100% B, 20–21 min from 100% to 2% B, and 21 to 25 min 2% B. The flow rate was set at 0.4 ml/min, and the injection volume was 10 μl. Ionization was achieved in negative and positive ion mode (ESI+ and ESI–) at 350°C. The mass spectrometric parameters were: sheath gas and aux gas flow rate 40 and 10 units, respectively; capillary voltage, 30 V; and tube lens, 100 V for the positive mode and capillary voltage of −20 V and tube lens of −80 V for the negative mode. The mass range was adjusted from 113 to 1,000 m/z.

NMR samples were dissolved in 600 μl of deuterated chloroform ($CDCL_3$). All the ^1H NMR experiments were applied on 600.11 MHz, while ^{13}C NMR spectra were acquired at 150.90 MHz. During all the experiments, temperature was set at 300°K. Spectral width of ^1H NMR was set to 14 ppm, offset to 6.5 ppm, and scans number to 32. Concerning 2-D NMR experiments, proton spectra were registered according to the abovementioned parameters with 12 scans number for COSY, while carbon spectra width set to 240 ppm, offset to 110 ppm, and scans number to 32 and 160 at HSQC and HMBC, respectively.

Tyrosinase, Elastase, Collagenase, and Hyaluronidase Inhibition Assays

Tyrosinase, elastase, and collagenase assays were applied following the enzymatic methods described by Angelis et al. (2016) with some modifications, while the enzymatic assays for the inhibition of hyaluronidase were conducted as described by Kim et al. (2013), with some modifications. All the enzymatic assays provide the competitive inhibition activity of the compounds. Three concentrations of pure compounds, i.e., 500, 100, and 25 μM (final concentration in the well) were used on the above enzymatic assays. Experiments were performed in triplicates and twice in total while the final DMSO concentrations did not exceed 5% of total volume. The inhibition percentage was calculated by the formula: Inhibition (%) = [((X control − X control's blank) − (X sample − X sample's blank))/(X control − X control's blank)] × 100, where X control is the absorbance or fluoresces of the mixture consisting of buffer, enzyme, sample solvent, and substrate, and X sample is the absorbance or fluoresces of the mixture of buffer, enzyme, sample, or positive control solution and substrate. Blanks contained all the abovementioned components except the enzyme. Concerning tyrosinase, elastase, and collagenase enzymatic assays, the half maximal inhibitory concentration (IC50) of each positive control was used as standard of comparison, while at hyaluronidase enzymatic assay the maximal inhibitory concentration (IC100) was used.

Tyrosinase enzymatic assay: This assay measures the inhibition of the tested samples at the catalytic oxidation of L-DOPA to dopachrome by tyrosinase. Kojic acid (IC50 = 50 μM) was used as positive control. In a 96-well microplate, 80 μl of phosphate-buffered saline (PBS) (1/15 M, pH = 6.8), 40 μl of the tested sample

(dissolved in the PBS buffer), and 40 μl of mushroom tyrosinase (100 U/ml) (dissolved in PBS buffer) were mixed and incubated in the dark for 10 min at room temperature. Afterward, 40 μl of 2.5 mM L-DOPA (substrate) dissolved in PBS buffer was added, and the mixture was incubated for 15 min. The 96-well microplate was measured at 475 nm.

Elastase enzymatic assay: Elastase protocol monitors the release of *p*-nitroaniline from N-succinyl-Ala-Ala-Ala-p-nitroanilide that is stimulated by elastase. Elastatinal (IC50 = 0.5 μg/ml) was used as a positive control. In a 96-well microplate, 70 μl of Trizma buffer (50 mM, pH = 7.5), 10 μl of tested sample (dissolved in Trizma buffer), and 5 μl of elastase (0.45 U/ml) (dissolved in Trizma buffer) were mixed and incubated in the dark for 15 min at room temperature. Afterward, 15 μl of 2 mM N-succinyl-Ala-Ala-Ala-p-nitroanilide (substrate) dissolved in Trizma buffer was added, and the mixture was incubated for 30 min at 37°C. The 96-well microplate was measured at 405 nm.

Collagenase enzymatic assay: Collagenase fragmentates the fluorescence molecule MMP2. The inhibition of the enzyme was measured concerning the reduction of the fluorescent intensity that was produced. Chlorhexidine (IC50 = 50 μM) was used as a positive control. In a 96-well dark microplate, 120 μl of Tris-HCl buffer (50 mM, pH = 7.3), 40 μl of tested sample, and 40 μl of collagenase (50 μg/ml) from *C. histolyticum* (dissolved in Tris-HCl buffer) were incubated for 10 min at 37°C avoiding light exposure. Afterward, 40 μl of 50.0 μM MMP2 (substrate) (MCA-Pro-Leu-Ala-Nva-DNP-Dap-Ala-Arg-NH_2) dissolved in Tris-Cl buffer was added, and the mixture was incubated in dark for 30 min at 37°C. The fluorescent intensity of 96-well microplate was measured at an excitation maximum of 320 nm and an emission maximum of 405 nm.

Hyaluronidase enzymatic assay: The inhibition activity of this enzyme was calculated inversely proportional of the production of *N*-acetyl-D-glucosamine. Tannic acid (IC100 = 800 μM) was used as positive control; 100 μl of acetate buffer (0.1 M NaCl, pH = 3.5), 150 μl of tested sample (dissolved in acetate buffer), and 50 μl of hyaluronidase solution 1% w/v (dissolved in acetate buffer) were added in Eppendorfs. Afterward, 100 μl of BSA solution 0.2% w/v (dissolved in ddH_2O) was added in each Eppendorf and incubated for 20 min at 37°C. Then, 50 μl of hyaluronic acid solution 0.5% w/v (dissolved in ddH_2O) was added and incubated for 60 min at 37°C; 45 μl from each Eppendorf was transferred in new Eppedorfs containing 10 μl of sodium tetraborate solution 0.8 M (dissolved in ddH_2O), and heated for 3 min at 100°C and cooled down on ice. In each tube 300 μl of dimethylaminobenzaldehyde (DMAB) solution was added (10% w/v dissolved in 10 N HCl and then dissolved 10 times in acetic acid glacial) and incubated for 20 min at 37°C. Finally, 200 μl from the last Eppendorf was transferred in a 96-well microplate and measured at 586 nm.

RESULTS AND DISCUSSION

Liquid–Liquid Extraction of Phenolic Compounds from SO

Several extraction processes of phenolic compounds from SO have been reported previously, both in laboratory and large scale (Dachtler et al., 2003; Lee and Choe, 2006; Wang et al., 2009; Reshma et al., 2010; Dar et al., 2015). However, the described experimental procedures consume large amount of solvents (Wang et al., 2009; Reshma et al., 2010), in some cases the sesame oil-solvent ratio is 1:8 (Dar et al., 2015), and overnight experimental tasks are needed (Dachtler et al., 2003; Lee and Choe, 2006; Reshma et al., 2010; Dar et al., 2015). Also, a lot of the proposed procedures have many steps, like solvent extraction, crystallization, and saponification, working in very low (−40°C, 4°C) and high temperatures (70°C), facts leading to long experimental protocols and high energy consumption (Dachtler et al., 2003; Lee and Choe, 2006; Reshma et al., 2010; Dar et al., 2015).

To avoid all the abovementioned disadvantages, during the extraction process of SO phenols, two different liquid–liquid techniques were compared. Both ACE and CPE techniques use the centrifugal force to achieve a fast mixture and separation of the immiscible liquid phases during the extraction process (Xu et al., 2006; Hamzaoui et al., 2011). These two techniques are characterized as green eco-friendly processes due to the low solvent and energy consumption, with industrial applications (Meikrantz et al., 2002; Duan et al., 2005; Hamzaoui et al., 2011).

Selection of the Suitable Method for Liquid–Liquid Extraction

The initial step for the liquid–liquid extraction process was the selection of the most suitable solvent system for the quantitative recovery of bioactive ingredients from SO. Taking advantage of the nonpolar oil nature, SO was used as ingredient of the biphasic system. This fact allowed the treatment of large amount of raw material increasing thus the process efficiency (Angelis et al., 2017). More specifically, several systems were created and tested by TLC and HPLC (**Supplementary Table 2**). The results of this analysis demonstrated that the presence of water as a part of the polar phase (systems ES1-ES8) led to the creation of stable emulsion, and thus, in unsuitable biphasic systems. On the other hand the non-aqueous biphasic systems containing mainly acetonitrile, ethanol or methanol (ES11-ES17) resulted in better separation of the two phases. The following HPLC-DAD analysis showed that the addition of butanol in the biphasic systems (ES11-ES14) (**Supplementary Table 3**) resulted in an unsatisfactory recovery of the lignans from the feed oil phase. In contrast to these results the direct extraction of SO with acetonitrile, methanol or ethanol (systems ES15, ES16, and ES17, respectively) led to the better recovery of the targeted compounds. These three systems were tested using triple funnel extraction of SO with the corresponding solvent, and the recovered upper phases were analyzed by TLC (**Supplementary Figure 1**) and HPLC (**Supplementary Table 4**). Both techniques demonstrated that system ES15 (extraction with AcN) is the most effective in receiving the lignan fraction and, thus, was chosen for the liquid–liquid extraction of SO.

Liquid–Liquid Extraction Using ACE

ACE is a liquid–liquid extraction technique with numerous advantages, such as high mass transfer coefficient, high interfacial areas, low solvents consumption, and flexible phase ratios (Tamhane et al., 2014). To find the critical parameters for the analytical scale

ACE extraction of SO using acetonitrile it was necessary to standardize the solvents flow rate and rotor speed. After several trials, it was found that the flow rate of SO should be lower than 14 ml/min and the rotation of the annular rotor at 3,800 to 4,050 rpm. Under these conditions, the two phases of the biphasic system are mixed and separate rapidly into the extraction bowl eliminating thus the formation of an emulsion that affects the quality of the extraction. The first experiment aimed to check the extraction efficiency using acetonitrile as extraction solvent. For this purpose, 200 ml of SO were extracted with 600 ml of acetonitrile in three successive cycles (200 ml in each cycle). The experiment lasted 75 min and totally 2.02 g of SO extract was obtained. The quantitative HPLC analysis of the obtained extract showed the present of 1.05 g of sesamin and 0.36 g of sesamolin (5.25 mg of sesamin and 1.80 mg of sesamolin per ml of SO) (**Table 1**). To reduce the process time and to increase the efficiency of the method, the ACE extraction was repeated. The main difference from the previous experiment was that the flow rate of AcN was increased three times (24 ml/min), replacing the triple extraction. Thus, 200 ml of SO was extracted with 600 ml of AcN in a single run and in total time of 25 min. The procedure resulted in the recovery of 1.68 g of extract, which contains 0.84 g of sesamin and 0.29 g of sesamolin (**Table 1**).

As a result, it was observed the continuous receiving of lignans but reduced recovery. At these conditions, 4.20 mg of sesamin and 1.50 mg of sesamolin were obtained from each ml of SO. It is important to note that is the first time that ACE technique was applied for the extraction of bioactive compounds, not only from SO, but generally from edible oils.

Liquid–Liquid Extraction Using CPE

The experiment was repeated successfully using multi-dual mode method. SO was used as stationary phase while acetonitrile (mobile phase) was pumped through the SO in ascending mode. After passing approximately one column volume (240 ml) of mobile phase, the experiment stopped and the collected fractions (12 fractions of 20 ml) were analyzed by TLC.

As it is observed in the TLC analysis of CPE fractions (**Figure 2**), the first two fractions are fully enriched in SO extract. Thereafter, the next four fractions are highly concentrated, while the following fractions have a decreasing amount of SO extract. It has to be noted that even the appliance of concentrated spots on the TLC plate, the final fraction provides a negligible amount of the extract. The fact that after 12 fractions we obtained the total amount of SO extract proves the effectiveness of AcN as an extraction solvent. Moreover, it is important to underline the repeatability of CPE technique. The above procedure was repeated two more times by replacing each time the treated SO with the fresh one in descending mode (multi-dual mode process). All the repetitions (three runs) provide exactly the same phenomenon, a total recovery of lignans' extract after 12 fractions. The fractions of each run were combined, evaporated under vacuum, and weighted, yielding 1.97, 2.01, and 1.94 g, respectively. The quantitative HPLC analysis of the above extracts reveals that sesamin constituted approximately the 50% (1.01, 1.03, and 0.96 g) of total extract, while sesamolin was included also in high amount of approximately 18% (**Table 1**, repetitions a, b, and c).

Overall, the first experiment (i) of ACE provided an adequate extract yield, but with high solvent (ratio SO/AcN 1/3) and time consumption. Concerning the second ACE experiment (ii), the experimental time decreased at 1/3, but the solvent consumption remained the same, while the yield decreased for 17%. Although CPE gave a high amount of extract after reasonable time, the solvent needs decreased almost three times. In detail, after 44 min and with an extraction ratio of 1/1.2 of SO-AcN, CPE technique is able to obtain the total extract of sesame oil. The above seems to lead to the conclusion that CPE is the best extraction solution, because it is efficient on yield, time, and solvent consumption, with high repeatability. It should be highlighted that this technique was applied for the first time, concerning the recovery of lignan fraction from SO.

According to UPLC-HRMS analysis of SO extract, sesamin and sesamolin were detected in the SO extract. Sesamin molecular ion was 355.1176 m/z, and sesamolin molecular ion was 371.1142 m/z in positive mode. Also, other minor lignans as well as fatty acids were detected (**Supplementary Table 5**).

Separation of Sesamin and Sesamolin from Crude Extracts by CPC

Study of the CPC Solvent Systems

Crucial step in the innovated chromatographic process of CPC was to find the biphasic system needed for the separation (**Supplementary Table 1**) and then for the distribution of the target compounds by using TLC analysis. Based on this test, systems CS9, CS10, CS11, CS12, and CS16 were rejected because they do not meet the required specifications (**Supplementary Table 1**) while at systems CS1, CS2, CS14, and CS15, unsatisfactory distributions of sesamin and sesamolin in the TLC chromatograms were observed. Seven biphasic systems (CS3–CS8 and CS17) were further investigated using HPLC to calculate

TABLE 1 | Comparison of two extraction techniques used for the treatment of SO in regard to yield, time, and solvent consumption.

Extraction Technique	SO volume	Extraction Time	Yield, g/200 ml SO	Solvent consumption	Yield sesamin	Yield sesamolin
ACE	i. 200 mL	i. 75 min	i. 2.02	i. 600 mL AcN	i. 1.05 g	0.36 g
	ii. 200 mL	ii 25 min	ii.1.68	ii. 600 mL AcN	ii. 0.84 g	0.30 g
CPE	a. 200 mL	44 min	1.97	240 mL AcN	1.01 g	0.35 g
	b. 200 mL	44 min	2.01	240 mL AcN	1.03 g	0.36 g
	c. 200 mL	44 min	1.94	240 mL AcN	0.96 g	0.34 g

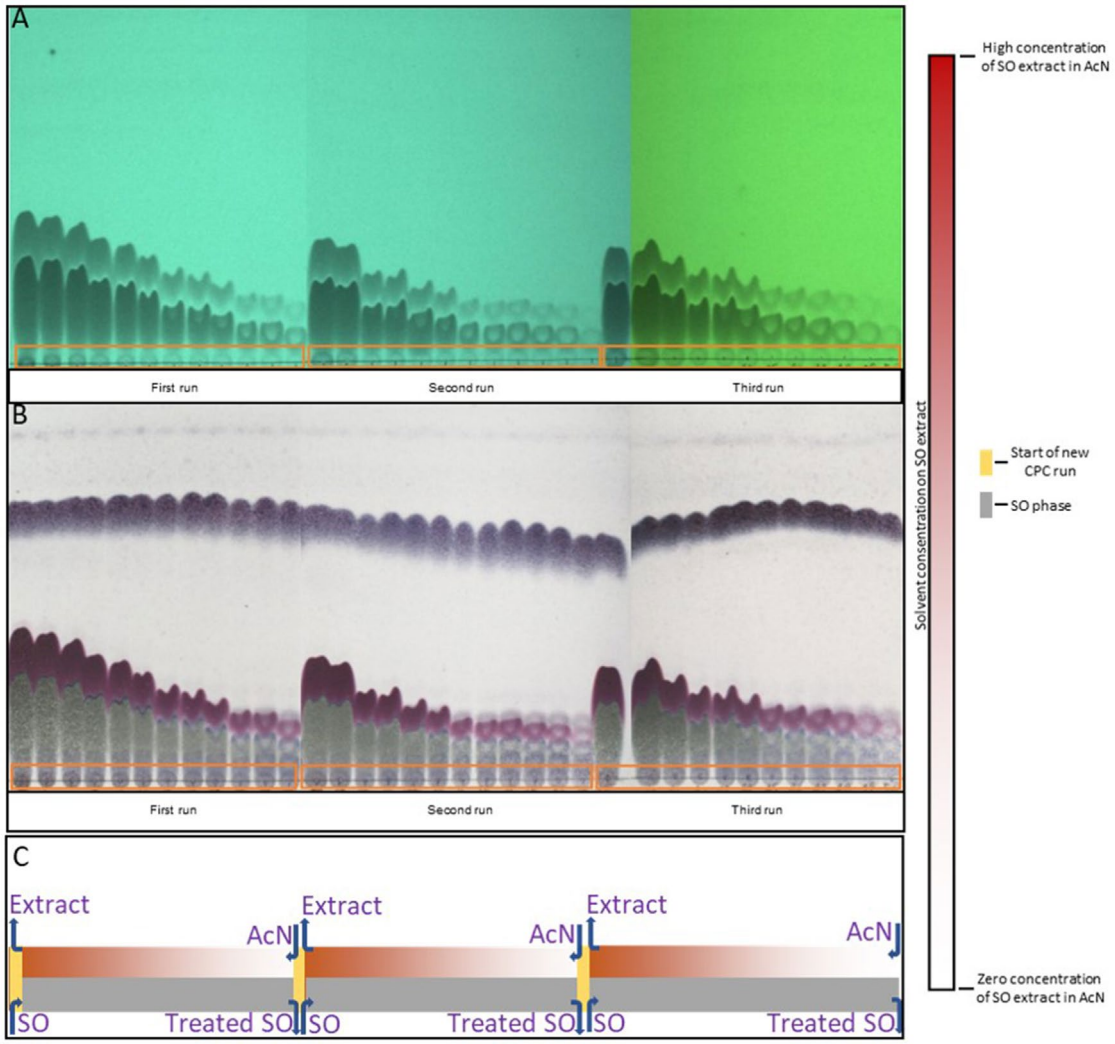

FIGURE 2 | TLC analysis of CPE fractions from three continuous runs in 254 nm **(A)** and in visible sprayed with vanillin solution **(B)**. Schematic presentation of concentration of extraction solvent in lignans during the extraction process **(C)**.

the partition coefficient values (K_Ds) of the target compounds and thus the suitability of the biphasic systems (based on the values of the separation factor α, which follow the rule K_{D1}/K_{D2}, $K_{D1} \geq K_{D2}$). The results of this analysis are given in **Table 2**.

TABLE 2 | Partition coefficient values (K_Ds) and separation factor (α) of sesamin and sesamolin in seven biphasic systems.

CPC Systems	Partition coefficient of sesamin	Partition coefficient of sesamolin	Separation factor (α) of sesamin and sesamolin
CS3	1.18	0.72	1.63
CS4	1.42	1.76	1.24
CS5	1.20	1.26	1.05
CS6	1.27	0.80	1.59
CS7	1.03	0.37	2.78
CS8	1.15	0.72	1.60
CS17	0.34	0.58	1.71

The study of K_Ds values and separation factors showed that five of the tested biphasic systems (CS3, CS6, CS7, CS8, and CS17) meet the criteria for a satisfactory separation of the target compounds (α > 1.5). Given that the higher value of α enables better separation of the two compounds and the treatment of higher amount of extract, system CS7 (n-Hex/EtOAc/EtOH/H_2O in proportion 2:3:3:2 v/v/v/v) seems to be the most effective (α = 2.78) and thus this system was chosen for the CPC analysis of the SO extract.

Purification of Lignans by Semi-Preparative FCPC200® and the Scale-Up Operation on a Preparative FCPC1000®

The capability of the selected method (elution–extrusion) and biphasic system (n-Hex/EtOAc/EtOH/H_2O in proportion 2:3:3:2 v/v/v/v) to efficiently isolate the two major lignans of SO extract was initially tested in semi-preparative column.

Except the phenolic part, SO extract contains high amounts of nonpolar fatty compounds, such as glycerides and fatty acids. Due to this nonpolar nature of the extract, the experiment was run in reverse mode by using as stationary phase the upper (nonpolar) phase of the system. This fact stabilizes the fatty compounds at the beginning of the column (due to the close affinity with the nonpolar phase) eliminating thus their co-elution with sesamin and sesamolin. After equilibrating the two phases into the column (Sf = 52.5%), 110 mg of crude SO extract was injected *via* a 10-ml injection loop. The elution step was completed by passing 350 ml of the aqueous mobile phase in descending mode and then the column content was extruded by passing 200 ml of the upper stationary phase also in descending mode. The experiment lasted 115 min while the separation process was monitored by UV at 255, 275, 288, and 320 nm (**Figure 3A**). All resulting fractions (55 fractions of 10 ml) were analyzed using TLC and fractions with similar chemical composition were put together. The result of this analysis was the recovery of 31.6 mg of sesamin and 14.1 mg of sesamolin both in a purity higher than 95% as this was calculated from the quantitative HPLC analysis.

The result obtained from semi-preparative analysis was very promising, and thus separation was scaled up to preparative CPC mode. The scaling up from 200 ml column (semi-preparative) to fivefold larger, 1L CPC column (preparative) can be easily applied, paying particular attention on rotational speed and

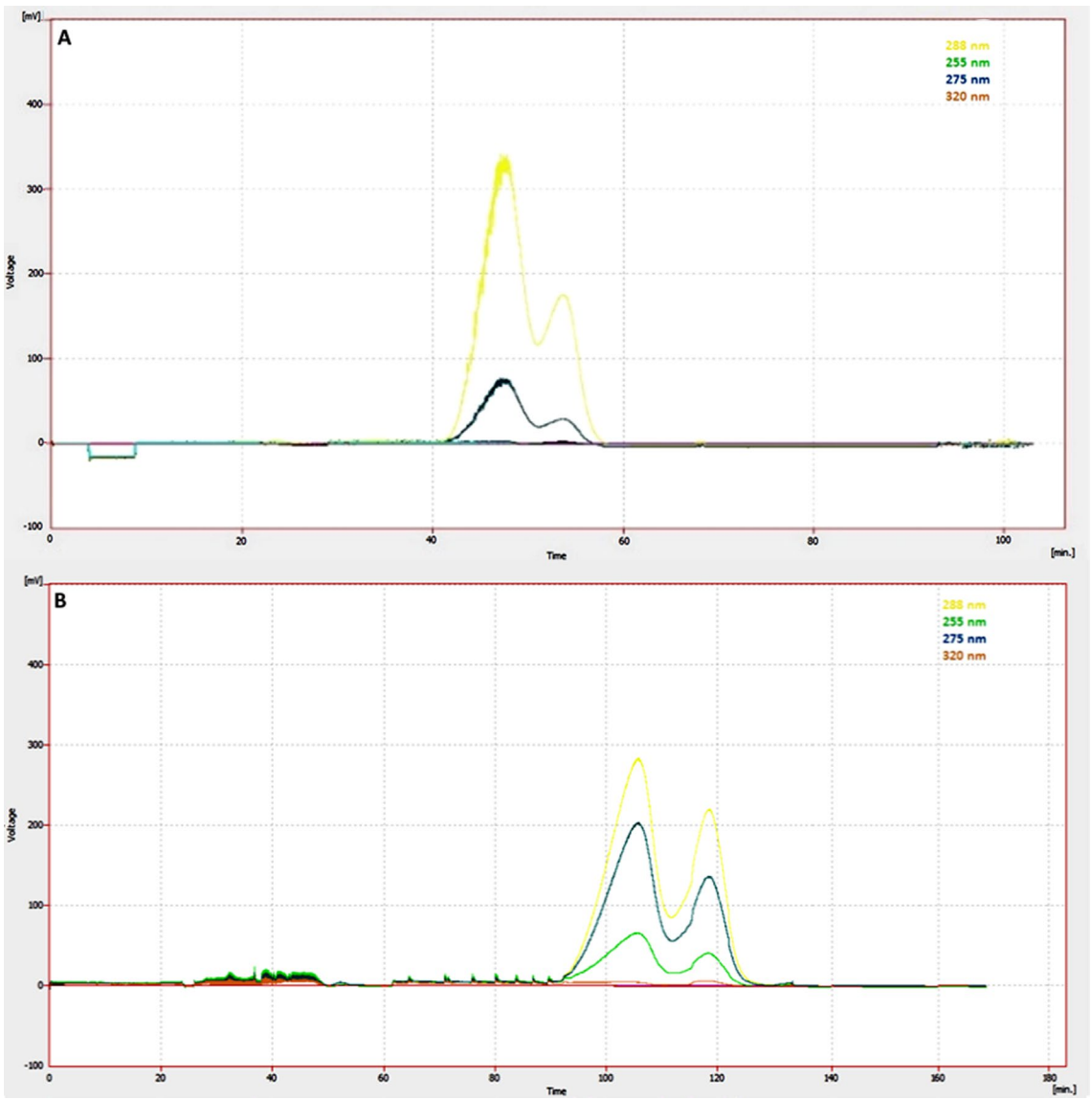

FIGURE 3 | UV Chromatogram (λ = 288, 275, 255, and 320 nm) of semi-preparative elution-extrusion CPC **(A)** in comparison to preparative elution-extrusion CPC **(B)**, indicating the better separation of the two main lignans during the scaling up from semi preparative to preparative mode. Biphasic solvent system: n-Hex/EtOAc/EtOH/H_2O in proportion 2:3:3:2 (v/v/v/v).

flow rate, two parameters that affect stationary phase retention (Fumat et al., 2016). After equilibrating the two phases into the column, 900 mg of SO extract was injected. The elution step of the experiment was completed after passing 1,600 ml of aqueous mobile phase in descending mode, and then the column was extruded by pumping 1,000 ml of the upper stationary phase also in descending mode. The CPC procedure was monitored with a UV detector, and the chromatogram (at 255, 275, 288, and 320 nm), presented in **Figure 3B**, shows a recovery of the target compounds according to their K_D values in the used biphasic system. By setting the rotational speed at 750 rpm and the flow rate of the eluent at 15 ml/min, the retention factor of stationary phase (Sf) was approx. 65%, much higher than Sf calculated for the semi-preparative CPC experiment (52.5%). Higher retention of the stationary phase led to higher theoretical plate number and thus in better fractionation of the extract. Indeed, the comparison of the CPC chromatograms obtained from semi-preparative and preparative analysis revealed that the preparative process resulted in better separation of the two major lignans (**Figure 3A, B**).

The preparative CPC process lasted 170 min while fraction collector was set to collect 20-ml fractions (total 130 fractions). All fractions were analyzed by TLC to check the quality of the separation. The analysis showed that the lignans were recovered during the elution step of the experiment while the fatty compounds were collected in the last fractions of the experiment during the extrusion of the column content. The fractions containing sesamin (fractions 51–64) and sesamolin (fractions 64–75) were subjected to quantitative HPLC analysis. The result of this analysis (presented as fractogram in **Figure 4**) showed that fractions 51 to 63 and 65 to 75 contain only sesamin and sesamolin, respectively, whereas only one fraction (64) contains a mixture of both compounds. Sesamin fractions were pooled and evaporated to dryness, yielding 276.07 mg, whereas the combined sesamolin fractions yielded 138.15 mg. The following UPLC-HRMS, NMR, and quantitative HPLC analysis of combined fractions showed that both sesamin and sesamolin were isolated in high purity (>95%) and good recovery (61.3% and 87.7% of the total amount of their SO extract content, respectively) verifying the efficient separation of these two bioactive compounds by using the proposed preparative elution–extrusion CPC method.

Except the isolation of the two major lignans, the preparative CPC analysis led to the additional separation of four minor lignans of SO extract, i.e., samin, sesamol, sesaminol, and episesaminol (**Figure 1**). In more details, fractions 13–18 (4.3 mg) samin, fractions 22–31 (9.4 mg) sesamol while fractions 35–39 (8.2 mg) and fractions 40–49 (6.6 mg) contained a mixture of sesaminol and episesaminol in ratios of approximately 85/15 and 45/55, respectively. It is important to note that samin and sesamol were recovered in one step separation procedure in high purity as this was determined by ^{1}H-NMR analysis (**Supplementary Figures 2–6**). The structure elucidation of the isolated compounds was achieved by studying HRMS/MS and NMR (1D and 2D) spectra and verified by comparison of the experimental data with the corresponding bibliographic data (Yamauchi et al., 2000; Dachtler et al., 2003; Kuo et al., 2011; Xia et al., 2016; Liu et al., 2018a; Liu et al., 2018b). Experimental data of ^{1}H and ^{13}C NMR of the isolated compounds are referred to at **Supplementary Table 6**.

Tyrosinase, Elastase, Collagenase, and Hyaluronidase Inhibition Activity of SO Compounds

All isolated lignans were evaluated for their tyrosinase, elastase, collagenase, and hyaluronidase inhibitory activities. For all the enzymatic assays, the IC50 of positive controls was used, with only exception being the hyaluronidase assay where the positive control was used at the IC100 concentration (see experimental part).

The tyrosinase inhibition assay showed that sesamol and sesamolin are able to inhibit the enzyme activity, in contrast to sesamin, samin, sesaminol, and episesaminol. In detail, sesamol exhibited an important inhibition activity at 500 μM (52.34%), while no activity was present at doses of 100 and 25 μM.

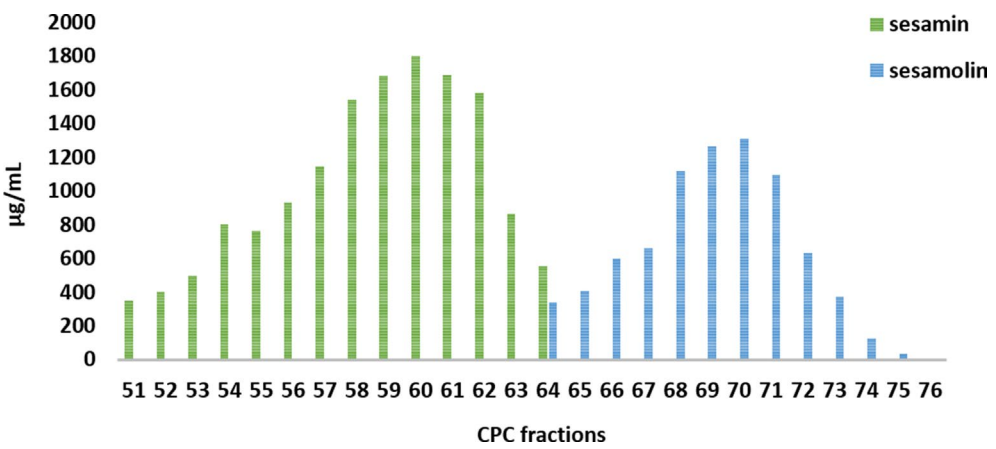

FIGURE 4 | Fractogram obtained from quantification analysis of preparative CPC fractions 51 to 76.

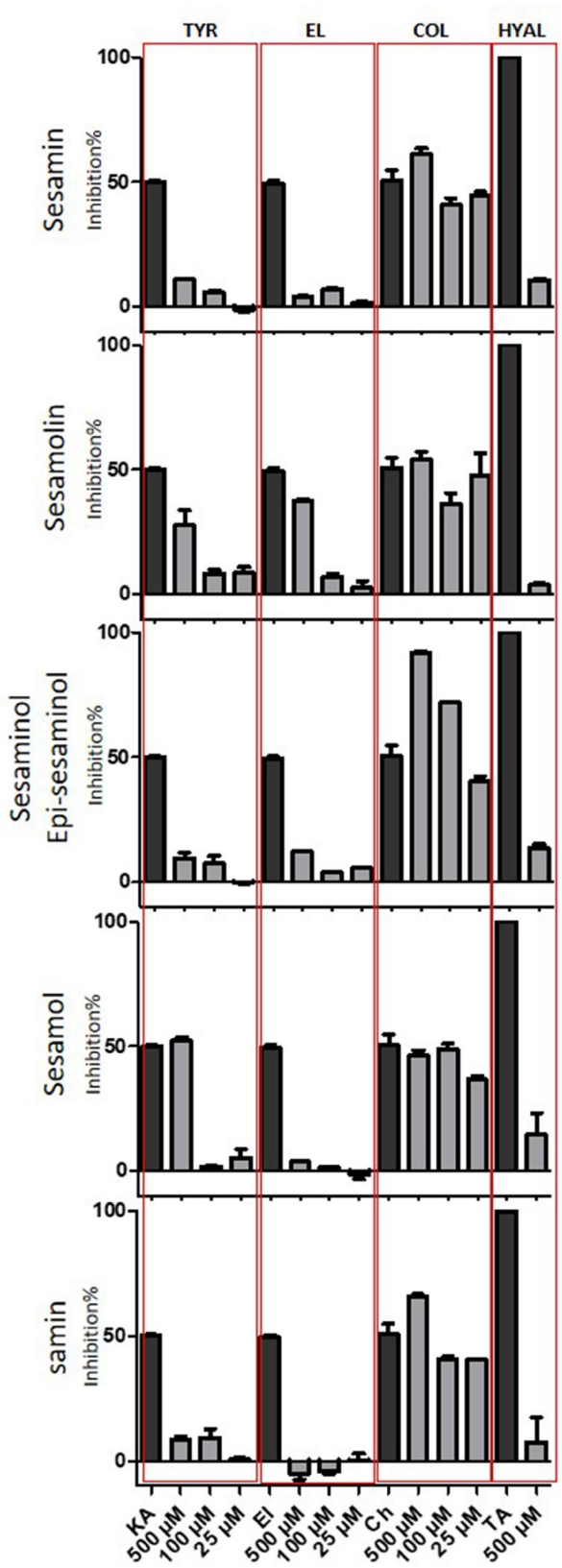

FIGURE 5 | Continued

FIGURE 5 | Tyrosinase, elastase, collagenase, and hyaluronidase inhibition activity of isolated compounds. Tested concentration for tyrosinase, elastase, and collagenase inhibition: 500, 100, and 25 μM. Tested concentration for hyaluronidase inhibition: 500 μM. Positive control for tyrosinase: Kojic acid (KA), Positive control for elastase: Elastatinal (El), Positive control for collagenase: Chlorexidine (Ch), Positive control for hyaluronidase: Tanic acid (TA).

Sesamolin presented moderate anti-tyrosinase activity at 500 μM (27.78%) and weak activity at 100 and 25 μM (**Figure 5**). These results are in agreement with literature data reporting the potent anti-tyrosinase activity of sesamol and sesamolin (Srisayam et al., 2017). The above results demonstrate a potent correlation between the structure of tested compounds and the anti-tyrosinase activity. Although sesamin, sesamolin, sesaminol, and episesaminol are structurally related compounds, only sesamolin inhibited the tyrosinase activity, showing that sesamol moiety seems necessary for the enzyme inhibition.

All tasted compounds expressed important activity on collagenase assay. The sesaminol/epi-sesaminol mixture revealed the highest anti-collagenase activity with inhibition values of 91.99% at 500 μM, 71.94% at 100 μM, and 40.36% at 25 μM. Sesamin presented moderate anti-collagenase activity with inhibition value of 61.16% at 500 μM, 40.77% at 100 μM, and 44.71% at 25 μM. Samin revealed anti-collagenase activity with inhibition values of 65.66% at 500 μM, 40.65% at 100 μM, and 40.33% at 25 μM. Sesamolin also presented moderate activity with inhibition value of 54.05% at 500 μM, 36.20% at 100 μM, and 47.83% at 25 μM, while sesamol revealed the lowest anti-collagenase activity with inhibition values of 46.19% at 500 μM, 48.20% at 100 μM, and 36.57% at 25 μM (**Figure 5**). To our knowledge, this is the first report connecting SO lignans with collagenase activity.

Regarding the elastase and hyaluronidase inhibition assays, all the tested compounds were found to be non-effective compared with the positive controls. The only exception was sesamolin, which presents a moderate anti-elastase activity at the highest dose of 500 μM with inhibition value of 37.24% (**Figure 5**).

CONCLUSION

This study constitutes a holistic procedure for the swift isolation of sesamin and sesamolin in high purity, using techniques with scale up to pilot and industrial prospects. Two different approaches were used for the extraction of SO lignans based on innovative liquid–liquid techniques, ACE and CPE, to obtain both sesamin and sesamolin in high amounts. However, CPE needs almost one third of solvent volume that was required from ACE to obtain the total extract. The green characteristic is not the only advantage of CPE. Also, this procedure is less time-consuming. CPC, as the superior liquid–liquid solid support-free technique, can treat the SO extract, giving high recovery of sesamin and sesamolin with purity over 95% with the minimum time consumption. The ability of CPC technique to analyze high portions of sample has as a result the isolation of other minor compounds from the SO extract in high purity.

Obtaining compounds in pure form permitted the realization of enzymatic assays. As a result, significant anti-collagenase activity was observed from all the isolated molecules.

DATA AVAILABILITY STATEMENT

All datasets (generated/analyzed) for this study are included in the manuscript and the supplementary files.

AUTHOR CONTRIBUTIONS

DM, AA and LS conceived and designed the experiments. DM and AA performed the phytochemical and analytical experiments and wrote the paper. DM and SM performed the biological experiments and analyzed the data. NA, SM, and LS critically revised the manuscript. All authors read and approved the final manuscript.

FUNDING

The research work was supported by the Hellenic Foundation for Research and Innovation (HFRI) and the General Secretariat for Research and Technology (GSRT), under the HFRI PhD Fellowship grant (GA. 14498). The present work was co-funded by the European Union (ERDF) and Greek national funds through the Operational Program "Competitiveness, Entrepreneurship and Innovation," under the call "STRENGTHENING RESEARCH AND INNOVATION INFRASTRUCTURES" (project code: 5002803).

This work has benefited from HAITOGLOU BROS S.A. with its kind offer of sesame oil.

SUPPLEMENTARY MATERIAL

The Supplementary Material for this article can be found online at: https://www.frontiersin.org/articles/10.3389/fphar.2019.00723/full#supplementary-material.

REFERENCES

Agalou, A., Thrapsianiotis, M., Angelis, A., Papakyriakou, A., Skaltsounis, A.-L., Aligiannis, N., et al. (2018). Identification of novel melanin synthesis inhibitors from Crataegus pycnoloba using an *in vivo* zebrafish phenotypic assay. *Front. Pharmacol.* 9, 265. doi: 10.3389/fphar.2018.00265

Angelis, A., Hamzaoui, M., Aligiannis, N., Nikou, T., Michailidis, D., Gerolimatos, P., et al. (2017). An integrated process for the recovery of high added-value compounds from olive oil using solid support free liquid–liquid extraction and chromatography techniques. *J. Chromatogr. A* 1491, 126–136. doi: 10.1016/j.chroma.2017.02.046

Angelis, A., Hubert, J., Aligiannis, N., Michalea, R., Abedini, A., Nuzillard, J. M., et al. (2016). Bio-guided isolation of methanol-soluble metabolites of common spruce (Picea abies) bark by-products and investigation of their dermo-cosmetic properties. *Molecules* 21, 1–15. doi: 10.3390/molecules21111586

Anilakumar, K. R., Pal, A., Khanum, F., and Bawa, A. S. (2010). Nutritional, medicinal and industrial uses of sesame (Sesamum indicum L). seeds—an overview. *Agric. Conspec. Sci.* 75, 159–168.

Barbosa, C. V., da, S., Silva, A. S., de Oliveira, C. V. C., Massa, N. M. L., de Sousa, Y. R. F., et al. (2017). Effects of sesame (Sesamum indicum L). Supplementation on creatine kinase, lactate dehydrogenase, oxidative stress markers, and aerobic capacity in semi-professional soccer players. *Front. Physiol.* 8, 196. doi: 10.3389/fphys.2017.00196

Berthod, A., Maryutina, T., Spivakov, B., Shpigun, O., and Sutherland, I. A. (2009). Countercurrent chromatography in analytical chemistry (IUPAC Technical Report). *Pure Appl. Chem.* 81, 355–387. doi: 10.1351/PAC-REP-08-06-05

Chung, B.-H., Lee, J. J., Kim, J.-D., Jeoung, D., Lee, H., Choe, J., et al. (2010). Angiogenic activity of sesamin through the activation of multiple signal pathways. *Biochem. Biophys. Res. Commun.* 391, 254–260. doi: 10.1016/j.bbrc.2009.11.045

Dachtler, M., Van De Put, F. H. M., Stijn, F. V., Beindorff, C. M., and Fritsche, J. (2003). On-line LC-NMR-MS characterization of sesame oil extracts and assessment of their antioxidant activity. *Eur. J. Lipid Sci. Technol.* 105, 488–496. doi: 10.1002/ejlt.200300835

Dar, A. A., and Arumugam, N. (2013). Lignans of sesame: purification methods, biological activities and biosynthesis—a review. *Bioorg. Chem.* 50, 1–10. doi: 10.1016/j.bioorg.2013.06.009

Dar, A. A., Verma, N. K., and Arumugam, N. (2015). An updated method for isolation, purification and characterization of clinically important antioxidant lignans—sesamin and sesamolin, from sesame oil. *Ind. Crops Prod.* 64, 201–208. doi: 10.1016/j.indcrop.2014.10.026

Dossa, K., Diouf, D., Wang, L., Wei, X., Zhang, Y., Niang, M., et al. (2017). The emerging oilseed crop Sesamum indicum enters the "Omics" Era. *Front. Plant Sci.* 8, 1154. doi: 10.3389/fpls.2017.01154

Duan, W., Song, C., Wu, Q., Zhou, X., and Zhou, J. (2005). Development and performance of a new annular centrifugal contactor for semi-industrial scale. *Sep. Sci. Technol.* 40, 1871–1883. doi: 10.1081/SS-200064531

Duan, W., Sun, T., and Wang, J. (2015). Separation of Nd3+ and Fe3+ by non-equilibrium solvent extraction using an annular centrifugal contactor. *Sep. Purif. Technol.* 146, 108–113. doi: 10.1016/j.seppur.2015.03.044

Food and Agriculture Organization of the United Nations (FAO) (2017). Production statistics—Crops, Crops Processed—knoema.com. Available at: https://knoema.com/FAOPRDSC2017/production-statistics-crops-crops-processed?tsId=1023090 [Accessed March 1, 2017].

Fumat, N., Berthod, A., and Faure, K. (2016). Effect of operating parameters on a centrifugal partition chromatography separation. *J. Chromatogr. A* 1474, 47–58. doi: 10.1016/j.chroma.2016.10.014

Goll, J., Audo, G., and Minceva, M. (2015). Comparison of twin-cell centrifugal partition chromatographic columns with different cell volume. *J. Chromatogr. A* 1406, 129–135. doi: 10.1016/j.chroma.2015.05.077

Grougnet, R., Magiatis, P., Laborie, H., Lazarou, D., Papadopoulos, A., and Skaltsounis, A.-L. (2012). Sesamolinol glucoside, disaminyl ether, and other lignans from sesame seeds. *J. Agric. Food Chem.* 60, 108–111. doi: 10.1021/jf2040687

Hammann, S., Englert, M., Müller, M., and Vetter, W. (2015). Accelerated separation of GC-amenable lipid classes in plant oils by countercurrent chromatography in the co-current mode. *Anal. Bioanal. Chem.* 407, 9019–9028. doi: 10.1007/s00216-015-9068-5

Hamzaoui, M., Hubert, J., Hadj-Salem, J., Richard, B., Harakat, D., Marchal, L., et al. (2011). Intensified extraction of ionized natural products by ion pair centrifugal partition extraction. *J. Chromatogr. A* 1218, 5254–5262. doi: 10.1016/j.chroma.2011.06.018

Jeon, J.-S., and Kim, C. Y. (2013). Preparative separation and purification of flavonoids and stilbenoids from Parthenocissus tricuspidata stems by dual-mode centrifugal partition chromatography. *Sep. Purif. Technol.* 105, 1–7. doi: 10.1016/j.seppur.2012.11.010

Jeon, J. S., Park, C. L., Syed, A. S., Kim, Y. M., Cho, I. J., and Kim, C. Y. (2016). Preparative separation of sesamin and sesamolin from defatted sesame meal *via* centrifugal partition chromatography with consecutive sample injection. *J. Chromatogr. B Analyt. Technol. Biomed. Life Sci.* 1011, 108–113. doi: 10.1016/j.jchromb.2015.12.062

Jing, X., Ning, P., Cao, H., Sun, Z., and Wang, J. (2017). Separation of V(V) and Cr(VI) in leaching solution using annular centrifugal contactors. *Chem. Eng. J.* 315, 373–381. doi: 10.1016/j.cej.2017.01.014

Kim, J. S., Seo, Y. C., No, R. H., and Lee, H. Y. (2013). Improved cosmetic activity by optimizing the Lithospermum erythrorhizon extraction process. *Cytotechnology* 67, 51–65. doi: 10.1007/s10616-013-9657-0

Kumar, G. M., Neelam, I., Ajitha, A., Uma, V., and Rao, M. (2014). Centrifugal partition chromatography: an overview. *Int. J. Pharm. Res. Anal.* 4, 353–360.

Kuo, P. C., Lin, M. C., Chen, G. F., Yiu, T. J., and Tzen, J. T. C. (2011). Identification of methanol-soluble compounds in sesame and evaluation of antioxidant potential of its lignans. *J. Agric. Food Chem.* 59, 3214–3219. doi: 10.1021/jf104311g

Lee, J., and Choe, E. (2006). Extraction of lignan compounds from roasted sesame oil and their effects on the autoxidation of methyl linoleate. *J. Food Sci.* 71, 430–436. doi: 10.1111/j.1750-3841.2006.00137.x

Liu, L., Li, Z., Chen, C., Li, H., Xu, L., and Yu, Z. (2018a). Efficient dealkylation of aryl alkyl ethers catalyzed by Cu2O. *Tetrahedron* 74, 2447–2453. doi: 10.1016/j.tet.2018.03.070

Liu, W. J., Chen, Y. J., Chen, D. N., Wu, Y. P., Gao, Y. J., Li, J., et al. (2018b). A new pair of enantiomeric lignans from the fruits of Morinda citrifolia and their absolute configuration. *Nat. Prod. Res.* 32, 933–938. doi: 10.1080/14786419.2017.1371163

Meikrantz, D. H., Macaluso, L. L., Flim, W. D., Heald, C. J., Mendoza, G., and Meikrantz, S. B. (2002). A new annular centrifugal contactor for pharmaceutical processes. *Chem. Eng. Commun.* 189, 1629–1639. doi: 10.1080/00986440214582

Michel, T., Destandau, E., Pecher, V., Renimel, I., Pasquier, L., André, P., et al. (2011). Two-step centrifugal partition chromatography (CPC) fractionation of Butea monosperma (Lam). biomarkers. *Sep. Purif. Technol.* 80, 32–37. doi: 10.1016/j.seppur.2011.04.002

Miyahara, Y., Hibasami, H., Katsuzaki, H., Imai, K., and Komiya, T. (2001). Sesamolin from sesame seed inhibits proliferation by inducing apoptosis in human lymphoid leukemia Molt 4B cells. *Int. J. Mol. Med.* 7, 369–371. doi: 10.3892/ijmm.7.4.369

Nakai, M., Harada, M., Nakahara, K., Akimoto, K., Shibata, H., Miki, W., et al. (2003). Novel antioxidative metabolites in rat liver with ingested sesamin. *J. Agric. Food Chem.* 51, 1666–1670. doi: 10.1021/jf0258961

Ning, Z., Wang, C., Liu, Y., Song, Z., Ma, X., Liang, D., et al. (2018). Integrating strategies of herbal metabolomics, network pharmacology, and experiment validation to investigate frankincense processing effects. *Front. Pharmacol.* 9, 1–18. doi: 10.3389/fphar.2018.01482

Obukowicz, M. G., Welsch, D. J., Salsgiver, W. J., Martin-Berger, C. L., Chinn, K. S., Duffin, K. L., et al. (1998). Novel, selective delta6 or delta5 fatty acid desaturase inhibitors as antiinflammatory agents in mice. *J. Pharmacol. Exp. Ther.* 287, 157–166. doi: 10.1007/BF02562269

Ohnmacht, S., Nava, P., West, R., Parker, R., and Atkinson, J. (2008). Inhibition of oxidative metabolism of tocopherols with ω-N-heterocyclic derivatives of vitamin E. *Bioorg. Med. Chem.* 141, 520–529. doi: 10.1016/j.bmc.2008.07.020

Park, S.-H., Ryu, S.-N., Bu, Y., Kim, H., Simon, J. E., and Kim, K.-S. (2010). Antioxidant components as potential neuroprotective agents in sesame (Sesamum indicum L). *Food Rev. Int.* 26, 103–121. doi: 10.1080/87559120903564464

Penalvo, J. L., Hopia, A., and Adlercreutz, H. (2006). Effect of sesamin on serum cholesterol and triglycerides levels in LDL receptor-deficient mice. *Eur. J. Nutr.* 45, 439–444. doi: 10.1007/s00394-006-0617-8

Reshma, M. V., Balachandran, C., Arumughan, C., Sunderasan, A., Sukumaran, D., Thomas, S., et al. (2010). Extraction, separation and characterisation of sesame oil lignan for nutraceutical applications. *Food Chem.* 120, 1041–1046. doi: 10.1016/j.foodchem.2009.11.047

Roullier, C., Chollet-Krugler, M., Bernard, A., and Boustie, J. (2009). Multiple dual-mode centrifugal partition chromatography as an efficient method for the purification of a mycosporine from a crude methanolic extract of Lichina pygmaea. *J. Chromatogr. B Analyt. Technol. Biomed. Life Sci.* 877, 2067–2073. doi: 10.1016/j.jchromb.2009.05.040

Sarkis, J. R., Michel, I., Tessaro, I. C., and Marczak, L. D. F. (2014). Optimization of phenolics extraction from sesame seed cake. *Sep. Purif. Technol.* 122, 506–514. doi: 10.1016/j.seppur.2013.11.036

Srisayam, M., Weerapreeyakul, N., and Kanokmedhakul, K. (2017). Inhibition of two stages of melanin synthesis by sesamol, sesamin and sesamolin. *Asian Pac. J. Trop. Biomed.* 7, 886–895. doi: 10.1016/j.apjtb.2017.09.013

Sutherland, I. A. (2007). Recent progress on the industrial scale-up of counter-current chromatography. *J. Chromatogr. A* 1151, 6–13. doi: 10.1016/j.chroma.2007.01.143

Tamhane, T. V., Joshi, J. B., and Patil, R. N. (2014). Performance of annular centrifugal extractors: CFD simulation of flow pattern, axial mixing and extraction with chemical reaction. *Chem. Eng. Sci.* 110, 134–143. doi: 10.1016/j.ces.2013.08.016

Toribio, A., Boudesocque, L., Richard, B., Nuzillard, J.-M., and Renault, J.-H. (2011). Preparative isolation of glucosinolates from various edible plants by strong ion-exchange centrifugal partition chromatography. *Sep. Purif. Technol.* 83, 15–22. doi: 10.1016/j.seppur.2011.07.001

Ungureanu, C., Marchal, L., Chirvase, A. A., and Foucault, A. (2013). Centrifugal partition extraction, a new method for direct metabolites recovery from culture broth: case study of torularhodin recovery from Rhodotorula rubra. *Bioresour. Technol.* 132, 406–409. doi: 10.1016/j.biortech.2012.11.105

Wang, X., Lin, Y., Geng, Y., Li, F., and Wang, D. (2009). Preparative separation and purification of sesamin and sesamolin from sesame seeds by high-speed counter—current chromatography. *Cereal Chem.* 86, 23–25. doi: 10.1094/CCHEM-86-1-0023

Wu, J. H. Y., Hodgson, J. M., Clarke, M. W., Indrawan, A. P., Barden, A. E., Puddey, I. B., et al. (2009). Inhibition of 20-hydroxyeicosatetraenoic acid synthesis using specific plant lignans: in vitro and human studies. *Hypertension* 54, 1151–1158. doi: 10.1161/HYPERTENSIONAHA.109.139352

Xia, S., Gan, L., Wang, K., Li, Z., and Ma, D. (2016). Copper-catalyzed hydroxylation of (hetero)aryl halides under mild conditions. *J. Am. Chem. Soc.* 138, 13493–13496. doi: 10.1021/jacs.6b08114

Xu, J.-Q., Duan, W.-H., Zhou, X.-Z., and Zhou, J.-Z. (2006). Extraction of phenol in wastewater with annular centrifugal contactors. *J. Hazard. Mater.* 131, 98–102. doi: 10.1016/j.jhazmat.2005.09.011

Yamauchi, S., Yamamoto, N., and Kinoshita, Y. (2000). Stereoselective synthesis of the optically active samin type of lignan from l-glutamic acid. *Biosci. Biotechnol. Biochem.* 64, 878–881. doi: 10.1271/bbb.64.878

Zhang, H., Miao, H., Wang, L., Qu, L., Liu, H., Wang, Q., et al. (2013). Genome sequencing of the important oilseed crop Sesamum indicum L. *Genome Biol.* 14, 1–9. doi: 10.1186/gb-2013-14-1-401

Conflict of Interest Statement: The authors declare that the research was conducted in the absence of any commercial or financial relationships that could be construed as a potential conflict of interest.

frontiers in Pharmacology

ORIGINAL RESEARCH
published: 07 February 2020
doi: 10.3389/fphar.2020.00037

Lignans: Quantitative Analysis of the Research Literature

Andy Wai Kan Yeung[1], Nikolay T. Tzvetkov[2,3], Aneliya A. Balacheva[2], Maya G. Georgieva[2], Ren-You Gan[4], Artur Jozwik[5], Bożena Pyzel[5], Jarosław O. Horbańczuk[5], Ettore Novellino[6], Alessandra Durazzo[7]*, Massimo Lucarini[7], Emanuela Camilli[7], Eliana B. Souto[8,9], Atanas G. Atanasov[5,10,11,12]* and Antonello Santini[6]**

[1] Oral and Maxillofacial Radiology, Applied Oral Sciences and Community Dental Care, Faculty of Dentistry, The University of Hong Kong, Hong Kong, China, [2] Department of Biochemical Pharmacology and Drug Design, Institute of Molecular Biology "Roumen Tsanev", Bulgarian Academy of Sciences, Sofia, Bulgaria, [3] Pharmaceutical Institute, University of Bonn, Bonn, Germany, [4] Institute of Urban Agriculture, Chinese Academy of Agricultural Sciences, Chengdu, China, [5] The Institute of Genetics and Animal Breeding, Polish Academy of Sciences, Magdalenka, Poland, [6] Department of Pharmacy, University of Napoli Federico II, Napoli, Italy, [7] CREA-Research Centre for Food and Nutrition, Rome, Italy, [8] Department of Pharmaceutical Technology, Faculty of Pharmacy, University of Coimbra (FFUC), Polo das Ciências da Saúde, Azinhaga de Santa Comba, Coimbra, Portugal, [9] CEB-Centre of Biological Engineering, University of Minho, Campus de Gualtar, Braga, Portugal, [10] Institute of Neurobiology, Bulgarian Academy of Sciences, Sofia, Bulgaria, [11] Department of Pharmacognosy, University of Vienna, Vienna, Austria, [12] Ludwig Boltzmann Institute for Digital Health and Patient Safety, Medical University of Vienna, Spitalgasse, Vienna, Austria

The current study provides a comprehensive overview and analysis of the lignan literature. Data for the current study were extracted from the electronic Web of Science Core Collection database *via* the search string TOPIC = ("lignan*") and processed by the VOSviewer software. The search yielded 10,742 publications. The ratio of original articles to reviews was 14.6:1. Over 80% of the analyzed papers have been published since the year 2000 and nearly 50% since the year 2010. Many of the publications were focused on pharmacology, chemistry, and plant sciences. The United States and Asian countries, such as China, Japan, South Korea, and India, were the most productive producers of lignan publications. Among the 5 most productive institutions was the University of Helsinki in Finland, the country that ranked 9th. Nineteen journals collectively published 3,607 lignan publications and were considered as core journals. Their impact factor did not correlate with the proportion of uncited papers. Highly cited publications usually mentioned phytoestrogen, isoflavone, daidzein, enterodiol, enterolactone, equol, genistein, and isoflavonoid. Cancer (e.g., breast cancer), cardiovascular disease, and antioxidation were the major themes. Clinical trials were estimated to contribute to 0.2–1.1% of the analyzed body of literature, so more of them should be conducted in the future to substantiate the beneficial effects and optimal dose of lignan intake in humans. Moreover, researchers can refer to these findings for future research directions and collaborations.

Keywords: lignans, pharmacology, chemistry, plant science, cancer, citation analysis, VOSviewer, Web of Science

OPEN ACCESS

Edited by:
Alexander N. Shikov, Saint-Petersburg State Chemical Pharmaceutical Academy, Russia

Reviewed by:
Heikki Vuorela, University of Helsinki, Finland
Claire Elizabeth Robertson, University of Westminster, United Kingdom

****Correspondence:***
Andy Wai Kan Yeung
ndyeung@hku.hk
Alessandra Durazzo
alessandra.durazzo@crea.gov.it
Atanas G. Atanasov
atanas.atanasov@univie.ac.at
Antonello Santini
asantini@unina.it

Specialty section:
This article was submitted to Ethnopharmacology, a section of the journal Frontiers in Pharmacology

Received: *23 August 2019*
Accepted: *14 January 2020*
Published: *07 February 2020*

Citation:
Yeung AWK, Tzvetkov NT, Balacheva AA, Georgieva MG, Gan R-Y, Jozwik A, Pyzel B, Horbańczuk JO, Novellino E, Durazzo A, Lucarini M, Camilli E, Souto EB, Atanasov AG and Santini A (2020) Lignans: Quantitative Analysis of the Research Literature. Front. Pharmacol. 11:37. doi: 10.3389/fphar.2020.00037

INTRODUCTION

The current study aimed to perform a quantitative analysis on the literature of lignans to unveil the major contributors in terms of institutions, countries/regions, and journals. By analyzing the publication and citation data, the major research themes present in the lignan literature were identified and further discussed.

Lignans are 1,4-diarylbutan compounds derived from the shikimic acid biosynthetic pathway (Lewis and Davin, 1999; Imai et al., 2006). In the 1970s, it was still commonly believed that lignans were synthesized in plants only (Hartwell, 1976). It was only in the 1980s when scientists identified lignans produced by microbes living in humans and animals (Axelson et al., 1982). Geographically, the intakes are greater in the European population relative to the Asian population (Bhakta et al., 2006). The main common dietary lignans are secoisolariciresinol, lariciresinol, matairesinol, pinoresinol, medioresinol, and syringaresinol (Durazzo et al., 2018); the range of components is very wide and efforts on isolation of new compounds are being carried out (Eklund and Raitanen, 2019; Xiao et al., 2019). Plant lignans are metabolized to enterodiol and enterolactone, called enterolignans or mammalian lignans (Landete, 2012).

The recent work of Durazzo et al. (2018) well summarized the occurrence of lignans in food groups and existing lignan databases at European level. As reported by Durazzo et al. (2018), the main sources of dietary lignans are oilseeds such as flax, soy, rapeseed, and sesame; whole-grain cereals such as wheat, oats, rye, and barley; legumes; various vegetables and fruits (particularly berries); beverages (i.e., coffee, tea, and wine); and, recently, lignans are also determined in dairy products, meat, and fish (Valsta et al., 2003; Milder et al., 2005a; Milder et al., 2005b; Peñalvo et al., 2005; Thompson et al., 2006; Penalvo et al., 2007; Kuhnle et al., 2008a; Kuhnle et al., 2008b; Durazzo et al., 2009; Kuhnle et al., 2009a; Kuhnle et al., 2009b; Smeds et al., 2009; Moreno-Franco et al., 2011; Smeds et al., 2012; Durazzo et al., 2013a; Durazzo et al., 2013b; Mulligan et al., 2013; Durazzo et al., 2014b; Turfani et al., 2017; Angeloni et al., 2018; Angeloni et al., 2019).

Within the bioactive compounds realm (Santini et al., 2018; Santini and Novellino, 2018; Daliu et al., 2019; Durazzo et al., 2019), the class of lignans is of interest for their potential biological activities, i.e., estrogenic and antiestrogenic, antioxidant, anti-inflammatory, metabolism-modulating, anti-proliferative, and anticancerogenic properties (Baumgartner et al., 2011; Teponno et al., 2016; Wang et al., 2016; Linder et al., 2019; Zálešák et al., 2019). Moreover, it is worth mentioning that the spectrum of biological activities attributed to lignans is being enlarged, i.e., related to newly discovered compounds belonged to this group (Zhang et al., 2014; Gnabre et al., 2015; Su and Wink, 2015; Hongthong et al., 2016; Azam et al., 2019; Zhuang et al., 2019).

Several studies showed that consumption of lignan-rich diets, which contain vegetables, fruits, and whole grain products, may protect against chronic diseases, particularly hormone-dependent cancer and cardiovascular diseases (Ward et al., 2009; Peterson et al., 2010; Buck et al., 2011; Guglielmini et al., 2012; Penalvo and López-Romero, 2012; Zamora-Ros et al., 2012; Lowcock et al., 2013; Durazzo et al., 2014a; Rodríguez-García et al., 2019). Proper evaluation of adherence, efficacy, and communication aspects should be taken into account as well as the retrospective analysis of databases as per recent studies in the field (Iolascon et al., 2016; Scala et al., 2016; Guerriero et al., 2017; Menditto et al., 2018).

The overview presented in the current study should be helpful to readers in better understanding the lignan research community, identifying potential research directions and collaboration partners, and conducting more in-depth literature searches of chemicals/chemical classes of interest.

MATERIALS AND METHODS

In July 2019, we queried the Web of Science (WoS) Core Collection online database, owned by Clarivate Analytics, to identify lignan publications with the following search string: TOPIC = ("lignan*"). This search identified publications mentioning the word "lignan" or its derivatives in the title, abstract, or keywords. No additional filters were placed on the search.

Data Extraction

Several aspects of each publication identified from the search were recorded, namely: (1) publication year; (2) institutions; (3) countries/regions of the institutions; (4) journal title; (5) WoS journal category; (6) type of publication; (7) language; and (8) number of total citations received. By using the "Export Records to File" function of WoS, full records and cited references of the identified publications were exported as "tab-delimited text files" to VOSviewer for additional processing.

The VOSviewer software (v.1.6.11, 2019) was used to analyze the titles and abstracts of publications, by breaking down the paragraphs into words and phrases, associating them with the citation data of the publications, and presenting the results in the form of a bubble map (Van Eck and Waltman, 2009). Default parameters were used for the analyses and visualizations. The size of a bubble represents the frequency of appearance of a term (multiple appearances of a word counted once, single use of the same word in a paper equally weighted). Two bubbles are positioned more closely to each other if the terms co-appeared more often in the analyzed publications. The color represents the averaged citations per publication (CPP). To simplify the bubble map, we analyzed and visualized words that appeared in at least 1% (n = 108) of the publications.

Apart from analyzing the whole dataset, we additionally probed into the articles published by the most prolific journals to see how many of them were uncited. According to Bradford's law of scattering, the core journals for a body of literature are defined as the prolific journals that collectively published 1/3 of the papers (Vickery, 1948). Using the current analyzed dataset, we tested if the core journals had their impact factor negatively correlated to the proportion of uncited papers, which was previously demonstrated in another field (Yeung, 2019). Pearson's correlation test was performed using SPSS 25.0 (IBM, New York, USA). Test results were significant if $p < 0.05$.

RESULTS

The literature search resulted in 10,742 publications. The earliest publications on lignans indexed in WoS were published in 1970, which isolated new lignans at that time and identified their structures (Corrie et al., 1970). Over 80% of the analyzed papers have been published since the year 2000, and nearly 50% since the year 2010. The numbers of original articles (n = 9,422) and reviews (n = 644) were in the ratio of 14.6:1. Reviews were more cited (CPP = 56.8) than original articles (CPP = 22.5). The majority of the publications were written in English (n = 10,483; 97.6%). Contributions came from 4,748 institutions located in 141 countries/regions and were published in 1,509 journals. The top five contributors with regard to WoS category, journal, institution, and country/region are listed in **Table 1**. It is worth mentioning that *Molecules* was the 6th most productive journal, with 208 lignan publications (1.9%) and CPP of 11.9. Nineteen journals collectively published 3,607 lignan publications and were considered as core journals (**Table 2**). Their impact factor did not correlate with the proportion of uncited papers (r = -0.257, p = 0.289). Though University of Helsinki was among the top 5 most productive institutions, Finland was ranked 9th in terms of countries/regions (n = 437, 4.1%). The 5 most productive countries were all from Asia, except the United States.

There were 311 terms that appeared in at least 1% (n = 108) of the 10,742 lignan publications (**Figure 1**). The highly cited publications usually mentioned phytoestrogen (4.3%, n = 463, CPP = 64.6), isoflavone (3.6%, n = 391, CPP = 64.9), or related terms such as daidzein (2.3%, n = 243, CPP = 84.1), enterodiol (2.6%, n = 280, CPP = 51.4), enterolactone (4.6%, n = 496, CPP = 48.0), equol (1.5%, n = 158, CPP = 82.3), genistein (2.4%, n = 260, CPP = 84.2), and isoflavonoid (1.2%, n = 134, CPP = 99.8). These terms were often mentioned together with cancer (6.1%, n = 655, CPP = 51.8), breast cancer (2.2%, n = 237, CPP = 51.8), or cardiovascular disease (1.5%, n = 157, CPP = 61.9). Some of the main common dietary lignans were frequently mentioned, such as lariciresinol (1.4%, n = 147; CPP = 27.3), matairesinol (2.5%, n = 264; CPP = 44.1), pinoresinol (3.4%, n = 368; CPP = 30.1), secoisolariciresinol (2.6%, n = 279; CPP = 36.9), syringaresinol (1.4%, n = 146; CPP = 23.1). The structures of these chemicals are shown in **Figure 2**. The top 20 recurring terms are listed in **Table 3**.

The keywords listed by authors and WoS (KeyWords Plus) were collectively analyzed. There were 88 keywords that appeared in at least 1% (n = 108) of the lignan publications, and the 20 most common ones are listed in **Table 4**. The keywords suggested that antioxidation (4.3%) and apoptosis (3.2%) were two frequently investigated themes, and that *in vitro* (5.0%) studies were prevalent.

To analyze the temporal changes in the keywords, we separately assessed lignan publications in three time periods: 1990s and before, 2000s, and 2010s. The top 20 recurring keywords for each of the three periods are listed in **Table 5**. Antioxidant activity rose to popularity since the 2000s. Apoptosis, cytotoxicity, and oxidative stress became popular in the 2010s.

TABLE 1 | The top five contributors in terms of Web of Science category, journal, institution, and country/region of publications concerning lignans.

Contributor	Publication count (% of total)	Citation per manuscript
Web of Science category		
Pharmacology pharmacy	2,522 (23.5%)	20.5
Chemistry medicinal	2,520 (23.5%)	18.9
Plant sciences	2,050 (19.1%)	22.9
Biochemistry molecular biology	1,796 (16.7%)	24.8
Chemistry multidisciplinary	1,509 (14.0%)	16.3
Journal		
Phytochemistry	587 (5.5%)	31
Journal of Natural Products	345 (3.2%)	27.1
Planta Medica	332 (3.1%)	18.9
Chemical and Pharmaceutical Bulletin	266 (2.5%)	28.4
Journal of Agricultural and Food Chemistry	213 (2.0%)	54.5
Organization		
Chinese Academy of Sciences	473 (4.4%)	13.8
University of Helsinki	246 (2.3%)	81.9
Chinese Academy of Medical Sciences Peking Union Medical College	195 (1.8%)	14.0
Kunming Institute of Botany	193 (1.8%)	12.9
Universidade de Sao Paulo	186 (1.7%)	18.1
Country/Territory		
China	2,482 (23.1%)	13.0
United States	1,321 (12.3%)	41.2
Japan	1,305 (12.1%)	24.5
South Korea	691 (6.4%)	15.5
India	638 (5.9%)	16.5

TABLE 2 | Core journals publishing lignan papers.

Journal	Impact factor	Proportion of uncited lignan papers (in %)
Phytochemistry	2.905	1.5
Journal of Natural Products	4.257	1.4
Planta Medica	2.746	17.8
Chemical & Pharmaceutical Bulletin	1.405	0.8
Journal of Agricultural and Food Chemistry	3.571	3.8
Molecules	3.060	15.9
Tetrahedron Letters	2.259	1.1
Tetrahedron	2.379	1.8
Natural Product Research	1.999	13.7
Journal of Organic Chemistry	4.745	3.4
Fitoterapia	2.431	13.4
Biochemical Systematics and Ecology	1.127	12.1
Journal of Ethnopharmacology	3.414	2.5
Journal of Asian Natural Products Research	1.170	7.1
Bioorganic & Medicinal Chemistry Letters	2.448	2.8
Food Chemistry	5.399	4.8
Phytochemistry Letters	1.338	15.8
Bioscience, Biotechnology, and Biochemistry	1.297	3.2
Archives of Pharmacal Research	2.458	5.4

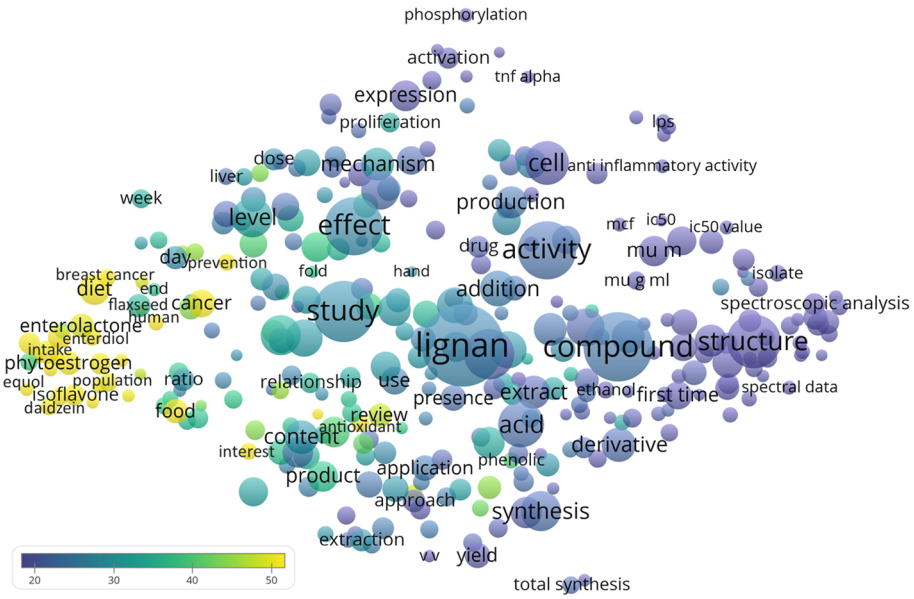

FIGURE 1 | Bubble map visualizing words from titles and abstracts of the 10,742 lignan publications. VOSviewer software was used to evaluate the recurring terms. Only the 311 terms that appeared in at least 1% (n = 108) of the publications were analyzed and visualized. The size of a bubble represents the frequency of appearance of a term (multiple appearances within one publication were treated as one appearance). Two bubbles are positioned more closely to each other if the terms co-appeared more often. The color represents the averaged citations per publication.

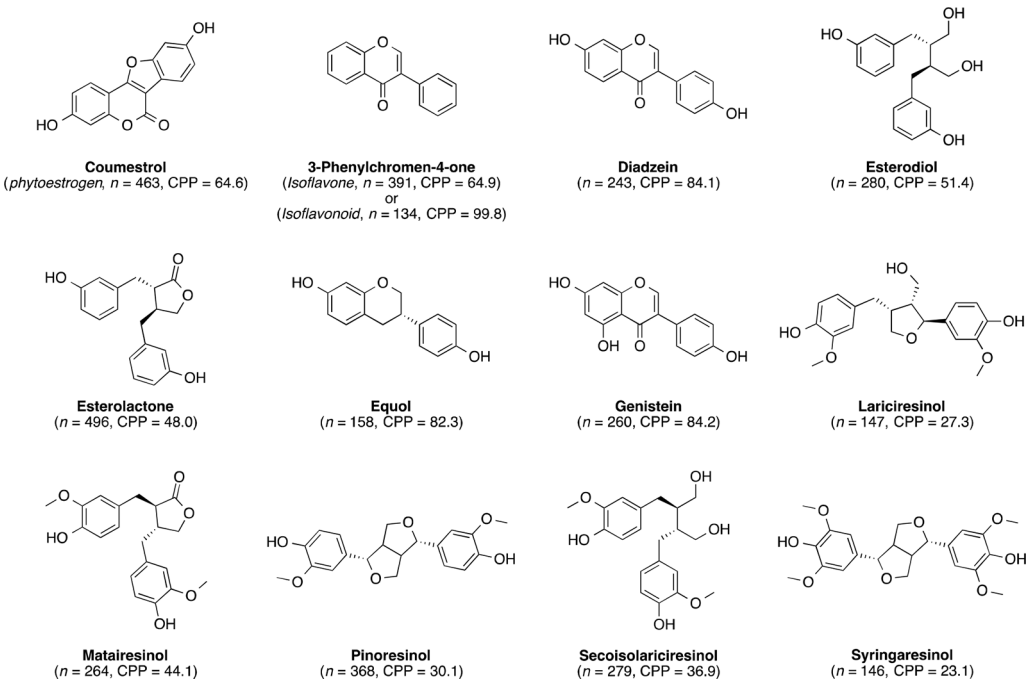

FIGURE 2 | Chemical structures of key single phytochemicals or representatives of chemical classes that were often discussed in the evaluated lignan publications. In parentheses are the cited compound classes (*italic*), number of publications (*n*), and citations per publication (CPP) for each chemical or representative chemical class.

TABLE 3 | The top 20 recurring terms from titles and abstracts.

Term	Appearance (% of 10,742 publications)
Lignan	5,700 (53.1%)
Compound	3,995 (37.2%)
Study	3,120 (29.0%)
Effect	2,878 (26.8%)
Activity	2,843 (26.5%)
Structure	2,443 (22.7%)
Analysis	2,121 (19.7%)
Acid	1,768 (16.5%)
Cell	1,629 (15.2%)
Level	1,367 (12.7%)
Concentration	1,365 (12.7%)
Synthesis	1,347 (12.5%)
Treatment	1,217 (11.3%)
Value	1,197 (11.1%)
Group	1,186 (11.0%)
Plant	1,144 (10.6%)
Addition	1,085 (10.1%)
Data	1,065 (9.9%)
Derivative	974 (9.1%)
Content	949 (8.8%)

TABLE 4 | The top 20 recurring keywords.

Keyword	Occurrence (% of 10,742 publications)
Lignans	3,825 (35.6%)
Lignan	1,358 (12.6%)
Constituents	1,217 (11.3%)
Derivatives	536 (5.0%)
Neolignans	536 (5.0%)
In-vitro	535 (5.0%)
Flavonoids	509 (4.7%)
Phytoestrogens	488 (4.5%)
Antioxidant activity	458 (4.3%)
Identification	438 (4.1%)
Cells	435 (4.0%)
Leaves	433 (4.0%)
Antioxidant	399 (3.7%)
Glycosides	388 (3.6%)
Flaxseed	383 (3.6%)
Inhibition	366 (3.4%)
Enterolactone	347 (3.2%)
Apoptosis	345 (3.2%)
Acid	344 (3.2%)
Expression	334 (3.1%)

DISCUSSION

The current literature analysis on lignan publications revealed the large publication shares from Asian countries, which were consistent with related bodies of literature such as antioxidants and curcumin (Yeung et al., 2019b; Yeung et al., 2019c). Examples of some highly cited original research papers recently published by Asian teams in the 2010s, without international collaborations, are discussed here. For instance, a Chinese paper reported results from sesame transcriptomes that provide useful information for understanding the relevant lignan biosynthesis molecular mechanism (Wei et al., 2011). Another Chinese team tested the effects of new lignans and neolignans on inhibiting nitric oxide production in mouse macrophages and against serum deprivation-induced PC12 cell damage (Xiong et al., 2011). These papers received over 100 citations. Meanwhile, Korean teams published the anti-inflammatory effects of several lignans isolated from *Schiandra chinensis* (Oh et al., 2010), and the hepatoprotective effect of pinoresinol isolated from *Forsythiae Fructus* (Kim et al., 2010). These papers were cited over 50 times. In Japan, a randomized controlled trial was conducted, and results found that oral intake of flaxseed (*Linum usitatissimum* L.) lignan could lower blood cholesterol level and risk of hepatic diseases in hypercholesterolemic men (Fukumitsu et al., 2010). Another Japanese team described an efficient synthetic route to synthesize herbindoles as naturally occurring forms (Saito et al., 2012). In India, researchers extracted, separated, and characterized sesame oil lignan (Reshma et al., 2010) and reported a phylogenetic analysis of *L. usitatissimum* L. (Barvkar et al., 2012). These Japanese and Indian papers had around 40 citations each. All these examples demonstrate the variety of the lignan research field, which ranged from basic sciences to human clinical trials.

Similar to the related research fields of berries, dietary natural products, and functional foods (Yeung et al., 2018a; Yeung et al., 2018b; Yeung et al., 2019d), the bubble map suggested that cancer and cardiovascular diseases were highly cited topics for lignan research. Readers can refer to comprehensive reviews on the relationship between phytoestrogens (such as lignans and isoflavonoids) and Western diseases (such as breast cancer and coronary heart disease) (Adlercreutz and Mazur, 1997; Rietjens et al., 2017). Their modulatory effects on steroid biosynthetic enzymes, hormone concentrations, and cellular events seem to be beneficial against cancer development (Adlercreutz and Mazur, 1997; Rietjens et al., 2017). In the early 1990s, a Finnish-Japanese collaboration probed into the low mortality in hormone-dependent cancer among the Japanese and found that they had high intake of soybean products rich in phytoestrogens, as demonstrated by a high concentration of isoflavonoids (and lignans to a lesser extent) excreted in their urine (Adlercreutz et al., 1991). In the year 1997, a case-control study published in *Lancet* reported that a high intake of phytoestrogens particularly lignan enterolactone and isoflavone equol could substantially reduce breast cancer risk in women (Ingram et al., 1997). Later, another paper reviewed data on existing epidemiologic studies and suggested that lignans and flavonoids have beneficial effects on cardiovascular diseases and lung cancer, but not other cancers (Arts and Hollman, 2005). The issues of low bioavailability might partly explain the differences in the results obtained between studies using cell/animal models and humans, particularly for the anti-cancer effects (Yang et al., 2001).

In addition, the bubble map can also relate to some of the potential biological activities of lignans, e.g., estrogenic and antiestrogenic, antioxidant, anti-inflammatory, and anticancerogenic properties (Baumgartner et al., 2011; Teponno et al., 2016; Wang et al., 2016; Linder et al., 2019; Zálešák et al.,

TABLE 5 | The top 20 recurring keywords in each decade.

1990s and before	Occurrence (% of 2,144)	2000s	Occurrence (% of 3,312)	2010s	Occurrence (% of 5,295)
Lignans	593 (27.7)	Lignans	1,304 (39.4)	Lignans	1,928 (36.4)
Lignan	192 (9.0)	Lignan	467 (14.1)	Constituents	708 (13.4)
Constituents	148 (6.9)	Constituents	361 (10.9)	Lignan	699 (13.2)
Neolignans	108 (5.0)	Phytoestrogens	254 (7.7)	In-vitro	366 (6.9)
Phytoestrogens	96 (4.5)	Neolignans	180 (5.4)	Flavonoids	324 (6.1)
Genistein	86 (4.0)	Derivatives	179 (5.4)	Antioxidant activity	313 (5.9)
Breast-cancer	60 (2.8)	Enterolactone	157 (4.7)	Antioxidant	307 (5.8)
Derivatives	60 (2.8)	Flaxseed	152 (4.6)	Cells	298 (5.6)
Identification	57 (2.7)	In-vitro	143 (4.3)	Derivatives	297 (5.6)
Cancer	50 (2.3)	Antioxidant activity	140 (4.2)	Leaves	295 (5.6)
Women	48 (2.2)	Flavonoids	138 (4.2)	Apoptosis	272 (5.1)
Chemistry	47 (2.2)	Phyto-estrogens	132 (4.0)	Identification	266 (5.0)
Flavonoids	47 (2.2)	Breast-cancer	127 (3.8)	Expression	253 (4.8)
Bark	46 (2.1)	Inhibition	119 (3.6)	Glycosides	252 (4.8)
Acid	45 (2.1)	Metabolism	119 (3.6)	Neolignans	248 (4.7)
Inhibition	44 (2.1)	Identification	115 (3.5)	Phenolic-compounds	210 (4.0)
Podophyllotoxin	44 (2.1)	Acid	114 (3.4)	Oxidative stress	209 (3.9)
Diet	42 (2.0)	Mammalian lignans	114 (3.4)	Flaxseed	203 (3.8)
Estrogens	42 (2.0)	Cells	113 (3.4)	Inhibition	203 (3.8)
Route	42 (2.0)	Podophyllotoxin	113 (3.4)	Cytotoxicity	194 (3.7)

2019), especially with antioxidant and anti-inflammatory activity being identified as frequently mentioned terms, whereas they were strong interests in phytoestrogen and cancer.

By limiting to "articles" (excluding other publication types such as reviews), a quick query of "clinical trial*" within the analyzed body of literature returned with 50 hits only. After evaluation, we found that there were only 19 randomized clinical trials, which was equivalent to 0.2% of the 10,742 lignan publications. A follow-up search in PubMed database with a query of "lignan*" and limited article type to "Clinical Trial" returned with 121 hits, which was equivalent to 1.1% of the analyzed publications. With such a small ratio of clinical trials in the lignan research literature, we believe that more clinical trials should be conducted to substantiate the beneficial effects and optimal dose of lignan intake on humans. In addition, researchers are currently experiencing common difficulties in estimating the dietary intakes of lignans (and also other non-nutritive substances) because they are not routinely included in the food composition tables, and there exists variability in contents reactive to soil quality, sun exposure, etc. All these complicate the works concerning the dose of lignan intake.

This study inherited some limitations, such as using indexed data based on a single database (WoS). Furthermore, the latest research trends, if any, might remain undetected due to a lack of time to accumulate publication and citation counts. Similar to previous literature analyses on curcumin and resveratrol (Yeung et al., 2019a; Yeung et al., 2019b), we did not analyze the authorship of the lignan publications, as there existed many Chinese authors with similar initials that caused inaccurate counting. Analyzing authorship by authors' full names was also not practical, as many publication records listed author initials only. Moreover, the analysis cannot evaluate the scientific methods used to determine the research findings (e.g., distinguish between *in vivo* work used to determine mechanistic relationships at a molecular level, and disease associations elucidated from population research). For an analysis of over 10,000 publications, this requires additional automatic labeling of the documents (data tagging), which is currently very limited in the literature databases. For Web of Science, for example, there are only a few publication types, e.g., articles, reviews, editorials. Besides, lignan sub-types and method of action in metabolizers are not analyzed.

Overall, the current report identified the terms and themes in the lignan research literature, being important in terms of publication and citation data. Results revealed several recurring or highly cited themes, implying that the bibliometric analysis was able to quantitatively highlight the topics in the field deemed important by the field experts.

CONCLUSIONS

To summarize, a bibliometric analysis was conducted to evaluate publications on lignans. The current findings revealed that the United States and Asian countries, such as China, Japan, South Korea, and India, were the most productive countries. Some productive institutions were based outside these countries, such as the University of Helsinki in Finland. Many of the publications were focused on pharmacology (23.5%), chemistry (23.5%), and plant sciences (19.1%). Over 80% of the analyzed papers have been published since year 2000, and nearly 50% since year 2010. The highly cited publications usually mentioned specific terms such as phytoestrogen, isoflavone, daidzein, enterodiol, enterolactone, equol, genistein, isoflavonoid, cancer, breast cancer, or cardiovascular disease. Some frequently mentioned and discussed main common dietary lignans were

lariciresinol, matairesinol, pinoresinol, secoisolariciresinol, and syringaresinol.

DATA AVAILABILITY STATEMENT

The datasets generated for this study are available on request to the corresponding authors.

AUTHOR CONTRIBUTIONS

AY, AD, AA, and AS conceived the work, performed data collection and analysis, and drafted the manuscript. All authors critically revised the manuscript and approved the submission of the manuscript.

FUNDING

AA acknowledges the support by the Polish KNOW (Leading National Research Centre) Scientific Consortium "Healthy Animal—Safe Food," decision of the Ministry of Science and Higher Education No. 05-1/KNOW2/2015. EN and AS acknowledge the support of the research project Nutraceutica come supporto nutrizionale nel paziente oncologico, CUP: B83D18000140007.

REFERENCES

Adlercreutz, H., and Mazur, W. (1997). Phyto-oestrogens and Western diseases. *Ann. Med.* 29, 95–120. doi: 10.3109/07853899709113696

Adlercreutz, H., Honjo, H., Higashi, A., Fotsis, T., Hämäläinen, E., Hasegawa, T., et al. (1991). Urinary excretion of lignans and isoflavonoid phytoestrogens in Japanese men and women consuming a traditional Japanese diet. *Am. J. Clin. Nutr.* 54, 1093–1100. doi: 10.1093/ajcn/54.6.1093

Angeloni, S., Navarini, L., Sagratini, G., Torregiani, E., Vittori, S., and Caprioli, G. (2018). Development of an extraction method for the quantification of lignans in espresso coffee by using HPLC-MS/MS triple quadrupole. *J. mass Spectrom.* 53, 842–848. doi: 10.1002/jms.4251

Angeloni, S., Navarini, L., Khamitova, G., Sagratini, G., Vittori, S., and Caprioli, G. (2019). Quantification of lignans in 30 ground coffee samples and evaluation of theirs extraction yield in espresso coffee by HPLC-MS/MS triple quadrupole. *Int. J. Food Sci. Nutr.* 6, 1–8. doi: 10.1080/09637486.2019.1624693

Arts, I. C., and Hollman, P. C. (2005). Polyphenols and disease risk in epidemiologic studies. *Am. J. Clin. Nutr.* 81, 317S–325S. doi: 10.1093/ajcn/81.1.317S

Axelson, M., Sjövall, J., Gustafsson, B., and Setchell, K. (1982). Origin of lignans in mammals and identification of a precursor from plants. *Nature* 298, 659–660. doi: 10.1038/298659a0

Azam, S., Jakaria, M., Kim, I.-S., Kim, J., Haque, M. E., and Choi, D.-K. (2019). Regulation of toll-like receptor (TLR) signaling pathway by polyphenols in the treatment of age-linked neurodegenerative diseases: focus on TLR4 signaling. *Front. In Immunol.* 10, 1000. doi: 10.3389/fimmu.2019.01000

Barvkar, V. T., Pardeshi, V. C., Kale, S. M., Kadoo, N. Y., and Gupta, V. S. (2012). Phylogenomic analysis of UDP glycosyltransferase 1 multigene family in *Linum usitatissimum* identified genes with varied expression patterns. *BMC Genomics* 13, 175. doi: 10.1186/1471-2164-13-175

Baumgartner, L., Sosa, S., Atanasov, A. G., Bodensieck, A., Fakhrudin, N., Bauer, J., et al. (2011). Lignan derivatives from *Krameria lappacea* roots inhibit acute inflammation *in vivo* and pro-inflammatory mediators *in vitro*. *J. Natural Prod.* 74, 1779–1786. doi: 10.1021/np200343t

Bhakta, D., Higgins, C. D., Sevak, L., Mangtani, P., Adlercreutz, H., Mcmichael, A. J., et al. (2006). Phyto-oestrogen intake and plasma concentrations in South Asian and native British women resident in England. *Br. J. Nutr.* 95, 1150–1158. doi: 10.1079/BJN20061777

Buck, K., Vrieling, A., Zaineddin, A. K., Becker, S., Hüsing, A., Kaaks, R., et al. (2011). Serum enterolactone and prognosis of postmenopausal breast cancer. *J. Clin. Oncol.* 29, 3730–3738. doi: 10.1200/JCO.2011.34.6478

Corrie, J. E. T., Green, G. H., Ritchie, E., and Taylor, W. C.(1970). The chemical constituents of Australian *Zanthoxylum* species. V. The constituents of *Z. pluviatile* Hartley; the structures of two new lignans. *Aust. J. of Chem.* 23, 133–145. doi: 10.1071/CH9700133

Daliu, P., Santini, A., and Novellino, E. (2019). From pharmaceuticals to nutraceuticals: Bridging disease prevention and management. *Expert Rev. Clin. Pharmacol.* 12, 1–7. doi: 10.1080/17512433.2019.1552135

Durazzo, A., Raguzzini, A., Azzini, E., Foddai, M., Narducci, V., Maiani, G., et al. (2009). Bioactive molecules in cereals. *Tec. Molitoria Int.* 60, 150–162.

Durazzo, A., Azzini, E., Turfani, V., Polito, A., Maiani, G., and Carcea, M. (2013a). Effect of cooking on lignans content in whole-grain pasta made with different cereals and other seeds. *Cereal Chem.* 90, 169–171. doi: 10.1094/CCHEM-05-12-0065-N

Durazzo, A., Zaccaria, M., Polito, A., Maiani, G., and Carcea, M. (2013b). Lignan content in cereals, buckwheat and derived foods. *Foods* 2, 53–63. doi: 10.3390/foods2010053

Durazzo, A., Carcea, M., Adlercreutz, H., Azzini, E., Polito, A., Olivieri, L., et al. (2014a). Effects of consumption of whole grain foods rich in lignans in healthy postmenopausal women with moderate serum cholesterol: a pilot study. *Int. J. Food Sci. Nutr.* 65, 637–645. doi: 10.3109/09637486.2014.893283

Durazzo, A., Turfani, V., Narducci, V., Azzini, E., Maiani, G., and Carcea, M. (2014b). Nutritional characterisation and bioactive components of commercial carobs flours. *Food Chem.* 153, 109–113. doi: 10.1016/j.foodchem.2013.12.045

Durazzo, A., Lucarini, M., Camilli, E., Marconi, S., Gabrielli, P., Lisciani, S., et al. (2018). Dietary lignans: definition, description and research trends in databases development. *Molecules* 23, 3251. doi: 10.3390/molecules23123251

Durazzo, A., Lucarini, M., Souto, E. B., Cicala, C., Caiazzo, E., Izzo, A. A., et al. (2019). Polyphenols: a concise overview on the chemistry, occurrence and human health. *Phytother. Res.* 33, 2221–2243. doi: 10.1002/ptr.6419

Eklund, P., and Raitanen, J.-E. (2019). 9-Norlignans: occurrence, properties and their semisynthetic preparation from hydroxymatairesinol. *Molecules* 24, 220. doi: 10.3390/molecules24020220

Fukumitsu, S., Aida, K., Shimizu, H., and Toyoda, K. (2010). Flaxseed lignan lowers blood cholesterol and decreases liver disease risk factors in moderately hypercholesterolemic men. *Nutr. Res.* 30, 441–446. doi: 10.1016/j.nutres.2010.06.004

Gnabre, J., Bates, R., and Huang, R. C. (2015). Creosote bush lignans for human disease treatment and prevention: perspectives on combination therapy. *J. Tradit. Complement. Med.* 5, 119–126. doi: 10.1016/j.jtcme.2014.11.024

Guerriero, F., Orlando, V., Monetti, V. M., Russo, V., and Menditto, E. (2017). Biological therapy utilization, switching, and cost among patients with psoriasis: retrospective analysis of administrative databases in Southern Italy. *ClinicoEconomics Outcomes Res.* 9, 741–748. doi: 10.2147/CEOR.S147558

Guglielmini, P., Rubagotti, A., and Boccardo, F. (2012). Serum enterolactone levels and mortality outcome in women with early breast cancer: a retrospective cohort study. *Breast Cancer Res. Treat* 132, 661–668. doi: 10.1007/s10549-011-1881-8

Hartwell, J. L. (1976). Types of anticancer agents isolated from plants. *Cancer Treat Rep.* 60, 1031–1067.

Hongthong, S., Kuhakarn, C., Jaipetch, T., Piyachaturawat, P., Jariyawat, S., Suksen, K., et al. (2016). A new neolignan, and the cytotoxic and anti-HIV-1 activities of constituents from the roots of *Dasymaschalon sootepense*. *Natural Prod. Commun.* 11, 809–813. doi: 10.1177/1934578X1601100628

Imai, T., Nomura, M., and Fukushima, K. (2006). Evidence for involvement of the phenylpropanoid pathway in the biosynthesis of the norlignan agatharesinol. *J. Plant Physiol.* 163, 483–487. doi: 10.1016/j.jplph.2005.08.009

Ingram, D., Sanders, K., Kolybaba, M., and Lopez, D. (1997). Case-control study of phyto-oestrogens and breast cancer. *Lancet* 350, 990–994. doi: 10.1016/S0140-6736(97)01339-1

Iolascon, G., Gimigliano, F., Moretti, A., Riccio, I., Di Gennaro, M., Illario, M., et al. (2016). Rates and reasons for lack of persistence with anti-osteoporotic drugs: analysis of the Campania region database. *Clin. cases In Mineral Bone Metab.* 13, 126–129. doi: 10.11138/ccmbm/2016.13.2.127

Kim, H.-Y., Kim, J.-K., Choi, J.-H., Jung, J.-Y., Oh, W.-Y., Kim, D. C., et al. (2010). Hepatoprotective effect of pinoresinol on carbon tetrachloride–induced hepatic damage in mice. *J. Pharmacol. Sci.* 112, 105–112. doi: 10.1254/jphs.09234FP

Kuhnle, G. G., Dell'aquila, C., Aspinall, S. M., Runswick, S. A., Mulligan, A. A., and Bingham, S. A. (2008a). Phytoestrogen content of beverages, nuts, seeds, and oils. *J. Agric. Food Chem.* 56, 7311–7315. doi: 10.1021/jf801534g

Kuhnle, G. G., Dell'aquila, C., Aspinall, S. M., Runswick, S. A., Mulligan, A. A., and Bingham, S. A. (2008b). Phytoestrogen content of foods of animal origin: dairy products, eggs, meat, fish, and seafood. *J. Agric. Food Chem.* 56, 10099–10104. doi: 10.1021/jf801344x

Kuhnle, G. G., Dell'aquila, C., Aspinall, S. M., Runswick, S. A., Mulligan, A. A., and Bingham, S. A. (2009a). Phytoestrogen content of cereals and cereal-based foods consumed in the UK. *Nutr. Cancer* 61, 302–309. doi: 10.1080/01635580802567141

Kuhnle, G. G., Dell'aquila, C., Aspinall, S. M., Runswick, S. A., Joosen, A. M., Mulligan, A. A., et al. (2009b). Phytoestrogen content of fruits and vegetables commonly consumed in the UK based on LC–MS and 13C-labelled standards. *Food Chem.* 116, 542–554. doi: 10.1016/j.foodchem.2009.03.002

Landete, J. M. (2012). Plant and mammalian lignans: a review of source, intake, metabolism, intestinal bacteria and health. *Food Res. Int.* 46, 410–424. doi: 10.1016/j.foodres.2011.12.023

Lewis, N. G., and Davin, L. B. (1999). "Lignans: biosynthesis and function," in *Comprehensive Natural Products Chemistry*, vol. 639-712 . Eds. D. Barton, K. Nakanishi and O. Meth-Cohn (Amsterdam, the Netherlands: Elsevier). doi: 10.1016/B978-0-08-091283-7.00027-8

Linder, T., Liu, R., Atanasov, A. G., Li, Y., Geyrhofer, S., Schwaiger, S., et al. (2019). Leoligin-inspired synthetic lignans with selectivity for cell-type and bioactivity relevant for cardiovascular disease. *Chem. Sci.* 10, 5815–5820. doi: 10.1039/C9SC00446G

Lowcock, E. C., Cotterchio, M., and Boucher, B. A. (2013). Consumption of flaxseed, a rich source of lignans, is associated with reduced breast cancer risk. *Cancer Causes Control* 24, 813–816. doi: 10.1007/s10552-013-0155-7

Menditto, E., Cahir, C., Aza-Pascual-Salcedo, M., Bruzzese, D., Poblador-Plou, B., Malo, S., et al. (2018). Adherence to chronic medication in older populations: application of a common protocol among three European cohorts. *Patient Prefer. Adherence* 12, 1975–1987. doi: 10.2147/PPA.S164819

Milder, I. E., Arts, I. C., Van De Putte, B., Venema, D. P., and Hollman, P. C. (2005a). Lignan contents of Dutch plant foods: a database including lariciresinol, pinoresinol, secoisolariciresinol and matairesinol. *Br. J. Nutr.* 93, 393–402. doi: 10.1079/BJN20051371

Milder, I. E., Feskens, E. J., Arts, I. C., De Mesquita, H. B. B., Hollman, P. C., and Kromhout, D. (2005b). Intake of the plant lignans secoisolariciresinol, matairesinol, lariciresinol, and pinoresinol in Dutch men and women. *J. Nutr.* 135, 1202–1207. doi: 10.1093/jn/135.5.1202

Moreno-Franco, B., García-González, Ñ., Montero-Bravo, A. M., Iglesias-Gutiérrez, E., ~beda, N., Maroto-Núnez, L., et al. (2011). Dietary alkylresorcinols and lignans in the Spanish diet: development of the alignia database. *J. Agric. Food Chem.* 59, 9827–9834. doi: 10.1021/jf2015446

Mulligan, A. A., Kuhnle, G. G., Lentjes, M. A., Van Scheltinga, V., Powell, N. A., Mctaggart, A., et al. (2013). Intakes and sources of isoflavones, lignans, enterolignans, coumestrol and soya-containing foods in the Norfolk arm of the European Prospective Investigation into Cancer and Nutrition (EPIC-Norfolk), from 7 d food diaries, using a newly updated database. *Public Health Nutr.* 16, 1454–1462. doi: 10.1017/S1368980012003904

Oh, S.-Y., Kim, Y. H., Bae, D. S., Um, B. H., Pan, C.-H., Kim, C. Y., et al. (2010). Anti-inflammatory effects of gomisin N, gomisin J, and schisandrin C isolated from the fruit of *Schisandra chinensis*. *Biosci. Biotechnol. Biochem.* 74, 285–291. doi: 10.1271/bbb.90597

Peñalvo, J. L., Haajanen, K. M., Botting, N., and Adlercreutz, H. (2005). Quantification of lignans in food using isotope dilution gas chromatography/mass spectrometry. *J. Agric. Food Chem.* 53, 9342–9347. doi: 10.1021/jf051488w

Penalvo, J. L., and López-Romero, P. (2012). Urinary enterolignan concentrations are positively associated with serum HDL cholesterol and negatively associated with serum triglycerides in US adults. *J. Nutr.* 142, 751–756. doi: 10.3945/jn.111.150516

Penalvo, J. L., Adlercreutz, H., Uehara, M., Ristimaki, A., and Watanabe, S. (2007). Lignan content of selected foods from Japan. *J. Agric. Food Chem.* 56, 401–409. doi: 10.1021/jf072695u

Peterson, J., Dwyer, J., Adlercreutz, H., Scalbert, A., Jacques, P., and Mccullough, M. L. (2010). Dietary lignans: physiology and potential for cardiovascular disease risk reduction. *Nutr. Rev.* 68, 571–603. doi: 10.1111/j.1753-4887.2010.00319.x

Reshma, M., Balachandran, C., Arumughan, C., Sunderasan, A., Sukumaran, D., Thomas, S., et al. (2010). Extraction, separation and characterisation of sesame oil lignan for nutraceutical applications. *Food Chem.* 120, 1041–1046. doi: 10.1016/j.foodchem.2009.11.047

Rietjens, I. M., Louisse, J., and Beekmann, K. (2017). The potential health effects of dietary phytoestrogens. *Br. J. Pharmacol.* 174, 1263–1280. doi: 10.1111/bph.13622

Rodríguez-García, C., Sánchez-Quesada, C., Toledo, E., Delgado-Rodríguez, M., and Gaforio, J. J. (2019). Naturally Lignan-rich foods: a dietary tool for health promotion? *Molecules* 24, 917. doi: 10.3390/molecules24050917

Saito, N., Ichimaru, T., and Sato, Y. (2012). Total synthesis of (–)-herbindoles A, B, and C *via* transition-metal-catalyzed intramolecular [2 + 2+ 2] cyclization between ynamide and diynes. *Org. Lett.* 14, 1914–1917. doi: 10.1021/ol300571b

Santini, A., and Novellino, E. (2018). Nutraceuticals-shedding light on the grey area between pharmaceuticals and food. *Expert Rev. Clin. Pharmacol.* 11, 545–547. doi: 10.1080/17512433.2018.1464911

Santini, A., Cammarata, S. M., Capone, G., Ianaro, A., Tenore, G. C., Pani, L., et al. (2018). Nutraceuticals: opening the debate for a regulatory framework. *Br. J. Clin. Pharmacol.* 84, 659–672. doi: 10.1111/bcp.13496

Scala, D., Menditto, E., Armellino, M. F., Manguso, F., Monetti, V. M., Orlando, V., et al. (2016). Italian translation and cultural adaptation of the communication assessment tool in an outpatient surgical clinic. *BMC Health Serv. Res.* 16, 163. doi: 10.1186/s12913-016-1411-9

Smeds, A. I., Jauhiainen, L., Tuomola, E., and Peltonen-Sainio, P. (2009). Characterization of variation in the lignan content and composition of winter rye, spring wheat, and spring oat. *J. Agric. Food Chem.* 57, 5837–5842. doi: 10.1021/jf9004274

Smeds, A. I., Eklund, P. C., and Willför, S. M. (2012). Content, composition, and stereochemical characterisation of lignans in berries and seeds. *Food Chem.* 134, 1991–1998. doi: 10.1016/j.foodchem.2012.03.133

Su, S., and Wink, M. (2015). Natural lignans from *Arctium lappa* as antiaging agents in *Caenorhabditis elegans*. *Phytochemistry* 117, 340–350. doi: 10.1016/j.phytochem.2015.06.021

Teponno, R. B., Kusari, S., and Spiteller, M. (2016). Recent advances in research on lignans and neolignans. *Natural Prod. Rep.* 33, 1044–1092. doi: 10.1039/C6NP00021E

Thompson, L. U., Boucher, B. A., Liu, Z., Cotterchio, M., and Kreiger, N. (2006). Phytoestrogen content of foods consumed in Canada, including isoflavones, lignans, and coumestan. *Nutr. Cancer* 54, 184–201. doi: 10.1207/s15327914nc5402_5

Turfani, V., Narducci, V., Durazzo, A., Galli, V., and Carcea, M. (2017). Technological, nutritional and functional properties of wheat bread enriched with lentil or carob flours. *LWT-Food Sci. Technol.* 78, 361–366. doi: 10.1016/j.lwt.2016.12.030

Valsta, L. M., Kilkkinen, A., Mazur, W., Nurmi, T., Lampi, A.-M., Ovaskainen, M.-L., et al. (2003). Phyto-oestrogen database of foods and average intake in Finland. *Br. J. Nutr.* 89, S31–S38. doi: 10.1079/BJN2002794

Van Eck, N. J., and Waltman, L. (2009). Software survey: VOSviewer, a computer program for bibliometric mapping. *Scientometrics* 84, 523–538. doi: 10.1007/s11192-009-0146-3

Vickery, B. C. (1948). Bradford's law of scattering. *J. Doc.* 4, 198–203. doi: 10.1108/eb026133

Wang, L., Ladurner, A., Latkolik, S., Schwaiger, S., Linder, T., HošEk, J., et al. (2016). Leoligin, the major lignan from edelweiss (*Leontopodium nivale* subsp. *alpinum*), promotes cholesterol efflux from THP-1 macrophages. *J. Natural Prod.* 79, 1651–1657. doi: 10.1021/acs.jnatprod.6b00227

Ward, H. A., Kuhnle, G. G., Mulligan, A. A., Lentjes, M. A., Luben, R. N., and Khaw, K.-T. (2009). Breast, colorectal, and prostate cancer risk in the European prospective investigation into cancer and nutrition–norfolk in relation to

phytoestrogen intake derived from an improved database. *Am. J. Clin. Nutr.* 91, 440–448. doi: 10.3945/ajcn.2009.28282

Wei, W., Qi, X., Wang, L., Zhang, Y., Hua, W., Li, D., et al. (2011). Characterization of the sesame (*Sesamum indicum* L.) global transcriptome using Illumina paired-end sequencing and development of EST-SSR markers. *BMC Genomics* 12, 451. doi: 10.1186/1471-2164-12-451

Xiao, H.-H., Lv, J., Mok, D., Yao, X.-S., Wong, M.-S., and Cooper, R. (2019). NMR applications for botanical mixtures: the use of HSQC data to determine lignan content in *Sambucus williamsii*. *J. Natural Prod.* 82, 1733–1740. doi: 10.1021/acs.jnatprod.8b00891

Xiong, L., Zhu, C., Li, Y., Tian, Y., Lin, S., Yuan, S., et al. (2011). Lignans and neolignans from *Sinocalamus affinis* and their absolute configurations. *J. Natural Prod.* 74, 1188–1200. doi: 10.1021/np200117y

Yang, C. S., Landau, J. M., Huang, M.-T., and Newmark, H. L. (2001). Inhibition of carcinogenesis by dietary polyphenolic compounds. *Annu. Rev. Nutr.* 21, 381–406. doi: 10.1146/annurev.nutr.21.1.381

Yeung, A. W. K., Aggarwal, B., Barreca, D., Battino, M., Belwal, T., Horbańczuk, O., et al. (2018a). Dietary natural products and their potential to influence health and disease including animal model studies. *Anim. Sci. Pap. Rep.* 36, 345–358.

Yeung, A. W. K., Mocan, A., and Atanasov, A. G. (2018b). Let food be thy medicine and medicine be thy food: a bibliometric analysis of the most cited papers focusing on nutraceuticals and functional foods. *Food Chem.* 269, 455–465. doi: 10.1016/j.foodchem.2018.06.139

Yeung, A. W. K., Aggarwal, B. B., Orhan, I. E., Horbańczuk, O. K., Barreca, D., Battino, M., et al. (2019a). Resveratrol, a popular dietary supplement for human and animal health: quantitative research literature analysis - a review. *Anim. Sci. Pap. Rep.* 37, 103–118.

Yeung, A. W. K., Horbańczuk, M., Tzvetkov, N. T., Mocan, A., Carradori, S., Maggi, F., et al. (2019b). Curcumin: total-scale analysis of the scientific literature. *Molecules* 24, 1393. doi: 10.3390/molecules24071393

Yeung, A. W. K., Tzvetkov, N. T., El-Tawil, O. S., Bungău, S. G., Abdel-Daim, M. M., and Atanasov, A. G. (2019c). Antioxidants: scientific literature landscape analysis. *Oxid. Med. Cell. Longevity* 2019, 8278454. doi: 10.1155/2019/8278454

Yeung, A. W. K., Tzvetkov, N. T., Zengin, G., Wang, D., Xu, S., Mitrović, G., et al. (2019d). The berries on the top. *J. Berry Res.* 9, 125–139. doi: 10.3233/JBR-180357

Yeung, A. W. K. (2019). Higher impact factor of neuroimaging journals is associated with larger number of articles published and smaller percentage of uncited articles. *Front. In Hum. Neurosci.* 12, 523. doi: 10.3389/fnhum.2018.00523

Zálešák, F., Bon, D.J.-Y.D., and Pospíšil, J. (2019). Lignans and Neolignans: plant secondary metabolites as a reservoir of biologically active substances. *Pharmacol. Res.* 146, 104284. doi: 10.1016/j.phrs.2019.104284

Zamora-Ros, R., Agudo, A., Luján-Barroso, L., Romieu, I., Ferrari, P., Knaze, V., et al. (2012). Dietary flavonoid and lignan intake and gastric adenocarcinoma risk in the European Prospective Investigation into Cancer and Nutrition (EPIC) study. *Am. J. Clin. Nutr.* 96, 1398–1408. doi: 10.3945/ajcn.112.037358

Zhang, C., Mao, X., Zhao, X., Liu, Z., Liu, B., Li, H., et al. (2014). Gomisin N isolated from *Schisandra chinensis* augments pentobarbital-induced sleep behaviors through the modification of the serotonergic and GABAergic system. *Fitoterapia* 96, 123–130. doi: 10.1016/j.fitote.2014.04.017

Zhuang, W., Li, Z., Dong, X., Zhao, N., Liu, Y., Wang, C., et al. (2019). Schisandrin B inhibits TGF-β1-induced epithelial-mesenchymal transition in human A549 cells through epigenetic silencing of ZEB1. *Exp. Lung Res.* 45, 157–166. doi: 10.1080/01902148.2019.1631906

Conflict of Interest: The authors declare that the research was conducted in the absence of any commercial or financial relationships that could be construed as a potential conflict of interest.

frontiers in Pharmacology

REVIEW
published: 28 February 2020
doi: 10.3389/fphar.2020.00151

Nordihydroguaiaretic Acid: From Herbal Medicine to Clinical Development for Cancer and Chronic Diseases

Gina Manda[1], *Ana I. Rojo*[2], *Elena Martínez-Klimova*[3], *José Pedraza-Chaverri*[3] *and Antonio Cuadrado*[1,2]*

[1] Department Cellular and Molecular Medicine, Victor Babes National Institute of Pathology, Bucharest, Romania, [2] Department of Biochemistry, Faculty of Medicine, Autonomous University of Madrid, Centro de Investigación Biomédica en Red sobre Enfermedades Neurodegenerativas (CIBERNED), Instituto de Investigación Sanitaria la Paz (idiPAZ), Instituto de Investigaciones Biomédicas "Alberto Sols" UAM-CSIC, Madrid, Spain, [3] Department of Biology, Faculty of Chemistry, National Autonomous University of Mexico (UNAM), Mexico City, Mexico

OPEN ACCESS

Edited by:
Salvatore Salomone,
University of Catania, Italy

Reviewed by:
Omidreza Firuzi,
Shiraz University of Medical Sciences, Iran
Laureano De La Vega,
University of Dundee, United Kingdom

***Correspondence:**
Antonio Cuadrado
antonio.cuadrado@uam.es

Specialty section:
This article was submitted to Experimental Pharmacology and Drug Discovery, a section of the journal Frontiers in Pharmacology

Received: 18 October 2019
Accepted: 05 February 2020
Published: 28 February 2020

Citation:
Manda G, Rojo AI, Martínez-Klimova E, Pedraza-Chaverri J and Cuadrado A (2020) Nordihydroguaiaretic Acid: From Herbal Medicine to Clinical Development for Cancer and Chronic Diseases. Front. Pharmacol. 11:151. doi: 10.3389/fphar.2020.00151

Nordihydroguaiaretic acid (NDGA) is a phenolic lignan obtained from *Larrea tridentata*, the creosote bush found in Mexico and USA deserts, that has been used in traditional medicine for the treatment of numerous diseases such as cancer, renal, cardiovascular, immunological, and neurological disorders, and even aging. NDGA presents two catechol rings that confer a very potent antioxidant activity by scavenging oxygen free radicals and this may explain part of its therapeutic action. Additional effects include inhibition of lipoxygenases (LOXs) and activation of signaling pathways that impinge on the transcription factor Nuclear Factor Erythroid 2-related Factor (NRF2). On the other hand, the oxidation of the catechols to the corresponding quinones my elicit alterations in proteins and DNA that raise safety concerns. This review describes the current knowledge on NDGA, its targets and side effects, and its synthetic analogs as promising therapeutic agents, highlighting their mechanism of action and clinical projection towards therapy of neurodegenerative, liver, and kidney disease, as well as cancer.

Keywords: catechol, quinone, electrophiles, NRF2, KEAP1, cytoprotection, oxidative stress, inflammation

INTRODUCTION

Nordihydroguaiaretic acid (NDGA), also called masoprocol {IUPAC name: 4-[4-(3,4-dihydroxyphenyl)-2,3-dimethylbutyl]benzene-1,2-diol}, is a phenolic lignan mainly extracted from the five plant species that constitute the genus *Larrea* (Arteaga et al., 2005; Peralta et al., 2018). A general source of NDGA is the leaves of *Larrea tridentata*, also known as "chaparral", "creosote bush", and "gobernadora", which is abundant in the deserts of Mexico and southwest USA (Arteaga et al., 2005). NDGA accounts for approximately 10% of the leaves' dry weight of *L. tridentata* and 80% of all flavonoids and lignans that are found in the resin of this plant (Floriano-Sanchez et al., 2006).

The leaves have been used in traditional medicine of the mentioned regions for the treatment of over 50 diseases, including rheumatism, arthritis, diabetes, pain, and inflammation (Arteaga et al., 2005). More

recently, NDGA started to be tested in other pathologies that are becoming prevalent as a result of population aging (Sadagurski et al., 2017). NDGA has been utilized as an antioxidant food preservative and as nutritional supplement, mainly in the form of chaparral tea. The best characterized effects of NDGA are: 1) the ROS scavenging nature of NDGA decreases the pro-oxidant effects of inflammation; 2) the inhibitory effects on lipoxygenases (LOX) activity, leading to the reduction of lipid hydroperoxides (5-HEPE and 5-HETE at 50 μM NDGA) that trigger oxidative stress due to their decomposition to free radicals (Mashima and Okuyama, 2015) the induction of ROS production through activation of NADPH-oxidases, MAPKs, etc. (Li Q. et al., 2016; Nagahora et al., 2017); 3) the activation of endogenous antioxidant responses mediated by NRF2. Most of the pleiotropic effects that have been attributed to this compound are briefly summarized in **Table 1**.

Despite the existence of many preclinical studies that highlight the therapeutic potential of NDGA, the fact is that most of its beneficial effects are not supported by clinical studies, as it usually happens with parapharmaceutical products (Abou-Gazar et al., 2004; Arteaga et al., 2005). Moreover, it was found that excessive consumption of this phytochemical may damage several organs including kidney and liver (Goodman et al., 1970; Evan and Gardner, 1979), hence raising awareness about the need of careful control of NDGA dosing and treatment length. Therefore, the clinical development of NDGA and its analogs is progressing slowly. This review will critically discuss the best characterized mechanisms and targets attributed to NDGA, safety concerns and the potential of NDAG analogs for clinical translation.

TABLE 1 | Some NDGA targets. The table summarizes some of the best characterized NDGA targets.

Molecular target	NDGA effect	References
5-LOX, 12-LOX, 15-LOX	Inhibition	(Tateson et al., 1988; Pavani et al., 1994; Vasquez-Martinez et al., 2007)
Lipoprotein lipase	Inhibition	(Kang et al., 2019)
Reactive oxygen species	Scavenging	(Floriano-Sanchez et al., 2006)
α-amylase, α-glucosidase and dipeptidyl peptidase 4	Inhibition	(Roskar et al., 2016)
mTORC1	Inhibition	(Zhang et al., 2012)
large conductance Ca^{2+}-activated K^+	activation	(Yamamura et al., 2002)
KEAP1	KEAP1 inhibition/ NRF2 activation	(Satoh et al., 2008; Rojo et al., 2012)
Insulin-like receptor-1 (Tyr kinase receptor)	Inhibition	(Youngren et al., 2005)
c-ErbB2/HER2/Neu (Tyr kinase receptor)	Inhibition	(Youngren et al., 2005; Rowe et al., 2008)
Transforming growth factor β type 1 receptor (Ser/Thr kinase receptor)	Inhibition	(Youngren et al., 2005; Li et al., 2009)
GSH	depletion	(Im and Han, 2007)
PTEN (Redox-sensitive phosphatase)	Inhibition	(Rojo et al., 2014)
DUSPs (Redox-sensitive phosphatase)	Inhibition	(Liu et al., 2012; Rios et al., 2014)

PTEN and DUSPs are postulated as NDGA targets based on information from other polyphenols (see text).

ANTIOXIDANT AND ELECTROPHILIC ACTIVITIES OF NDGA

NDGA presents two catechol rings that confer both cytoprotective and cytotoxic effects depending on the dosage and the context. The cytoprotective effect stems from the strong scavenging activity of NDGA against multiple types of Reactive Oxygen Species (ROS) such as peroxynitrite, singlet oxygen, hydroxyl radical, superoxide anion, and hypochlorous acid (Floriano-Sanchez et al., 2006). NDGA can donate one electron and one proton from each of its four hydroxyl groups contained in the two catechol rings, converting itself into an oxidized catechol-quinone (Yam-Canul et al., 2008). Since NDGA is a symmetrical molecule with two catechol groups, both catechols can be oxidized to quinones. The reactions involved in the oxidative modifications of NDGA have been described previously (Billinsky et al., 2007; Billinsky and Krol, 2008) (**Figure 1**). Briefly, at physiological pH, NDGA rapidly auto-oxidizes, resulting in the formation of a *semi*-quinone radical which is further converted in a second oxidation step to generate *ortho*-quinone and superoxide anion, mostly spontaneously or through peroxidases- and cytochrome p450-catalyzed reactions (Billinsky and Krol, 2008). *Ortho*-quinone may be converted back to the reactive *semi*-quinone by cellular NADPH-dependent reductases (O'brien, 1991; Monks et al., 1992; Chichirau et al., 2005). This redox cycle is highly toxic, as it evokes superoxide-generated oxidative stress, which may become deleterious at high concentrations of NDGA. The *ortho*-

Abbreviations: 4-VO, four-vessel occlusion; 5-HEPE, 5-hydoxyeicosapentaenoic acid; 5-HETE, 5-hydroxyeicosatetraenoic acid; AA, arachidonic acid; AD, Alzheimer's disease; ALS, Amyotrophic Lateral Sclerosis; ARE, Antioxidant Response Element; ALT, alanine aminotransferase; AST, aspartate aminotransferase; beta-TrCP, beta-transducin repeat-containing protein; BTB, broad complex, Tramtrack, Bric-a-brac; bZip, basic region-leucine zipper; COX, cyclooxygenase; CUL3/RBX1, cullin 3 and RING-box protein 1; DGR, double glycine repeat; DHA, docosahexaenoic acid; DPP, dipeptidyl Peptidase 3; DUSPs, dual specificity phosphatases; EPA, eicosapentaenoic acid; EWL, egg white lysozyme; FAM117B, Family with sequence similarity 117 member B; GSH, glutathione; HD, Huntington's disease; HO-1, heme oxygenase-1; HPETEs, hydroperoxy eicosatetraenoic acids; IGF-1R, insulin-like Growth Factor 1 Receptor; IGF-I, insulin-like growth factor-1; IKBKB, inhibitor of Nuclear Factor Kappa B Kinase Subunit Beta; IP-10, interferon-gamma inducible protein-10; IRF-1, interferon regulatory factor-1; KEAP1, Kelch-like erythroid cell–derived protein with Cap'n'collar homology (ECH)-associated protein 1; LDH, lactate dehydrogenase; LOXs, lipoxygenases; LTA4, leukotriene A4; LTB4, leukotriene B4; LTBR1/2, leukotriene B4 receptor 1 or 2; MAD2L1, mitotic Arrest Deficient 2 Like 1; MAF, small musculo aponeurotic fibrosarcoma proteins; MCAO, middle cerebral artery occlusion; MCC, mutated in colorectal cancers; MCMBP, minichromosome maintenance complex component; MCP-1, monocyte chemoattractant protein-1; MMP, matrix metalloproteinases; NDGA, nordihydroguaiaretic acid; NO, nitric oxide; NRF2, Nuclear factor erythroid 2-related factor 2; OGD, oxygen-glucose deprivation; PALB2, partner and localizer of BRCA2; PD, Parkinson's disease; PGAM5, PGAM Family Member 5, Mitochondrial Serine/Threonine Protein Phosphatase; PI3K, phosphatidylinostisol 3-kinase; PKD, polycystic kidney disease; PPARγ, peroxisome proliferator-activated receptor gamma; PTEN, phosphatase and tensin homolog; PUFA, polyunsaturated fatty acids; ROS, reactive oxygen species; SLK, STE20 like kinase; Sp1, specificity protein 1; SQSTM1, Sequestosome 1; tBHQ, tert-Butylhydroquinone; TDP-43, TAR DNA binding protein 43; TGF-β, transforming growth factor β; TMZ, temozolomide.

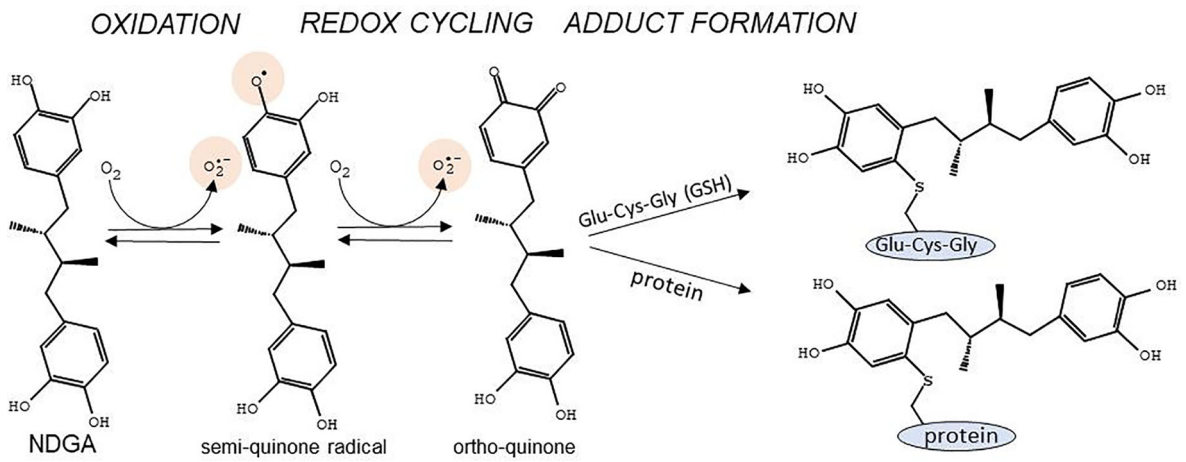

FIGURE 1 | Main reactions for conversion of the catechol rings of NDGA into *semi*-quinone and *ortho*-quinone, and adduct formation with cysteines in glutathione (Glu-Cys-Gly) or in proteins. Of note are the generation of the *semi*-quinone free radical as well as superoxide anion during the redox cycling reactions. Adapted with permission from (Billinsky et al., 2007). Copyright (2007) American Chemical Society.

quinone is a highly electrophilic Michael reaction acceptor (Talalay et al., 1988) that reacts with sulfur neutrophiles such as cysteine residues in glutathione (GSH) and in various proteins (Powis, 1987). Adduct formation of *ortho*-quinone with GSH results in increased excretion of these compounds, but at the cost of depleting the GSH pool, hence leading to a shift in the redox balance towards deleterious oxidative stress. On the other hand, adduct formation with cysteines in critical proteins may lead to changes in signaling pathways that trigger cytoprotective mechanisms through NRF2 activation (**Figure 1**).

Therefore, the effect of NDGA on cell physiology depends on the balance between its protective effect, which is mediated by its antioxidant nature and electrophilic interaction with several signaling proteins, and its toxic effect, which is related to enhanced superoxide formation and GSH depletion. This balance is narrowly dependent on NDGA concentration. Although not analyzed for NDGA, diphenols provide cytoprotection at low doses, whilst being toxic at high doses (Satoh et al., 2013). In this context, NDGA has a redox potential and a geometric distribution of atoms that make it suitable for interaction with cysteines in proteins over a small range of concentrations at which GSH levels are not substantially depleted. Moreover, NRF2 activation by NDGA (described in detail later in this review) leads to increased expression of the two subunits that conform the glutamate-cysteine ligase (GCLC and GCLM) which is the rate-limiting enzyme in GSH biosynthesis, hence contributing to the maintenance of the cellular GSH pool.

NDGA IS A PAN-LIPOXYGENASE INHIBITOR

Lipoxygenases (LOXs) are non-heme iron-containing enzymes (six isoforms have been identified in humans) that catalyze the stereospecific oxygenation of *cis*,*cis*-1,4-pentadiene moieties of polyunsaturated fatty acids (PUFAs), such as arachidonic acid, eicosapentaenoic acid and docosahexaenoic acid, and formation of their corresponding hydroperoxy-derivatives, which may be further reduced by glutathione peroxidases. For instance, LOXs catalyze the formation of hydroperoxyeicosatetraenoic acids (HPETEs) from arachidonic acid (**Figure 2A**). HPETEs are subsequently reduced and transformed into bioactive eicosanoids such as 5-hydroxyeicosatetraenoic acid (5-HETE) and 5-hydroxyeicosapentaenoic acid (5-HEPE) which can be further metabolized to hepoxilins, lipoxins, and resolvins. These metabolites are versatile signaling molecules that play an important role in many physiological and pathological processes. Of utmost importance for the immune response is the 5-LOX-mediated generation of leukotriene A4 (LTA4) and its further transformation, by LTA4 hydrolase, into the pro-inflammatory leukotriene B4 (LTB4). LTB4 regulates inflammatory pathways and immune responses against infection and tissue injury (Brandt and Serezani, 2017).

LOXs were the first identified molecular targets of NDGA (Tang et al., 1996; Tang and Honn, 1997; Tong et al., 2002; Floriano-Sanchez et al., 2006; Czapski et al., 2012), which was initially defined as a pan-LOX inhibitor with micromolar and sub-micromolar IC_{50} values (**Table 2**). Accordingly, the biologic effects of NDGA were firstly explained from the LOX inhibition perspective in various pathologic conditions. For catalysis, the iron component of the LOX enzymes must cycle between Fe^{2+} and Fe^{3+} states (**Figure 2B**) and the potent antioxidant activity of NDGA is halting iron in the Fe^{2+} state (Nelson et al., 1991). As shown in **Table 2**, micromolar and sub-micromolar NDGA concentrations inhibit various LOX isoforms including both 15-LOX-1 and 15-LOX-2. Compared to the FDA approved 5-LOX inhibitor zileuton (IC_{50} = 0.15 μM) (Braeckman et al., 1995), NDGA has a lower IC_{50} value (IC_{50} = 0.097 μM) for human 5-LOX (Estrada-Valencia et al., 2019).

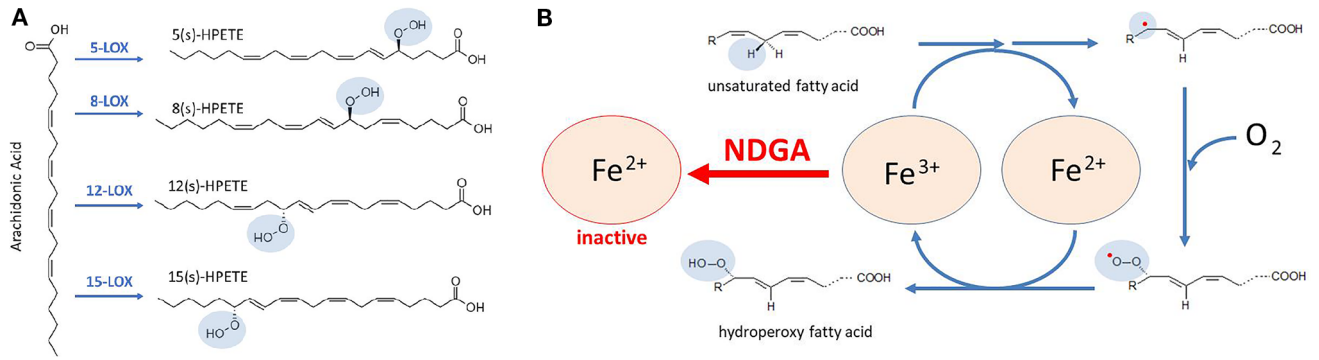

FIGURE 2 | Catalytic mechanism proposed for lipoxygenases (LOXs) inhibition by NDGA. **(A)** conversion of arachidonic acid to HPETEs by specific LOX enzymes that are targeted by NDGA. **(B)** LOXs contain a non-heme Fe in the catalytic center that allows redox cycling of the enzyme, coupled with oxygen consumption. In the first reactions, unsaturated fatty acids, such as arachidonic acid, undergo a hydrogen abstraction and electron rearrangement, converting Fe^{3+} to Fe^{2+}, and yielding a free radical (red dot). Then, a molecule of oxygen is taken to form a peroxy radical. Finally, the conversion of peroxy radical to hydroperoxy fatty acid is coupled to the regeneration of Fe^{3+}. NDGA maintains Fe in the Fe^{2+} form, hence breaking the redox cycle of LOXs and resulting in its inactivation.

TABLE 2 | Inhibitory action of NDGA on lipoxygenases (LOXs).

LOX	IC_{50} (μM)	Extracts from:	References
Arachidonate 5-lipoxygenase (5-LOX)	0.8	Leukocytes	(Tateson et al., 1988)
Arachidonate 12-lipoxygenase (12-LOX)	2.6	SF9 cells transfected with human LOX genes	(Vasquez-Martinez et al., 2007)
Arachidonate 5-lipoxygenase-1 (15-LOX-1)	0.25		
Arachidonate 15-lipoxygenase-2 (15-LOX-2)	0.11		
Arachidonate 12/15-lipoxygenase 15/12-LOX	0.1		
Arachidonate 12-lipoxygenase (12-LOX)	3-5	Human platelets	(Pavani et al., 1994)
Arachidonate 5-lipoxygenase (5-LOX)	2.3	Nucleated platelets	(Chen et al., 2005)
Arachidonate 12-lipoxygenase (12-LOX)	1.6		
Arachidonate 15-lipoxygenase (15-LOX)	1.7		
Arachidonate 5-lipoxygenase (5-LOX)	0.91	Rabbit reticulocytes	(Hope et al., 1983)
Soybean lipoxygenase	0.45	Soybean	(Whitman et al., 2002)

IC_{50} values established in vitro.

NDGA REGULATES THE KEAP1/NRF2 AXIS

A more profound antioxidant action of NDGA than its ROS-scavenging activity is probably related to the activation of the endogenous antioxidant system through the inhibition of the redox sensor KEAP1 (Kelch-like Erythroid Cell–derived Protein with Cap'n'collar Homology (ECH)-associated Protein 1) (**Figure 3A**). KEAP1 is a homodimeric protein that comprises three functional domains: a Broad complex, Tramtrack, Bric-a-brac (BTB) homodimerization domain, an intervening region (IVR) and a C-terminal Kelch domain with a double glycine repeat (DGR) (Canning et al., 2015). KEAP1 is an ubiquitin E3 ligase adapter that binds certain proteins at the Kelch domain and presents them to the E3 ligase complex formed by Cullin 3 and RING-box protein 1 (CUL3/RBX1), leading to their ubiquitination and proteasomal degradation (Zhang and Hannink, 2003; Cullinan et al., 2004; Kobayashi et al., 2004). Therefore, KEAP1 inhibition results in accumulation of these proteins.

The exceptional feature of KEAP1 is that it is a redox sensor. Human KEAP1 contains 27 cysteine residues and several of them can be modified by sulfhydryl reactions under oxidant conditions and by adduct formation with electrophiles, such as NDGA. The most sensitive cysteines for adduct formation are C151, C273, and C288 (Yamamoto et al., 2008). Although experimental evidence is still lacking for NDGA, another catechol, hydroxytyrosol butyrate, appears to interact with the above mentioned cysteines *in vivo* (Funakohi-Tago et al., 2018). However, a single point mutant, C151S, was sufficient to yield KEAP1 refractory to inhibition by the diphenolic compound tert-butylhydroquinone (tBHQ) (Zhang and Hannink, 2003) as well as by carnosic acid, a catechol-type electrophilic compound (Satoh et al., 2008). Therefore, it is tempting to speculate that NDGA inhibits KEAP1 through conversion to its quinone form, followed by adduct formation with C151 of KEAP1 (Satoh et al., 2008).

The best characterized protein interacting with KEAP1 is the transcription factor NRF2, which is considered a master regulator of multiple homeostatic responses (Cuadrado et al., 2018; Cuadrado et al., 2019). NRF2 is a basic region-leucine zipper (bZip) transcription factor that forms heterodimers with the small muscle aponeurotic fibrosarcoma proteins (MAF) K, G, and F (Katsuoka and Yamamoto, 2016). The heterodimer recognizes an enhancer sequence termed Antioxidant Response Element (ARE) that is present in the regulatory regions of over 250 genes (Ma, 2013; Hayes and Dinkova-Kostova, 2014). These

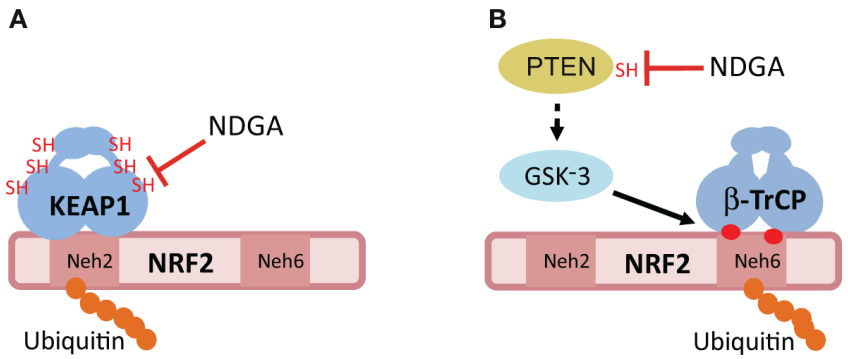

FIGURE 3 | Hypothetical mechanisms of NRF2 activation by NDGA. **(A)** The E3 ligase adapter KEAP1 recognizes the Neh2 domain of NRF2, leading to its ubiquitination and proteasomal degradation. NDGA might inhibit KEAP1 by making adducts with specific cysteines of KEAP1, including Cys151. **(B)** The Neh6 domain of NRF2 is a target for phosphorylation by the Glycogen Synthase Kinase-3 (GSK-3). This phosphorylation creates a site for recognition by the E3 ligase adapter beta-TrCP, leading to its ubiquitination and proteasomal degradation. GSK-3 is inhibited by phosphorylation at its N-terminus by several kinases including AKT. NDGA might inhibit GSK-3 indirectly through adduct formation with the catalytic Cys124 of PTEN. Inhibition of PTEN results in sustained activation of AKT and inhibition of GSK-3, therefore allowing NRF2 to escape this degradation pathway. See text for details of both mechanisms.

genes encode a network of enzymes involved in phase I, II, and III biotransformation reactions, antioxidant metabolism (e.g. generation of NADPH-, glutathione- and thioredoxin-mediated reactions), lipid and iron catabolism, interaction with other transcription factors, as well as autophagy (Hayes and Dinkova-Kostova, 2014; Cuadrado et al., 2019). Although the crystal structure of NRF2 has not yet been reported, its primary sequence reveals several domains termed (Neh)1-6 (NRF2-ECH homology). Under basal homeostatic conditions, the Kelch domains of the KEAP1 homodimer bind one molecule of NRF2 at two N-terminal amino acid sequences in the Neh2 domain: the low affinity binding site (aspartate, leucine, and glycine; DLG) and the high affinity binding site (glutamate, threonine, glycine, and glutamate; ETGE) (Mcmahon et al., 2006; Tong et al., 2006). Thereafter, KEAP1-bound NRF2 is directed to ubiquitination by CUL3/RBX1 and its subsequent degradation by the proteasome. As a result, the constantly synthesized NRF2 is continuously degraded, having a very short half-life of about 20–45 min, depending on the cell type (Mcmahon et al., 2004). However, in an oxidant environment or in the presence of electrophiles (e.g. NDGA), KEAP1 switches towards an inactive form which is no longer capable of promoting NRF2 ubiquitination. As such, NRF2 is stabilized by avoiding proteasomal degradation, and supports cellular adaptation to oxidative stress (Rojo et al., 2012). Definite evidence that NDGA increases NRF2 stability by disrupting the KEAP1/NRF2 interaction was obtained using a chimeric protein that contains the enhanced green fluorescence protein fused to the Neh2 domain of NRF2 (Rojo et al., 2012). The Neh2 tag conferred instability to the chimeric protein and this was prevented in the presence of NDGA. In fact, NDGA promotes the stabilization of the NRF2 protein and upregulation of its gene target *HMOX1* that encodes heme-oxygenase-1 (HO-1), hence conferring cytoprotection against the hydrogen peroxide-induced damage in mouse fibroblasts (Rojo et al., 2012) and against 3-nitropropionic acid in cerebellar granule cells (Guzman-Beltran et al., 2008). Moreover, NDGA induces the nuclear translocation of NRF2 *in vivo* in the rat kidney, leading to the activation of its transcriptional signature and consequent protection against renal oxidative injury and apoptosis in a model of ischemia reperfusion (Zuniga-Toala et al., 2013).

Although for the moment there is no clear experimental evidence, the inhibition of KEAP1 by NDGA might also impact the stability and function of other KEAP1 substrates, besides NRF2. These substrates are still poorly defined but they all share a motif that is identical to or resembles the ETGE motif in the high affinity binding site of NRF2. Empirical evidence for association to KEAP1 has been shown for SQSTM1 (Sequestosome 1), MCM3 (Minichromosome Maintenance Complex Component 3), MCMBP (Minichromosome Maintenance Complex Binding Protein), MCC (Mutated In Colorectal Cancers), the metallopeptidase DPP3 (Dipeptidyl Peptidase 3), SLK (STE20 Like Kinase), MAD2L1 (Mitotic Arrest Deficient 2 Like 1), FAM117B (Family With Sequence Similarity 117 Member B), IKBKB (Inhibitor Of Nuclear Factor Kappa B Kinase Subunit Beta), PGAM5 (PGAM Family Member 5, Mitochondrial Serine/Threonine Protein Phosphatase), and PALB2 (Partner and localizer of BRCA2) (Lo and Hannink, 2006; Goldfarb et al., 2014; Orthwein et al., 2015). However, it should be noted that the disruption of the KEAP1/NRF2 interaction by NDGA might not represent a general mechanism for other KEAP1 substrates and therefore experimental work is needed, not only to establish mechanistic interactions but also to know if these proteins might be functional effectors underlining the anti-tumor and anti-inflammatory activities of NDGA. At least in the case of SQSTM1, there is some indirect evidence indicating that NDGA alters this interaction and inhibits *Mycobacterium tuberculosis* growth in infected macrophages by inducing autophagy (Guzman-Beltran et al., 2016). SQSTM1 is a crucial autophagy protein involved in transporting KEAP1 to autophagosomes. It contains a STGE motif that, upon

phosphorylation at the serine residue, resembles the high affinity binding site for KEAP1 (Komatsu et al., 2010). Accordingly, it is possible that, in addition to the induction of autophagy genes through NRF2 activation (Pajares et al., 2016; Pajares et al., 2018), NDGA might modulate autophagy by disrupting the KEAP1/SQSTM1 interaction.

NDGA ELICITS DUAL EFFECTS ON VARIOUS SIGNALING CASCADES

Studies in cell culture indicate that, depending on the context, NDGA may either inhibit or activate the PI3K/AKT axis and the three main MAPK cascades, namely ERK1/2, p38, and JNK. At high concentrations, NDGA disrupts the activation of ERK and AKT signaling pathways activated by IGF-I (insulin-like growth factor-1) and induces apoptosis (Meyer et al., 2007), the effect being highly important for cancer treatment but also for unwanted side-effects. At least in the case of the PI3K/AKT pathway, the NDGA-mediated inhibition resembles the effect of high concentrations of hydrogen peroxide, which lead to elevated levels of intracellular ROS and ceramide. These intermediary molecules trigger the down-regulation of AKT by dephosphorylation and subsequent proteolysis (Martin et al., 2002). However, low micromolar concentrations of NDGA were found in most reports to activate the mentioned kinase pathways. This effect is most likely due to the redox cycling nature of NDGA which, depending on dosing and cell type, induces a mild oxidative stress and alteration of redox sensitive cysteines in particular proteins by sulfhydryl modification, as well as GSH depletion. For instance, NDGA-mediated apoptosis in the murine prolymphocytic cell line FL5.12 was shown to be independent of LOX inhibition but was partially related to p38 activation, and was prevented by the antioxidant N-acetyl cysteine (Deshpande and Kehrer, 2006). In fact, redox cycling polyphenols like NDGA can alter the balance between phosphorylation and dephosphorylation by inhibiting redox-sensitive phosphatases (Ostman et al., 2011). An example is PTEN (Phosphatase and Tensin Homolog) in which a catalytic cysteine is required to form a covalent intermediate with the phosphate group in order to be eliminated from the substrate protein. Evidence gathered with the diphenolic compound tBHQ indicates that this cysteine is susceptible to form adducts with the oxidized benzoquinone form of tBHQ, hence triggering PTEN inhibition and consequent AKT activation (Ostman et al., 2011; Rojo et al., 2014). Assuming that the catechol quinone derived from NDGA oxidation behaves as this benzoquinone, it is most likely that NDGA is activating the PI3K/AKT pathway by inhibiting PTEN.

The modulation of MAPKs by NDGA is less clear. It is noteworthy that dual specificity phosphatases (DUSPs), which are involved in shutting down these pathways, exhibit a catalytic cysteine, similar to PTEN. Therefore, a comparable inhibitory effect of NDGA as described for PTEN is suggested, resulting in MAPK activation (Rios et al., 2014). NDGA seems to use this mechanism also in the case of JNK for protection against cerebral ischemia/reperfusion (Liu et al., 2012). The JNK upstream kinase ASK1 is sensitive to oxidative stress through interaction with thioredoxin, and it was demonstrated that the electrophile acrolein alkylates thioredoxin reductase-1 and thioredoxin-activating JNK (Randall et al., 2013). More experimental work is required to determine if NDGA inhibits catalytic cysteines, in particular phosphatases and other proteins, and impacts the signaling networks that are critically involved in various pathologies.

NDGA CAN ACTIVATE NRF2 IN A KEAP1-INDEPENDENT MANNER

As described above, NDGA inhibits the redox sensor KEAP1, leading to NRF2 activation. However, the fact that NDGA can stabilize the protein levels of NRF2, even in fibroblasts derived from *Keap1*-knockout mouse embryos, points towards other mechanisms besides KEAP1 inhibition for regulating NRF2 stability. It was found that NDGA stabilizes NRF2 in a KEAP1-independent manner through phosphorylation of its Neh6 domain (Rojo et al., 2012). In fact, the Neh6 domain was shown to confer instability to a chimera made of cyan fluorescent protein and the Neh6 domain, and this effect was prevented by NDGA. In this domain, NRF2 presents two motifs, DSGIS and DSAPGS, that, upon phosphorylation, are converted into a degradation signal recognized by the E3 ligase adapter beta-TrCP (beta-transducin repeat-containing protein) (Cuadrado, 2015). This protein connects phospho-NRF2 with the CUL1-RBX1 ubiquitin ligase complex, and promotes its degradation (**Figure 3B**). The kinase involved in phosphorylation of the DSAPGS motif was not identified (Chowdhry et al., 2013), but it is known that the DSGIS motif is phosphorylated by the serine/threonine protein kinases GSK-3α and GSK-3β (Cuadrado, 2015). GSK-3 is an active kinase under resting conditions, but it is inhibited upon growth factor signaling by phosphorylation of its N-terminal domain (Serine 21 and Serine 9 in GSK-3α and GSK3β, respectively) (Rada et al., 2011; Rada et al., 2012). A very well established kinase involved in GSK-3 phosphorylation is AKT (Van Weeren et al., 1998; Woodgett, 2005). NDGA mimics growth factor signaling to activate AKT, rendering GSK-3 inactive and preventing the formation of the DSGIS phosphodegron (Rada et al., 2011; Rada et al., 2012). It has also been reported that p38 inhibits human GSK-3β through phosphorylation of T390 (Thornton et al., 2008) and therefore NDGA might also contribute to inhibition of GSK-3 and subsequent stabilization of NRF2 *via* activation of the p38 pathway, but this mechanism needs remains to be demonstrated.

NDGA AS A THERAPEUTIC AGENT

NDGA Protects Against Renal Damage

Deterioration of renal function is associated with impairment of the electrolyte and acid balance, resulting in irreversible kidney damage and renal necrosis. Therapy may include hemo- and

peritoneal dialysis, and a kidney transplant is required in severe cases. All these therapeutic strategies are helping in alleviating symptoms, but cannot prevent or reverse renal damage. In this context, NDGA has emerged as a novel promising candidate considering that oxidative stress and inflammation are the major pathological mechanisms of nephrotoxicity.

Firstly, the antioxidant capacity of NDGA has been evaluated in renal dysfunction induced by ferric-nitrilotriacetate. NDGA prevented the reduction in the expression of key antioxidant enzymes, such as glutathione-S-transferase, glutathione-reductase, glucose-6-phosphate dehydrogenase, and catalase, that are induced by ferric-nitrilotriacetate. Accordingly, NDGA increased GSH concentration and reduced the levels of oxidative damage markers such as lipid peroxides and oxygen peroxide (Ansar et al., 1999). Similar results were obtained in a later study of streptozotocin-induced nephropathy in rats. Administration of NDGA prevented the increase in renal malondialdehyde levels and the decrease in the renal GSH content, superoxide dismutase and catalase activities, paralleled by the decrease of proteinuria (Anjaneyulu and Chopra, 2004). Moreover, the effect of NDGA on $K_2Cr_2O_7$-induced nephrotoxicity and the associated oxidative/nitrosative stress indicates that when this drug is administered in mini osmotic pumps, it can reduce the levels of the oxidative and nitrosative stress markers 4-hydroxy-2-nonenal and 3-nitrotyrosine, respectively (Yam-Canul et al., 2008). Histologic analysis of slices from $K_2Cr_2O_7$-treated rats showed extensive tubular damage, and most of cortical tubules exhibited epithelial atrophy and casts. Interestingly, $K_2Cr_2O_7$/NDGA-treated rats had lesser tissue damage and fewer epithelial tubular cells were affected. In addition, the levels of urinary N-acetyl-β-d-glucosaminidase, serum creatinine and serum glutathione peroxidase activity were actually normalized after NDGA treatment (Yam-Canul et al., 2008). These results are further supported in rodent models of the human idiopathic nephrotic syndrome, which is based on puromycin aminonucleoside-induced nephrosis. Ultrastructural investigations by electron microscopy showed that podocyte morphology was changed after induction of nephrosis but recovered after NDGA administration. Moreover, protein excretion in urine was significantly lower in the animal groups treated with NDGA than in the control groups (Lee et al., 2009). In diabetic nephropathy, NDGA was also shown to improve renal function by decreasing the ratio of urinary albumin to creatinine, paralleled by a decrease in serum lipid peroxide levels (Gad, 2012). Moreover, NDGA was shown to accelerate the recovery of the renal function after cisplatin treatment. In line with the results of previous studies, NDGA pretreatment prevented oxidative and nitrosative stress, as well as inflammation (restoration of the levels of the anti-inflammatory IL-10 cytokine in the kidney), and preserved the renal function (Mundhe et al., 2019). In a model of polycystic kidney disease, which is characterized by increased levels of renal cyclooxygenase (COX)-derived eicosanoids, NDGA decreased the levels of prostaglandin PGF_2 and LOX-derived metabolites, but this inhibition was not clearly associated with changes in the renal function or disease progression (Ibrahim et al., 2015). In conclusion, NDGA exerts renal protective actions in preclinical models, hence suggesting its therapeutic potential for the treatment of patients with kidney failure and other associated complications.

NDGA Protects Against Liver Disease

The role of NDGA in liver protection has been widely addressed experimentally using various models that mimic key hallmarks of acute hepatotoxicity. Diverse studies have pointed out that both metabolic syndrome and liver damage induced by an unbalanced diet, were improved when NDGA was co-administered. Obesity, insulin resistance, hepatic steatosis and liver fibrosis were attenuated by NDGA in mice fed with high trans-fat, cholesterol, and fructose diet (Han et al., 2019). In mice submitted to a typical American "fast food" diet, NDGA normalized insulin sensitivity, but not glucose intolerance, body and fat pad weight, ALT, AST, and liver triglycerides (Chan et al., 2018). By contrast, in mice fed with a high-fat diet for 8 weeks, NDGA reduced weight gain, fat pad mass and hepatic triglyceride accumulation, and improved serum lipid parameters (Zhang et al., 2016). Further analysis showed that this NDGA effect is underlined by the activation of the AMP-activated protein kinase (AMK) in the liver and in HepG2 hepatocytes. Specific analysis of the mechanism through which NDGA exerts its anti-hypertriglyceridemic action was determined in response to a high-fructose diet. Oral administration of NDGA decreased the plasma levels of glucose, insulin, triglycerides and fatty acids, increased hepatic mitochondrial fatty acid oxidation and attenuated hepatic accumulation of triglycerides (Zhang et al., 2016). In addition, chronic administration of NDGA to obese mice (ob/ob) significantly improved plasma triglycerides levels, inflammatory chemokines levels, hyperinsulinemia, insulin sensitivity and glucose intolerance, while enhancing the rate of fatty acid oxidation (Zhang et al., 2013). Type 2 diabetes mellitus is a complex disease with alterations in metabolic and inflammatory markers which could be spontaneously developed by Stillman Salgado rats. Dain et al. (2016) analyzed in these rats the effects of ω-3 polyunsaturated fatty acids supplementation with or without NDGA added, and they observed that NDGA treatment ameliorated inflammatory, metabolic, and oxidative stress markers (Dain et al., 2016).

NDGA deeply impacts the transcriptomic profile of the liver. Global transcriptional changes have been analyzed in response to chronic administration of NDGA in the context of a high-fructose diet. NDGA upregulated the expression of several genes involved in fatty acid oxidation (*ACOX1*, *CPT1B*, *CPT2*, *ACADVL*, *ECI1,* and *EHHADH*) and *PPARα*, which is the transcription factor considered as the master regulator of fatty acid oxidation. On the other hand, the expression of some lipogenic genes and relevant transcriptional factors were reduced in the NDGA-treated animals (*GCKR, GCK, ACLY, FASN, SCD1, ELOVL2, ELOVL5, FADS1 FADS2, DGAT2, ARF3, HMGCR, INSIG1, INSIG2*). NDGA differentially affected the genes encoding fatty acid transporters, acetyl CoA synthetases, elongases, fatty acid desaturases, and lipid clearance proteins (Zhang et al., 2015). Some of these findings were validated by qRT-PCR and immunoblot in independent studies. NDGA

downregulated the protein level of SREBP-1 and therefore of its target genes, *ACC* and *FAS*. In turn, it upregulated the levels of proteins involved in fatty acid oxidation, such as PPARα, PGC-1, CPT-1L, UCP2 and UCP3 (Lee et al., 2010). The transcription factor PPARα plays a crucial role in the response to NDGA. Both the mRNA and nuclear protein levels of PPARα were upregulated by NDGA (Lee et al., 2010; Zhang et al., 2013). In fact, NDGA increased *PPARα* promoter activity in AML12 hepatocytes. Very relevant, reduction of PPARα expression by siRNA abrogated its stimulatory effect on fatty acid catabolism. Likewise, no stimulatory effect of NDGA on hepatic fatty acid oxidation was observed in the liver of PPARα-deficient mice (Zhang et al., 2013). These findings suggest that NDGA ameliorates hypertriglyceridemia and steatosis primarily by altering the expression of genes encoding key enzymes and transcription factors involved in *de novo* lipogenesis and fatty acid oxidation.

Altogether, these studies strongly suggest that the antioxidant and anti-inflammatory properties of NDGA are involved in its kidney protective effect; whereas its role in liver is closely related to its capacity to increase lipid catabolism. However, we might be aware that NDGA concentration is a key issue to correctly interpret the experimental data. For instance, NDGA exhibits adverse pro-oxidant effects on clone-9 rat hepatocyte cultures in the concentration range of 20-100 μM, while it has beneficial antioxidant effects on rat alveolar macrophages and Chinese hamster lung fibroblasts at concentrations below 10 μM (Robison et al., 1990). As it will be discussed in section *Adverse Effects of NDGA*, a growing body of evidence supports the fact NDGA is deeply impacting kidney and liver physiology, precluding is clinical development.

NDGA Protects Against Neurodegeneration

Extensive data from animal models and human samples provide strong evidence for an early role of redox and neurotransmitter imbalance, inflammation, mitochondrial dysfunction, and altered proteostasis as common mechanisms in the pathogenesis of neurodegenerative diseases that are clinically characterized by progressive loss of neurons and compromised motor or cognitive functions (Ibanez et al., 2004; Alzheimer'sassociation, 2016). Existing therapeutic approaches do not control the unrelenting progression of neurodegeneration, and the therapeutic approaches designed to target individual signaling pathways have failed in clinical studies. As we have reviewed here, NDGA exerts protective effects against various deleterious signals involved in neurodegeneration.

NDGA Modulates Oxidative Stress in the Brain

Compared with other organs, the brain consumes very high oxygen amounts, has low antioxidant defense mechanisms and a high content of polyunsaturated fatty acids that are readily prone to be oxidized. Mitochondrial impairment, resulting in ROS overproduction, is also an underlying mechanism of neurodegeneration (Cenini et al., 2019). These features make the brain especially vulnerable to oxidative stress-induced damage. Therefore, the use of antioxidant compounds which are able to restore the redox balance may greatly help to keep under control the susceptibility of the brain to oxidative damage.

The intrinsic antioxidant activity of NDGA was evidenced in rat brain homogenates by measuring the production of thiobarbituric acid reactive substances, formation of peroxy-lipids and carbonyl-proteins. These redox markers were significantly reduced when the brain extracts were incubated with NDGA (Shishido et al., 2001; Czapski et al., 2012). The neuroprotective effect of NDGA has been also evaluated in neuronal cultures submitted to generic oxidant compounds such as oxygen peroxide (Guzman-Beltran et al., 2008) or iodoacetate (Cardenas-Rodriguez et al., 2009) used as inhibitor of glyceraldehyde-3-phosphate dehydrogenase. In both experimental settings, the neuroprotective effects exerted *in vitro* by NDGA were associated with the prevention of oxidative stress. Additionally, NDGA prevented the increase in ROS and calcium levels, as well as neuronal injury in an *in vitro* model of Alzheimer's disease (AD), consisting in the treatment of neuronal cultures with amyloid beta (Aβ) (Goodman et al., 1994). Moreover, Guzman-Beltran et al. (2008) demonstrated that NDGA protects neurons against 3-nitropropionic acid, a chemical model of Huntington Disease (HD), through the activation of the NRF2 transcription factor. Furthermore, this study pointed out the stimulatory activity of NDGA on the NRF2 target *HMOX1*, which has an important role in neuroprotection (Guzman-Beltran et al., 2008).

Further demonstration of the antioxidant activity of NDGA in the brain has been done using *in vivo* models characterized by increased oxidative stress. For instance, diabetic encephalopathy is a chronic complication of diabetes mellitus that affects the central nervous system. Plasma and brain samples of diabetic rats exhibited higher levels of oxidative stress markers, gamma-glutamyltranspeptidase activity, and hydro-/lipoperoxides than those found in control rats. Interestingly, the levels of those markers were reduced when the rats were injected monthly with NDGA for 12 months (Diaz-Gerevini et al., 2019). In the striatal neurons of the R6/2 mouse model of HD, NDGA markedly reduced the levels of 4-HNE (marker of lipid peroxidation) and preserved mitochondrial morphology and ATP generation. These beneficial effects of NDGA were associated with an increase of the lifespan of HD mice (Lee et al., 2011).

NDGA Regulates Neurotransmission

Alterations in the cholinergic neurotransmission at the cortex and hippocampus are important hallmarks in many forms of dementia (Wilcock et al., 1982; Muir, 1997). In fact, acetylcholinesterase (AChE) inhibitors are currently the main therapeutic tool for restoring acetylcholine levels in the pathogenesis of AD (Arvanitakis et al., 2019). Virtual screening of diverse natural products against AChE revealed that NDGA was among the top scored compounds with an IC_{50} value of 46.2 μM. Moreover, structural modifications of NDGA were performed *in silico* to obtain derivatives with improved blood brain barrier penetration and improved activity in the central nervous system. The new NDGA derivatives were more lipophilic, less flexible and had lower molecular weight than

NDGA. AchE binding analysis showed higher binding affinity for the designed ligands, probably due to higher hydrogen bonding and π–π interactions (Remya et al., 2013).

Chronic excitotoxicity plays a role in many neurodegenerative diseases, having a particular relevance in amyotrophic lateral sclerosis (ALS). Excitotoxicity results from excessive activation of glutamate receptors, and leads to loss of neuronal structures including dendrites and cell bodies (Meldrum and Garthwaite, 1990; Limanaqi et al., 2019). Considering that synaptic accumulation of glutamate is detrimental to neurons, drugs like NDGA, that are capable of increasing glutamate uptake by the astrocytes, might be therapeutically beneficial (Lynch et al., 1989). Indeed, subcutaneous administration of NDGA for 30 days in mice, increased glutamate uptake in synaptosomes from the spinal cord (Boston-Howes et al., 2008). In turn, the effect of NDGA in a mouse model of ALS (SOD1-G93A mouse) is slightly controversial. Initially, oral NDGA administration significantly extended lifespan by 10%, slowed motor dysfunction and triggered a reduction in gliosis and neuron damage (West et al., 2004). However, a later study did not find that NDGA could extend life span of these mice when administered subcutaneously (Boston-Howes et al., 2008).

NDGA Limits Neuroinflammation

Chronic inflammation plays a critical role in neurodegenerative disease and therefore immunosuppressive/modulatory strategies hold great promise. For instance, immune interventions have been successfully applied in the clinic to treat multiple sclerosis (Rieckmann et al., 2008). Several studies analyzed the anti-inflammatory role of NDGA in the context of LOX inhibition and the resulting reduction of harmful arachidonic acid (AA)-derived metabolites. NDGA was shown to prevent ischemic/reperfusion damage in a model of cultured rat cortical neurons that were subjected to oxygen-glucose deprivation (OGD) (Liu et al., 2012). In this study, NDGA reduced the levels of phospho-JNK and phospho-c-JUN, preventing neuronal apoptosis through 12/15-LOX inhibition. In addition, NDGA protected neurons in stroke models based on permanent or transient occlusion of the middle cerebral artery followed by reperfusion (Liu et al., 2012). Moreover, NDGA significantly attenuated post-ischemic learning and memory impairment after transient four-vessel occlusion in rats. Furthermore, consecutive administration of NDGA for 4 days significantly reduced the post-ischemic neuronal death of pyramidal cells in the rat hippocampus (Shishido et al., 2001). In a Parkinson's disease model, the toxic effect of nitric oxide (NO) on GSH-depleted primary midbrain cultures was partially prevented by NDGA (Canals et al., 2003). The anti-inflammatory effects of NDGA were also evaluated in a spinal cord injury model which is characterized by inflammation. In this context, NDGA significantly decreased myeloperoxidase (MPO) levels, as an indicator of neutrophil activity, and also the number of macrophages/microglia cells. In addition, NDGA suppressed the expression of the pro-inflammatory cytokines IL-1β and TNF-α. Of utmost importance, histological analysis of the spinal cord showed an increased number of neurons after NDGA administration and the extent of secondary damage, measured as the number of apoptotic cells and proliferating astrocytes, was significantly decreased (Xue et al., 2013).

Modulation of the IFNγ response by NDGA deserves special attention. It has been proposed that in rat astrocytes, NDGA suppresses the pro-inflammatory response mediated by IFNγ in a LOX-independent manner (Jeon et al., 2005). Thus, in the presence of NDGA, the expression of pro-inflammatory factors such as IRF-1 (interferon regulatory factor-1), MCP-1 (monocyte chemotactic protein-1), interferon-gamma inducible protein-10 (IP-10), and the CXCL10 chemokine) were significantly reduced, as well as the levels of phospho-JAK and phospho-STAT. However, the 5-LOX products LTB4 and LTC4 were not detected in cells treated with IFNγ. In addition, two other 5-LOX inhibitors (Rev5901 and AA861) did not mimic the effect of NDGA, and addition of 5-LOX metabolites did not reverse the NDGA-driven suppression of STAT. These results suggest that NDGA regulates IFNγ-mediated inflammation through mechanisms that are not related to LOX inhibition and might be the result of combined mechanisms, possibly related to NRF2 activation (Cuadrado et al., 2018).

NDGA Prevents Proteinopathy

Proteinopathy is a pathological condition characterized by the formation of protein deposits in the form of amyloid fibrils. In the brain, protein aggregates encompass dimers, oligomers, protofilaments, and fibrils (Stefani, 2010). Thus, misfolded aggregates of α-synuclein are found in PD, β-amyloid (Aβ) plaques and hyper-phosphorylated TAU neurofibrillary tangles in AD, huntingtin in HD, superoxide dismutase 1, and TAR DNA binding protein 43 (TDP-43) in ALS, etc. A growing body of evidence supports a connection between NDGA and amyloidosis. Nusrat et al. (2016) studied this concept using egg white lysozyme (HEWL) as a model protein for amyloidosis. NDGA interferes with the amyloid fibrillogenesis process by hydrophobic interaction with the amino acid residues found in the highly prone amyloid fibril forming region of HEWL, as demonstrated by molecular docking results (Nusrat et al., 2016). Previous studies have also addressed the role of NDGA in Aβ or α-synuclein oligomerization. Particularly, by analyzing the fluorescence derived from the Aβ probe, thioflavin T, Yamada's group showed that NDGA inhibits Aβ fibril formation (Naiki et al., 1998; Ono et al., 2004) and disaggregates Aβ fibrils formed *in vitro* (Ono et al., 2002). These results were confirmed and extended to Aβ protofibrils in a later study, where the authors have combined fluorescence analysis of the thioflavin T probe with electron microscopy. However, the authors established that the NDGA-induced decrease in thioflavin T fluorescence was not accompanied by a reduction in Aβ aggregate size or quantity. To elucidate these controversial results, NDGA supplementation was given to AD transgenic mice (Tg2576) for 10 months starting at the age of 5 months. It was found that Aβ deposition, assessed immunohistochemically, was significantly decreased in the brain of NDGA-treated mice (Moss et al., 2004).

NDGA inhibits dose-dependently α-synuclein oligomerization (Takahashi et al., 2015) due to the binding of multiple molecules of NDGA per α-synuclein molecule (Haney et al., 2017). Recently, it

was shown that NDGA induced modest but progressive compaction of monomeric α-synuclein, hence preventing its aggregation into amyloid-like fibrils. This conformational remodeling preserved the dynamic adoption of α-helical conformations that are essential for physiologic membrane interactions (Daniels et al., 2019). The modulation of α-synuclein dynamics by NDGA was studied in connection with climbing ability in a *Drosophila* PD-model expressing normal human α-synuclein in neurons. Diet supplementation with NDGA for 24 days improved in a dose-dependent manner the locomotor dysfunction exhibited by the mutant flies (Siddique et al., 2012).

NDGA Has Anti-Cancer Action

NDGA exerts *in vitro* anti-cancer effects on various types of tumor and leukemia cell lines in the concentration range 1–100 μM. The mechanisms underlining the observed effects might differ depending on NDGA concentration and the type of cancer cells. In tumor-bearing animal models NDGA was tested in the dose range of 0.750–100 mg/kg body weight (Hernandez-Damian et al., 2014). As shown in **Table 3**, NDGA holds great promise as a therapeutic agent for several types of cancer, as extensively demonstrated by preclinical studies on tumor cell lines and animal/human tumors. The rationale behind the anti-tumor action resides in the fact that most cancer cells are characterized by low-grade oxidative stress and inflammation that provide a survival and growth advantage in the hostile tumor microenvironment, as well as resistance to therapy (Manda et al., 2015). **Table 4** summarizes the nine clinical studies on NDGA and its analog terameprocol (see section *NDGA-Analogs as Novel Therapeutic Small Molecules*), but only two of them have reported results. They will be discussed in the following subsections.

NDGA Exerts Anti-Cancer Effects by LOX Inhibition

Several types of cancer cells exhibit altered LOX expression or activity, and this is highly differentiated according to the involved LOX isoform, cancer cell type and the context. Moreover, the interplay between tumor cells and stroma (epithelial, endothelial and immune cells) is critically involved in tumor progression from the LOX perspective. As demonstrated in colorectal cancer (Mariani et al., 2014), inflammation and necrosis within the tumor niche lead to the recruitment of monocytes and their polarization towards a pro-inflammatory phenotype, hence reinforcing inflammation in the tumor microenvironment through increased production of pro-inflammatory cytokines (TNFα, IL-12 and IL-23). Moreover, stromal, epithelial and endothelial cells express LOXs (5-LOX, 12-LOX), and COX2 which generate potent inflammatory mediators (leukotrienes and prostaglandins) that trigger the recruitment of neutrophils, and consequently amplify inflammation through increased production of ROS and matrix metalloproteinases (MMP). If the inflammatory stimulus is switched-off, the stromal and epithelial cells expressing 15-LOX produce pro-resolving lipoxins, which block neutrophils migration, stimulate the phagocytosis of apoptotic cells by macrophages and polarize macrophages to an anti-inflammatory phenotype. If the stimulus is not resolved, stromal and epithelial cells amplify the inflammatory signals in the tumor niche (IL-1, IL-8, 5-LOX, and 12-LOX), hence inhibiting neutrophils' apoptosis and sustaining tumor growth and metastasis through increased production of ROS and MMPs.

The LOX status plays a critical role in several types of cancer. Increased levels of 12-HETE, the arachidonic acid metabolite derived from 12-LOX activity, promotes the proliferation of human colon, pancreatic and breast cancer cell lines, and plays an important role in cell adhesion and metastasis (Yang et al., 2012). AA turnover was found to be 10 times higher in prostate tumors than in the corresponding normal tissue, and elevated mRNA expression of 12-LOX was found more frequently in advanced stage, high-grade prostate cancer (Gao et al., 1995). 12-LOX sustains the proliferation of prostate cancer cells, favors their metastasis to the bone and stimulates angiogenesis (Tang and Honn, 1999). 12-HETE and 5-HETE, the products of 12-LOX and 5-LOX respectively, were shown to act as pro-growth and pro-survival factors for human prostate cancer cells by inducing a tumor-sustaining inflammatory and oxidative microenvironment. Additionally, 5-LOX promotes the growth of prostate tumor cells by over-activating the c-Myc oncogene, as demonstrated by a whole genome gene expression study (Sarveswaran et al., 2015). Furthermore, 5-LOX and 12-LOX appear to be promising biomarkers and therapeutic targets for prostate cancer stem cells (Yin et al., 2011).

In turn, low levels of the 15-LOX-2 isoform and consequently decreased 15-HETE formation were found as distinctive alterations of AA metabolism in prostate cancer cells. 15-LOX enzymes may exert anti-tumoral effects in particular types of tumors (Klil-Drori and Ariel, 2013) by promoting apoptosis, ferroptosis, or autophagy (Li et al., 2018). For instance, 15-LOX-1 contributes to inflammation resolution through its 13-HODE product (13-hydroxyoctadecadienoic acid) derived from linoleic acid, and has an important role in the terminal differentiation of normal cells. 15-LOX-1 is down-regulated in human colorectal polyps and cancers (Il Lee et al., 2011). In turn, the 5-LOX isoform contributes to tumorigenesis in colorectal cancer, mostly due to the infiltration of mast cells (Cheon et al., 2012; Mashima and Okuyama, 2015).

Altogether, these data highlight that 12- and 5-LOX inhibitors with antioxidant properties, like NDGA, could be efficiently used for targeting simultaneously critical pathological mechanisms in cancer such as proliferation, defective apoptosis, metastasis and angiogenesis, as well as the chronically enhanced oxidative stress in the tumor niche.

Anti-Cancer Effects of NDGA Are Mediated Also by Tyrosine Kinases

NDGA decreases tumor progression in various preclinical models by inhibiting metabolic enzymes that are critically involved in prostate, lung, esophageal and skin cancers (e.g. fatty acid synthase and LOX enzymes) (Lu et al., 2010). Additionally, NDGA inhibits tumor-relevant receptor tyrosine kinases and downstream signaling related to the IGF-1 receptor and the downstream protein serine/threonine kinase AKT, along with the c-ErbB2/HER2/Neu receptor in breast cancer cells and in tumor-bearing mice (Youngren et al., 2005; Li et al., 2009;

TABLE 3 | Some preclinical studies on the effect of NDGA and NDGA analogs in cancer.

Cells/Animal models	Compound	Concentration	Effect/Mechanism of action	Reference
Breast cancer cells: trastuzumab-naive and trastuzumab-refractory HER2-overexpressing SK-BR-3 and BT-474 human cells	NDGA	25-100 μM	Induces DNA fragmentation, cleavage of poly(ADP-ribose) polymerase and caspase-3, and promotes cell death of both trastuzumab-naive and trastuzumab-refractory HER2-overexpressing breast cancer cells. NDGA and trastuzumab suppressed proliferation and survival of trastuzumab-refractory cells to a greater degree than either agent alone	(Rowe et al., 2008)
SiHa cervical cancer cells (grade II squamous cell carcinoma)	NDGA	20-100 μM	Growth inhibition induced by up-regulating p21	(Gao et al., 2011)
Human SW 850 pancreatic and C4-I cervical cancer cells	NDGA	25 μM	Inhibits anchorage-independent growth of pancreatic and cervical tumor cells. Increases apoptosis (cells exhibiting fragmented DNA at 12 h post-exposure to NDGA). Disrupts the actin cytoskeleton and activates JNK and $p38^{mapk}$ before cell detachment	(Seufferlein et al., 2002)
Athymic NMRI/nu-nu mice transplanted with human SW 850 pancreatic and C4-I cervical cancer cells		90 μM	Moderately inhibits tumor growth *in vivo* (delays the growth of pancreatic and cervical human tumors in athymic mice)	
PC3 human prostate cancer cells	NDGA	20-50 μM	Inhibits cell growth in a concentration-dependent and increases intracellular calcium levels (EC_{50} = 30 μM)	(Huang et al., 2004)
	NDGA	10 and 20 μM	Inhibits cell migration and tumor metastasis. Suppresses neuropilin 1 (NRP1) function by downregulating its expression, leading to attenuated cell motility, cell adhesion to extracellular matrix, and FAK signaling in cancer cells	(Moody et al., 1998)
PC3 xenografts (14 and 28 days treatment)	NDGA	50 and 100 mg/kg	Blocks the expression and consequently the function of NRP1 in tumor xenografts	
NCI-H1264 lung cancer cells	NDGA	3–10 μM	Decrease tumor cell growth (3μM) and colony number (10μM)	(Moody et al., 1998)
Non-small-cell lung cancer xenografts (NCI-H157 or H1264 cells) in athymic BALB/c nude mice		0.1% in drinking water for 4 months	Inhibits lung cancer growth and prevents lung carcinogenesis	
Chemically induced (urethane) adenoma in A/J mice				
TA3 grown in CAF 1 Jax mice and 786A cells grown in A Swiss mice	NDGA	25–100 μM (TA3 cells) 42–126 μM (786A cells)	Inhibits the respiration rate of tumor cell lines by preventing electron flow through the respiratory chain, hence decreasing ATP levels, cell viability and culture growth rates.	(Pavani et al., 1994)
Human leukemic HL-60 and U-937 cell lines	NDGA	3–60 μM	Decreases cell viability in a dose-dependent manner • IC_{50} at 48 h in HL-60: 5.8 ± 0.5 • IC_{50} at 72 h in U-937 cells: 7.5 ± 1.0. Inhibits glucose uptake leukemic cell lines through a non-competitive mechanism.	(Leon et al., 2016)
Human red blood cells		0.1–100 μM	Blocks hexose transport in human red blood cells and displaces pre-bound cytochalasin B from erythrocyte ghosts (K_{Dapp}=4.5 μM), possibly through a direct interaction with the glucose transporter GLUT1.	
Lymphatic leukemia P388 cells, grown in the abdominal cavity of DBA2 mice	NDGA	0.01–30 μg/ml	Induces apoptotic death (IC_{50} = 0.66 μg/ml).	(Bibikova et al., 2017)
Multiple myeloma cells (RPMI-8226, LP-1, KMS-18 and KMS-11)	NDGA	0.1–40 μM	Inhibits FGFR3 autophosphorylation both *in vitro* (dramatic reduction induced by 0.5 μM NDGA) and *in vivo* (IC_{50} = 10 μM). Decreases MAPK activation which results in increased apoptosis.	(Meyer et al., 2008)
Acute lymphoblastic leukemia (ALL) (MOLT-4, Jurkat-FADD deficient)	NDGA	2 μM	Protects ALL cells from lipid peroxidation, ROS generation and cell death induced by the small molecule RSL3 (inducer of ferroptosis).	(Probst et al., 2017)
Proliferating C3, C33a, CEM-T4, and TC-1 cells	Terame procol	10–100 μM	Arrests proliferation at the G2 phase (10–40 μM). Reduces mRNA levels and protein production of the cyclin-dependent kinase CDC2 (40 μM), resulting in the inactivation of the maturation promoting factor CDC2/cyclin B complex.	(Heller et al., 2001)
C3-cell induced C57bl/6 mouse tumor model	Terame procol	20 mg/day intratumoral	Substantial tumoricidal activity that correlated with a reduction in tumor cell CDC2 protein levels.	
Leukemic cell lines (OCI-AML3, U937, U937neo, U937XIAP, Jurkat, Jurkatl2.1, HL-60, HL-60neo, HL-60Bcl-2, and HL60Bcl-XL c, KBM5 cells), and	Terame procol	5–40 μM	Inhibits growth and induces cell death in leukemic cell lines and blasts from AML patients. Significant inhibition of AKT phosphorylation was observed in M4N treated OCI-AML3 cells. The effects are not mediated by a mechanism not mediated by Cdc2 and survivin inhibition or by the extrinsic and the mitochondrial apoptotic pathways.	(Mak et al., 2007)

(Continued)

TABLE 3 | Continued

Cells/Animal models	Compound	Concentration	Effect/Mechanism of action	Reference
acute myeloid leukemia (AML) blasts				
Nude mice with xenografts of hepatocellular (Hep 3B) prostate (LNCaP) colorectal (HT-29) breast (MCF7) carcinomas; erythroleukemia (K-562)	Terame procol	2 mg/day for 3 weeks (i.p.) 300 mg/day for 3 weeks (oral)	Suppresses the *in vivo* growth of xenografts. Induces growth arrest and apoptosis in both xenograft tumors and in tumor cells grown in culture, accompanied by reduction in both Cdc2 and tumor-specific s37urvivin gene expression.	(Park et al., 2005)
ICR mice		44 mg/kg (5-40 min, 2–16 h)	Absolute bioavailability of oral M4N: approximately 88%. Minimal drug-related toxicity.	
Glioma stem-like cells (GSLC) Xenografted glioma	*dl*-NDGA (Nordy)	5–60 μM 13.5 mg/kg or 27 mg/kg every other day (8 times)	Inhibits self-renewal and induces differentiation of tumor stem cells *in vitro* (10 μM) and *in vivo.* Inhibits 5-LOX (19 μM). Reduces the GSLC pool through a decrease in the CD133+ population and abrogates clonogenicity. This occurs apparently *via* astrocytic differentiation, by up-regulating GFAP and down-regulating stemness related genes, rather than by inducing apoptosis of GSLCs.	(Wang et al., 2011)

TABLE 4 | Clinical trials with NDAG or its derivate terameprocol.

Compound	Identifier	Disease	Phase	Status	Results
NDGA	NCT00678015	hormone-sensitive non-metastatic prostate cancer	phase 2	terminated	(Friedlander et al., 2012)
NDGA	NCT00313534	Nonmetastatic Relapsed Prostate Cancer	phase 1	terminated	No
terameprocol	NCT00404248	Recurrent High-Grade Glioma	phase 1	completed	(Grossman et al., 2012)
terameprocol	NCT00154089	Cervical Intraepithelial Neoplasia	phase 1/2	completed	No
terameprocol	NCT00259818	Recurrent or Refractory Solid Tumors	phase 1	completed	No
terameprocol	NCT00057512	Refractory Malignant Tumors of the Head and Neck	phase 1	completed	No
terameprocol	NCT00664677	Leukemia	phase 1	terminated	No
terameprocol	NCT00664586	Refractory Solid Tumors	phase 1	terminated	No
terameprocol	NCT02575794	Recurrent High Grade Glioma	phase 1	active	No

See text for discussion of outcomes of the two studies that reported results.

Lu et al., 2010). Of utmost importance for cancer treatment, NDGA inhibits signaling pathways mediated by the transforming growth factor β (TGF-β) type I receptor which triggers Smad2 translocation to the nucleus and its subsequent phosphorylation (Li et al., 2009). As demonstrated in pancreatic cancer cells, TGF-β functions as a tumor suppressor in the early stage of neoplasia, but acts as a pro-tumoral stimulus at later stages (Truty and Urrutia, 2007). Therefore, the moment of NDGA administration during tumor progression may be critical for efficiently controlling tumor growth.

NDGA Promotes Death of Cancer Cells

Another mechanism through which NDGA seems to exert anti-tumoral effects is by directly promoting the death of various tumor cells or by sensitizing tumor cells to other anti-tumor agents. For instance, NDGA increases the susceptibility of prostate and colorectal tumor cells to TRAIL-induced apoptosis by up-regulating the expression of the death receptor 5 (Yoshida et al., 2007), and was also shown to sensitize refractory breast cancer cells to trastuzumab, a monoclonal antibody against HER2 (Rowe et al., 2008).

Precaution should be taken when using NDGA as anti-cancer agent, considering that, in particular types of cancer such as malignant glioma, NDGA can inhibit caspase 8 and 3, poly (ADP-ribose)polymerase cleavage and consequent CD95L-mediated apoptosis (Wagenknecht et al., 1998). Moreover, NDGA at low concentrations (< 0.3 μM) proved to moderately sustain the survival of some leukemic cancer cell lines, but becomes cytotoxic at higher, micromolar concentrations (Shaposhnikova et al., 2001). There is also evidence that LOX inhibitors like NDGA and baicailin can inhibit ferroptotic cell death caused by the accumulation of lipid-based ROS in acute lymphoblastic leukemia cells (Probst et al., 2017).

NDGA Inhibits Metastasis and Angiogenesis

NDGA impacts metastasis of tumor cells through LOX inhibition but also due to down-regulation of neuropilin 1, a single-pass transmembrane protein that functions as a "signaling platform" on the cell surface. Neuropilin 1 is over-expressed in breast, prostate, pancreatic, colon, and kidney cancers, and exerts important roles in tumor progression, angiogenesis and anti-cancer immunity (Rizzolio and Tamagnone, 2011). As shown in human PC3 prostate cells, decreased levels of neuropilin 1, induced by NDGA treatment, lead to alterations in the motility and cell-matrix adhesion, and attenuated tumor metastasis in a nude mice model of prostate cancer. Thus, neuropilin 1 suppression impacts on both tumor cells and the tumor microenvironment by down-regulating angiogenesis and extracellular matrix formation during the progression of metastasis (Li X. et al., 2016).

The formation of new capillaries from preexisting vessels is tightly regulated process that involves a complex network of cells,

soluble factors and extracellular matrix molecules (Nie et al., 2000). Therefore, the persistently deregulated angiogenesis found in cancer is critically involved in promoting tumor growth and metastasis. Vascular endothelial cells express LOX and the resulting eicosanoids have potent biologic activities in these cells. This is probably the reason why NDGA can efficiently limit angiogenesis and hence tumor outgrowth. The pan-LOX inhibitor NDGA and the selective 12-LOX inhibitor baicalein, both exhibiting also antioxidant properties, were shown to reduce the expression of the vascular endothelial growth factor (VEGF) in human prostate cancer PC3 cells through inhibition of Sp1 (specificity protein 1) which is the transcription factor responsible for 12-LOX-mediated stimulation of VEGF (Nie et al., 2006). Moreover, proliferation and angiogenesis are suppressed by NDGA in breast cancer through inhibition of the rapamycin complex 1 (mTORC1), as demonstrated both in cultured breast cancer cells and in xenograft models (Zhang et al., 2012). NDGA reduced the basal level of mTORC1 and suppressed mTORC1 downstream signaling (expression of cyclin D1, hypoxia-inducible factor-α, and VEGF) by disrupting the mTOR/raptor interaction.

Controversies on the Antioxidant Activity of NDGA in Cancer Treatment

As described above, most of the anti-tumor effects of NDGA are supported by its inhibitory action on LOX enzymes and other inflammatory pathways as well as inhibition of receptor tyrosine kinase signaling pathways. Meanwhile, the stimulating action of NDGA on the cytoprotective transcription factor NRF2 raises concerns in oncologic pathologies (Milkovic et al., 2017). Various types of cancers (Kitamura and Motohashi, 2018) are characterized by chronic activation of the cytoprotective NRF2 system which accounts, at least partially, for the selection of more aggressive neoplastic phenotypes by conferring survival and growth advantage, as well as resistance to therapy (Cuadrado et al., 2018). Of utmost importance for cancer recurrence is the unique pattern of persistent NRF2 activation in cancer stem cells which sustains stemness and shields these cells against anti-cancer therapies (Kim et al., 2018). Therefore, activation of the NRF2 pathway by NDGA might be deleterious in advanced stages of cancer. From the antioxidant perspective, NDGA therapy seems to be in fact relevant for chemoprevention in patients at risk and in early steps of carcinogenesis, when persistent exposure of normal cells to oxidative stress and carcinogens may trigger their neoplastic transformation. In this case, NRF2-mediated transcription of cytoprotective genes helps to restore the redox balance, as well as to avoid unwanted DNA mutations and cancer initiation. Nevertheless, intensive research is nowadays ongoing for better defining the boundaries between NRF2 positive and negative effects in cancer, and for establishing a precise rationale for undertaking NRF2 therapeutic targeting (Milkovic et al., 2017). It is worth mentioning that NDGA might turn into a pro-oxidant at higher doses (Biswal et al., 2000; Sahu et al., 2006) which sustains apoptosis of tumor cells, hence supporting the use of NDGA in cancer treatment either as monotherapy or as adjuvant for conventional therapeutic strategies.

NDGA Protects Normal Tissues Against the Deleterious Action of Anti-Cancer Therapies

Mundhe et al. (2015) found that NDGA ameliorated cisplatin-induced nephrotoxicity and was even capable of increasing *in vivo* the anti-tumoral properties of cisplatin in a 7,12-dimethyl benz[a] anthracene (DMBA)-induced breast cancer rat model (Mundhe et al., 2015). Cisplatin is toxic for the kidneys because it promotes the generation of ROS and inhibits the activity of the endogenous antioxidant defense system. The protective action of NDGA was mirrored by the reduction in the levels of serum creatinine and BUN (Blood Urea Nitrogen) and also by the increase of superoxide dismutases protein levels in the breast cancer tissue.

ADVERSE EFFECTS OF NDGA

Despite compelling preclinical evidence on the potential benefits of NDGA treatment in various pathologies, the major drawback for further clinical development is related to its important side-effects (Alderman et al., 1994; Lu et al., 2010). Most of the available information about safety issues in humans has been obtained from consumption of the chaparral infusion, which is a non-standardized mixture of compounds extracted from *Larrea*, in which NDGA is the main constituent and may generally contain uncontrolled carcinogens or tumor promoters (Gold and Slone, 2003; Bode and Dong, 2015). Nevertheless, preclinical data gathered with pure NDGA indicate that many of the toxic effects of chaparral tea can be attributed to this compound, particularly in kidney and liver damage.

Kidney toxicity associated with NDGA, leading to cystic nephropathy, was initially reported in rats (Goodman et al., 1970). Later on, a case report in humans further associated high consumption of chaparral tea with cystic renal disease and cystic adenocarcinoma of the kidney (Smith et al., 1994). The liver is also highly affected by high consumption of NDGA in the form of chaparral tea. Thus, prolonged consumption of this infusion for over 10 months led to severe non-viral hepatitis (Gordon et al., 1995). The effects can be attributed to NDGA since a later study in mice demonstrated that intraperitoneal administration of NDGA dose-dependently increases the levels alanine aminotransferase in serum (Lambert et al., 2002). The toxic effect may be related, at least in part, to the conversion of NDGA to its *ortho*-quinone form. Indeed, a study performed with clone-9 rat hepatocytes demonstrated that exposure to high concentrations of NDGA (up to 100 μM) caused lipid peroxidation, DNA double-strand breaks and cell death (Sahu et al., 2006). In addition to kidney and liver damage, other organs are also affected by prolonged or high NDGD dosing. A clinical trial addressing the pharmacokinetics and efficacy of NDGA in non-metastatic recurrent prostate cancer evidenced the following side-effects on 12 patients, at a dosage of 2000 mg/day given orally in three divided doses: diarrhea (12/12), fatigue (5/12), headache (4/12), abdominal distension, and nausea (3/12). Elevated levels of alanine aminotransferase (8/1), aspartate aminotransferase (6/12), bilirubin (3/12), and alkaline phosphatase (2/12) were registered (Friedlander et al., 2012).

Although, the reported toxic doses of NDGA in humans and experimental animals generally exceeded the traditional use of

the plant (Arteaga et al., 2005), based on the evidence of hepatotoxicity and nephrotoxicity the US Food and Drug Administration (FDA) removed NDGA from the list of Generally Regarded As Safe (GRAS) compounds. Moreover, food containing any added NDGA is deemed to be adulterated in violation of the act based upon an order published by FDA in the Federal Register in April 11, 1968.

The toxicity related to NDGA is most likely due to the oxidation of the catechol rings to their corresponding quinones, leading to adduct formation in proteins and glutathione depletion (Billinsky et al., 2007; Jeong et al., 2017). Moreover, catechol quinones form depurinating DNA adducts and DNA double strand brakes, leading to cancer and other diseases (Cavalieri et al., 2002). Therefore, NDGA analogues with potentially low toxicity are being developed by protecting the catechol groups from oxidation to their *ortho*-quinone derivative.

NDGA-ANALOGS AS NOVEL THERAPEUTIC SMALL MOLECULES

Several NDGA analogs are currently in various phases of development, aiming to increase therapeutic efficacy while limiting side-effects. **Figure 4** shows the most relevant NDGA analogs under clinical development.

Recently, a series of NDGA analogs with modified catechol rings were shown to correct metabolic alterations related to hepatic lipid metabolism in a high fructose diet-fed rat model of dyslipidemia, insulin resistance and hypertension (Singh et al., 2019). Oral gavage of these analogs reduced the hepatic and plasma levels of triacylglycerides. In particular, Nordy [(5,5-(2,3-dimethylbutane1,4-diyl)bis(benzo[*d*][1,3]dioxole); **Figure 4**] was very effective at inhibiting the expression of several genes involved in triacylglycerides synthesis (*Scd*, *Gpam* and *Dgat2*) and fatty acid elongation (*Elovl2* and *Elovl5*). These effects were consistent with inhibition of transcription factors SREBP-1c (sterol regulatory element binding transcription factor 1c) and ChREBP (carbohydrate-responsive element-binding protein). In contrast to NDGA, these analogues did not alter the expression of genes involved in hepatic fatty acid oxidation or transport.

In ischemic stroke, oxidative damage is a crucial factor. Novel NDGA analogs have been developed that combine potent ROS scavenging and NRF2 activation (Huang et al., 2018). **Compound 3a** of this study [(2Z, 5E)-2,5-bis (3,4-dihydroxybenzylidene)cyclopentanone; **Figure 4**] was more effective than the antioxidant edaravone in reducing brain infarction after cerebral ischemia-reperfusion injury in rats subjected to transient middle cerebral artery occlusion. However, this study did not compare the efficacy of this compound *vs.* NDGA in stroke protection or in overall toxicity and therefore, its benefit over NDGA remains to be ascertained.

High concentrations of NDGA are required to inhibit tumor growth, thus yielding toxicity. Therefore, an intensive search has been made to develop NDGA analogs with low toxicity. This is the case of tetra-O-methyl nordihydroguaiaretic acid, also called Terameprocol, M4N or EM-1421. As shown in **Figure 4**, in this

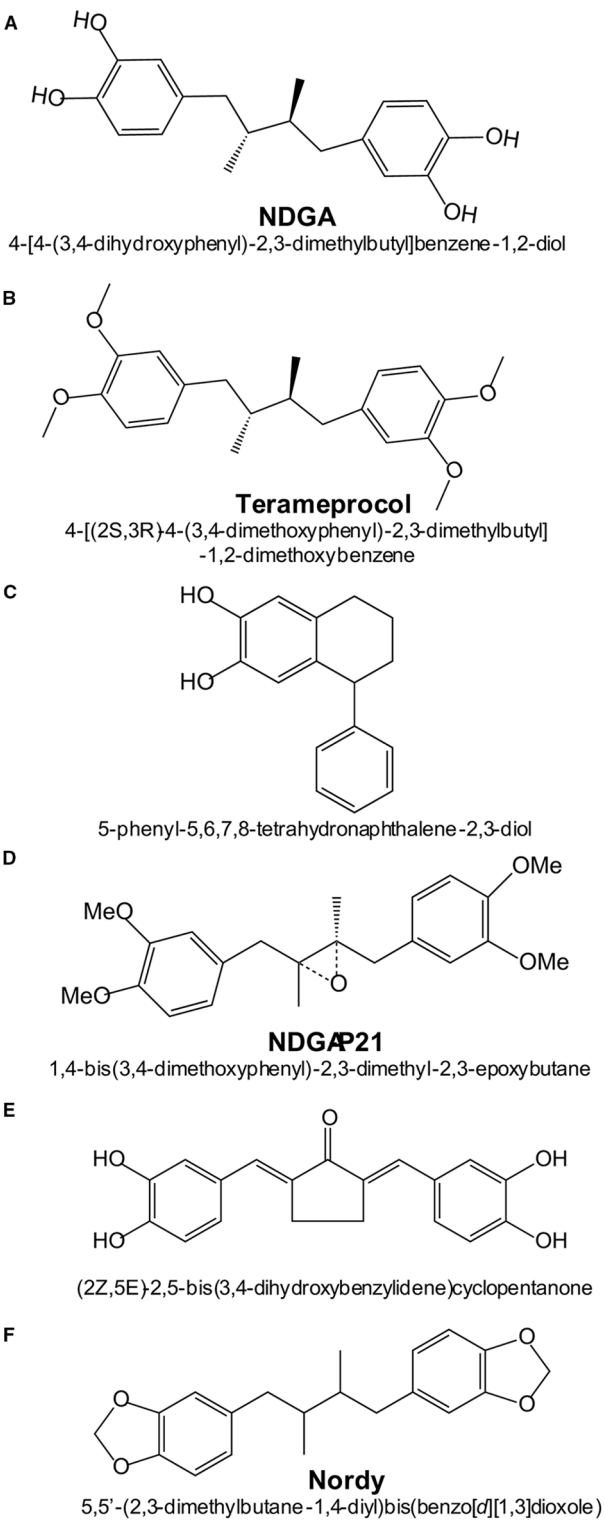

FIGURE 4 | Chemical structures and names of NDGA and NDGA-analogs: **(A)** NDGA (PubChem ID 4534); **(B)** Terameprocol (PubChem ID 476861); **(C)** Re-draw of NDGA-analog reported in (Blecha et al., 2007); **(D)** Re-draw of NDGA-analog reported in (Zhao et al., 2017); **(E)** Re-draw of NDGA-analog reported in (Huang et al., 2018).

molecule the four hydroxyl groups of the two catechol rings have been methylated, thus preventing the formation of catechol quinones. While NDGA intraperitoneally injected in mice has a LD_{50} value of 75 mg/kg, in a phase 1 clinical study it was found that Terameprocol is well-tolerated even at 1700 g/kg in humans (Chang et al., 2004). Terameprocol induces rapid cell death in combination with Etoposide and Rapamycin in prostate LNCaP cells, both *in vitro* and in animal experiments (Eads et al., 2009). Terameprocol entered Phase I/II clinical trials in patients with recurrent high grade lymphoma (Grossman et al., 2012) or advanced forms of leukemia (Tibes et al., 2015), but proved only low anti-tumor activity. Nevertheless, these clinical studies emphasized that Terameprocol has an improved toxicological profile as compared to NDGA and further reshaping could improve its anti-cancer activity. The pharmacological target appears to be the transcription factor Sp1 which controls a large number of genes, and therefore Terameprocol exerts pleiotropic effects: 1) it induces caspase-7 cleavage and inhibits autophagy by suppressing ATG5 and BNIP3; 2) it broadly modulates metabolic processes related to glucose-6-phosphate/glucose-1-phosphate/UDP-glucose; 3) it reduces glutathione levels by up-regulation of CHAC1, a key enzyme that affects the stress pathways; 4) it suppresses energy metabolism by inhibiting the mitochondrial electron transport system (like NDGA), along with the TCA cycle; 5) it induces oxidative stress by decreasing the content of glutathione and propionylcarnitine, a superoxide scavenger. Transcriptomic and metabolomic analysis using high-throughput screening methods (GC/LC-MS and deep RNA sequencing) revealed that Terameprocol is a global transcriptional repressor of genes that are dependent on the Sp1 transcription factor. Studies in glioblastoma primary cultures and cell lines have shown that Terameprocol, in combination with temozolomide (TMZ), down-regulates the expression of Cdk1 and survivin, while the survivin-2B variant was up-regulated (Castro-Gamero et al., 2013). In this study, Terameprocol decreased cell proliferation separately and synergistically with TMZ, enhanced the effects of radiotherapy, especially when associated with TMZ, induced apoptotic cell death, decreased the mitotic index and arrested the cell cycle mainly in the G2/M phase. Once again it was demonstrated that Terameprocol could be successfully used as co-therapy in various types of cancer.

Blecha *et al.* prepared a series of NDGA-analogs to be more potent and selective against MCF-7 breast cancer cells by targeting the IGF-1 receptor (IGF-1R) or 15-LOX (Blecha et al., 2007). The NDGA analogs consisted of introducing various substituents into one of the two catechol rings. One of the analogs (5-phenyl-5,6,7,8-tetrahydronaphthalene-2,3-diol) showed higher specificity for IGF-1R (Blecha et al., 2007). Zhao et al. demonstrated that the NDGA analog NDGA-P21 [1, 4-bis (3, 4-dimethoxy phenyl)-2, 3-dimethyl-2, 3-epoxy butane] was capable of inhibiting the *in vitro* proliferation of glioma cells and their stemness. Under the action of NDGA-P21, the cell cycle was arrested in the G0/G1 phase. However, NDGA-P21 has limited water solubility which is a major drawback for further clinical development (Zhao et al., 2017).

In a very interesting work, Asiamah et al. found that the oxidative cyclization of NDGA forms a dibenzocyclooctadiene, which may have therapeutic benefits (Asiamah et al., 2015). Certain NDGA-analogs may be more susceptible to cyclize. Only NDGA-analogs that have two catechols have the capacity to form dibenzocyclooctadienes. The formation of quinones may not be a necessary step for the formation of dibenzocyclooctadienes, and cyclization depends on radicals (Asiamah et al., 2015). Furthermore, in order to test the hypothesis of reactive intermediate metabolites of NDGA, Asiamah et al. (2015) synthesized catechol- and phenol-type analogs of NDGA, aiming to study the formation of quinone-types, and found that the phenol-type NDGA-analogs are probably safer for clinical applications. It was presumed that the formed quinone-type methide would depend on the substitution in the aromatic rings, but found no evidence that *para*-quinone methide was formed, thereby suggesting that the reactive intermediate metabolite of NDGA that is toxic for the liver is *ortho*-quinone methide (Asiamah and Krol, 2018). Altogether, compelling preclinical and clinical evidence highlighted that some of the newly designed NDGA analogs hold great promise as therapeutic agents for cancer treatment, either as monotherapy or in combination with conventional anti-cancer agents.

Regarding the role of NDGA-derivatives in neurodegenerative disease, Daniels et al. (2019) found that the cyclized NDGA analog prevented the aggregation of α-synuclein into amyloid-like fibrils by producing modified monomers of α-synuclein that are aggregation-resistant. Cyclized NDGA reduced neurodegeneration in a *Caenorhabditis elegans* α-synuclein-driven neurodegeneration model. The cyclized NDGA analog has to be capable of oxidation because this fact is critical for preventing α-synuclein aggregation (Daniels et al., 2019). Huang et al. (2018) synthesized NDGA-analogs containing curcumin's α, β-unsaturated ketone moiety (Huang et al., 2018). The analogs provided cytoprotection against oxidative damage. One of the analogs [(2Z,5E)-2,5-bis(3,4-dihydroxybenzylidene] cyclopentanone) promoted NRF2 translocation to the nucleus and the expression of heme oxigenase-1 *in vitro* in PC12 cells (pheochromocytoma of the rat adrenal medulla). This analog was proposed for the treatment of cerebral ischemia-reperfusion injury in stroke, especially due to its lower cytotoxicity compared to other analogs, protection against hydrogen peroxide and reduction of lipid peroxidation markers such as MDA.

CONCLUDING REMARKS

For over 60 years, preclinical studies in cell culture and rodents indicate that the lignan NDGA is a promising drug for prevention or therapy of several chronic diseases and cancer. However, very little progress has been made in the translation of these studies to a clinical setting. This fact may reflect the large variety of side effects described for NDGA. While NDGA might be considered as a multi-target small molecule that elicits anti-oxidant and anti-inflammatory responses at particular dose ranges, it is also clear that under many difficult-to-control conditions it may also produce harmful effects. In recent years a new impulse to this field has been given with the development of NDGA analogs that

might be more potent and target-selective, and at the same time exhibit lower toxicity due to prevention of the catechol conversion into quinone. This is the case of Terameprocol, currently used in several clinical trials on cancer. Also, some NDGA analogs are promising in neurodegenerative disorders and in metabolic syndrome. However, much work needs to be done in order to define and attain a safe pharmacological profile of NDGA derivatives. Increasing the knowledge about their pharmacokinetics, pharmacodynamics and mechanisms of action will be crucial to translate findings from traditional medicine to official medicine.

AUTHOR CONTRIBUTIONS

GM wrote the section addressing lipoxygenases and cancer, and participated in writing of all sections. EM-K, JP-C, and AR wrote the sections on liver and kidney diseases. AR wrote the section neurodegenerative diseases. AC wrote the remaining sections and participated in writing of all sections.

FUNDING

This work was supported by SAF2016-76520-R of the Spanish Ministry of Economy and Competiveness; P-024-FTPGB 2018 from the Spanish "Tatiana de Guzman el Bueno Foundation" and by the P_37_732/2016 grant (REDBRAIN) financed by the European Regional Development Fund, Competitiveness Operational Program 2014–2020. EM-K was financed by a Postdoctoral Scholarship from Consejo Nacional de Ciencia y Tecnología (CONACY, Mexico) with support from the Posgrado en Ciencias Biológicas at UNAM. Comunidad Autónoma de Madrid (grant B2017/BMD-3827).

REFERENCES

Abou-Gazar, H., Bedir, E., Takamatsu, S., Ferreira, D., and Khan, I. A. (2004). Antioxidant lignans from larrea tridentata. *Phytochemistry* 65, 2499–2505. doi: 10.1016/j.phytochem.2004.07.009

Alderman, S., Kailas, S., Goldfarb, S., Singaram, C., and Malone, D. G. (1994). Cholestatic hepatitis after ingestion of chaparral leaf: confirmation by endoscopic retrograde cholangiopancreatography and liver biopsy. *J. Clin. Gastroenterol.* 19, 242–247. doi: 10.1097/00004836-199410000-00016

Alzheimer'sassociation (2016). 2016 Alzheimer's disease facts and figures. *Alzheimers Dement* 12, 459–509. doi: 10.1016/j.jalz.2016.03.001

Anjaneyulu, M., and Chopra, K. (2004). Nordihydroguairetic acid, a lignin, prevents oxidative stress and the development of diabetic nephropathy in rats. *Pharmacology* 72, 42–50. doi: 10.1159/000078631

Ansar, S., Iqbal, M., and Athar, M. (1999). Nordihydroguairetic acid is a potent inhibitor of ferric-nitrilotriacetate-mediated hepatic and renal toxicity, and renal tumour promotion, in mice. *Carcinogenesis* 20, 599–606. doi: 10.1093/carcin/20.4.599

Arteaga, S., Andrade-Cetto, A., and Cardenas, R. (2005). Larrea tridentata (Creosote bush), an abundant plant of Mexican and US-American deserts and its metabolite nordihydroguaiaretic acid. *J. Ethnopharmacol.* 98, 231–239. doi: 10.1016/j.jep.2005.02.002

Arvanitakis, Z., Shah, R. C., and Bennett, D. A. (2019). Diagnosis and management of dementia: review. *JAMA* 322, 1589–1599. doi: 10.1001/jama.2019.4782

Asiamah, I., and Krol, E. S. (2018). Quadrupole linear ion-trap mass spectrometry studies on glutathione conjugates of nordihydroguaiaretic acid (NDGA) analogues reveals phenol-type analogues are without reactive metabolite-mediated toxic liability. *Cogent. Chem.* 4. doi: 10.1080/23312009.2018.1562858

Asiamah, I., Hodgson, H. L., Maloney, K., Allen, K. J., and Krol, E. S. (2015). Ring substitution influences oxidative cyclisation and reactive metabolite formation of nordihydroguaiaretic acid analogues. *Bioorg. Med. Chem.* 23, 7007–7014. doi: 10.1016/j.bmc.2015.09.039

Bibikova, M. V., Spiridonova, N. A., Korystova, A. F., Kublik, L. N., Levitman, M. K., Shaposhnikova, V. V., et al. (2017). Lipoxygenase inhibitors nordihydroguaiaretic acid and fungus lecanicillum lecanii extract induce death of lymphoid leukemia cells. *Bull. Exp. Biol. Med.* 163, 330–333. doi: 10.1007/s10517-017-3796-9

Billinsky, J. L., and Krol, E. S. (2008). Nordihydroguaiaretic acid autoxidation produces a schisandrin-like dibenzocyclooctadiene lignan. *J. Nat. Prod.* 71, 1612–1615. doi: 10.1021/np8001354

Billinsky, J. L., Marcoux, M. R., and Krol, E. S. (2007). Oxidation of the lignan nordihydroguaiaretic acid. *Chem. Res. Toxicol.* 20, 1352–1358. doi: 10.1021/tx700205j

Biswal, S. S., Datta, K., Shaw, S. D., Feng, X., Robertson, J. D., and Kehrer, J. P. (2000). Glutathione oxidation and mitochondrial depolarization as mechanisms of nordihydroguaiaretic acid-induced apoptosis in lipoxygenase-deficient FL5.12 cells. *Toxicol. Sci.* 53, 77–83. doi: 10.1093/toxsci/53.1.77

Blecha, J. E., Anderson, M. O., Chow, J. M., Guevarra, C. C., Pender, C., Penaranda, C., et al. (2007). Inhibition of IGF-1R and lipoxygenase by nordihydroguaiaretic acid (NDGA) analogs. *Bioorg. Med. Chem. Lett.* 17, 4026–4029. doi: 10.1016/j.bmcl.2007.04.092

Bode, A. M., and Dong, Z. (2015). Toxic phytochemicals and their potential risks for human cancer. *Cancer Prev. Res. (Phila)* 8, 1–8. doi: 10.1158/1940-6207.CAPR-14-0160

Boston-Howes, W., Williams, E. O., Bogush, A., Scolere, M., Pasinelli, P., and Trotti, D. (2008). Nordihydroguaiaretic acid increases glutamate uptake *in vitro* and *in vivo*: therapeutic implications for amyotrophic lateral sclerosis. *Exp. Neurol.* 213, 229–237. doi: 10.1016/j.expneurol.2008.06.010

Braeckman, R. A., Granneman, G. R., Locke, C. S., Machinist, J. M., Cavannaugh, J. H., and Awni, W. M. (1995). The pharmacokinetics of zileuton in healthy young and elderly volunteers. *Clin. Pharmacokinet* 29 Suppl 2, 42–48. doi: 10.2165/00003088-199500292-00007

Brandt, S. L., and Serezani, C. H. (2017). Too much of a good thing: how modulating LTB4 actions restore host defense in homeostasis or disease. *Semin. Immunol.* 33, 37–43. doi: 10.1016/j.smim.2017.08.006

Canals, S., Casarejos, M. J., De Bernardo, S., Rodriguez-Martin, E., and Mena, M. A. (2003). Nitric oxide triggers the toxicity due to glutathione depletion in midbrain cultures through 12-lipoxygenase. *J. Biol. Chem.* 278, 21542–21549. doi: 10.1074/jbc.M213174200

Canning, P., Sorrell, F. J., and Bullock, A. N. (2015). Structural basis of Keap1 interactions with Nrf2. *Free Radic. Biol. Med.* 88, 101–107. doi: 10.1016/j.freeradbiomed.2015.05.034

Cardenas-Rodriguez, N., Guzman-Beltran, S., Medina-Campos, O. N., Orozco-Ibarra, M., Massieu, L., and Pedraza-Chaverri, J. (2009). The effect of nordihydroguaiaretic acid on iodoacetate-induced toxicity in cultured neurons. *J. Biochem. Mol. Toxicol.* 23, 137–142. doi: 10.1002/jbt.20278

Castro-Gamero, A. M., Borges, K. S., Moreno, D. A., Suazo, V. K., Fujinami, M. M., De Paula Gomes Queiroz, R., et al. (2013). Tetra-O-methyl nordihydroguaiaretic acid, an inhibitor of Sp1-mediated survivin transcription, induces apoptosis and acts synergistically with chemo-radiotherapy in glioblastoma cells. *Invest. New Drugs* 31, 858–870. doi: 10.1007/s10637-012-9917-4

Cavalieri, E. L., Li, K. M., Balu, N., Saeed, M., Devanesan, P., Higginbotham, S., et al. (2002). Catechol ortho-quinones: the electrophilic compounds that form depurinating DNA adducts and could initiate cancer and other diseases. *Carcinogenesis* 23, 1071–1077. doi: 10.1093/carcin/23.6.1071

Cenini, G., Lloret, A., and Cascella, R. (2019). Oxidative Stress in neurodegenerative diseases: from a mitochondrial point of view. *Oxid. Med. Cell Longev* 2019, 2105607. doi: 10.1155/2019/2105607

Chan, J. K. W., Bittner, S., Bittner, A., Atwal, S., Shen, W. J., Inayathullah, M., et al. (2018). Nordihydroguaiaretic acid, a lignan from larrea tridentata (Creosote Bush), protects against american lifestyle-induced obesity syndrome diet-induced metabolic dysfunction in mice. *J. Pharmacol. Exp. Ther.* 365, 281–290. doi: 10.1124/jpet.117.243733

Chang, C. C., Heller, J. D., Kuo, J., and Huang, R. C. (2004). Tetra-O-methyl nordihydroguaiaretic acid induces growth arrest and cellular apoptosis by inhibiting Cdc2 and survivin expression. *Proc. Natl. Acad. Sci. U. S. A* 101, 13239–13244. doi: 10.1073/pnas.0405407101

Chen, T. Y., Shiao, M. S., and Pan, B. S. (2005). Inhibition of 12- and 15-lipoxygenase activities and protection of human and tilapia low density lipoprotein oxidation by I-Tiao-Gung (Glycine tomentella). *Lipids* 40, 1171–1177. doi: 10.1007/s11745-005-1482-1

Cheon, E. C., Strouch, M. J., Krantz, S. B., Heiferman, M. J., and Bentrem, D. J. (2012). Genetic deletion of 5-lipoxygenase increases tumor-infiltrating macrophages in Apc(Delta468) mice. *J. Gastrointest Surg.* 16, 389–393. doi: 10.1007/s11605-011-1761-x

Chichirau, A., Flueraru, M., Chepelev, L. L., Wright, J. S., Willmore, W. G., Durst, T., et al. (2005). Mechanism of cytotoxicity of catechols and a naphthalenediol in PC12-AC cells: the connection between extracellular autoxidation and molecular electronic structure. *Free Radic. Biol. Med.* 38, 344–355. doi: 10.1016/j.freeradbiomed.2004.10.035

Chowdhry, S., Zhang, Y., Mcmahon, M., Sutherland, C., Cuadrado, A., and Hayes, J. D. (2013). Nrf2 is controlled by two distinct beta-TrCP recognition motifs in its Neh6 domain, one of which can be modulated by GSK-3 activity. *Oncogene* 32, 3765–3781. doi: 10.1038/onc.2012.388

Cuadrado, A., Manda, G., Hassan, A., Alcaraz, M. J., Barbas, C., Daiber, A., et al. (2018). Transcription factor NRF2 as a therapeutic target for chronic diseases: a systems medicine approach. *Pharmacol. Rev.* 70, 348–383. doi: 10.1124/pr.117.014753

Cuadrado, A., Rojo, A. I., Wells, G., Hayes, J. D., Cousin, S. P., Rumsey, W. L., et al. (2019). Therapeutic targeting of the NRF2 and KEAP1 partnership in chronic diseases. *Nat. Rev. Drug Discovery* 18, 295–317. doi: 10.1038/s41573-018-0008-x

Cuadrado, A. (2015). Structural and functional characterization of Nrf2 degradation by glycogen synthase kinase 3/beta-TrCP. *Free Radic. Biol. Med.* 88, 147–157. doi: 10.1016/j.freeradbiomed.2015.04.029

Cullinan, S. B., Gordan, J. D., Jin, J., Harper, J. W., and Diehl, J. A. (2004). The Keap1-BTB protein is an adaptor that bridges Nrf2 to a Cul3-based E3 ligase: oxidative stress sensing by a Cul3-Keap1 ligase. *Mol. Cell Biol.* 24, 8477–8486. doi: 10.1128/MCB.24.19.8477-8486.2004

Czapski, G. A., Czubowicz, K., and Strosznajder, R. P. (2012). Evaluation of the antioxidative properties of lipoxygenase inhibitors. *Pharmacol. Rep.* 64, 1179–1188. doi: 10.1016/S1734-1140(12)70914-3

Dain, A., Repossi, G., Diaz-Gerevini, G. T., Vanamala, J., Das, U. N., and Eynard, A. R. (2016). Long chain polyunsaturated fatty acids (LCPUFAs) and nordihydroguaiaretic acid (NDGA) modulate metabolic and inflammatory markers in a spontaneous type 2 diabetes mellitus model (Stillman Salgado rats). *Lipids Health Dis.* 15, 205. doi: 10.1186/s12944-016-0363-8

Daniels, M. J., Nourse, J. B.Jr., Kim, H., Sainati, V., Schiavina, M., Murrali, M. G., et al. (2019). Cyclized NDGA modifies dynamic alpha-synuclein monomers preventing aggregation and toxicity. *Sci. Rep.* 9, 2937. doi: 10.1038/s41598-019-39480-z

Deshpande, V. S., and Kehrer, J. P. (2006). Oxidative stress-driven mechanisms of nordihydroguaiaretic acid-induced apoptosis in FL5.12 cells. *Toxicol. Appl. Pharmacol.* 214, 230–236. doi: 10.1016/j.taap.2005.12.011

Diaz-Gerevini, G. T., Dain, A., Pasqualini, M. E., Lopez, C. B., Eynard, A. R., and Repossi, G. (2019). Diabetic encephalopathy: beneficial effects of supplementation with fatty acids omega3 and nordihydroguaiaretic acid in a spontaneous diabetes rat model. *Lipids Health Dis.* 18, 43. doi: 10.1186/s12944-018-0938-7

Eads, D., Hansen, R., Oyegunwa, A., Cecil, C., Culver, C., Scholle, F., et al. (2009). Terameprocol, a methylated derivative of nordihydroguaiaretic acid, inhibits production of prostaglandins and several key inflammatory cytokines and chemokines. *J. Inflammation (Lond)* 6, 2. doi: 10.1186/1476-9255-6-2

Estrada-Valencia, M., Herrera-Arozamena, C., Pérez, C., Viña, D., Morales-García, J. A., Pérez-Castillo, A., et al. (2019). New flavonoid – N,N-dibenzyl (N-methyl)amine hybrids: Multi-target-directed agents for Alzheimer´s disease endowed with neurogenic properties. *J. Enzyme Inhib Med. Chem.* 34. doi: 10.1080/14756366.2019.1581184

Evan, A. P., and Gardner, K. D.Jr. (1979). Nephron obstruction in nordihydroguaiaretic acid-induced renal cystic disease. *Kidney Int.* 15, 7–19. doi: 10.1038/ki.1979.2

Floriano-Sanchez, E., Villanueva, C., Medina-Campos, O. N., Rocha, D., Sanchez-Gonzalez, D. J., Cardenas-Rodriguez, N., et al. (2006). Nordihydroguaiaretic acid is a potent *in vitro* scavenger of peroxynitrite, singlet oxygen, hydroxyl radical, superoxide anion and hypochlorous acid and prevents *in vivo* ozone-induced tyrosine nitration in lungs. *Free Radic. Res.* 40, 523–533. doi: 10.1080/10715760500419365

Friedlander, T. W., Weinberg, V. K., Huang, Y., Mi, J. T., Formaker, C. G., Small, E. J., et al. (2012). A phase II study of insulin-like growth factor receptor inhibition with nordihydroguaiaretic acid in men with non-metastatic hormone-sensitive prostate cancer. *Oncol. Rep.* 27, 3–9.

Funakohi-Tago, M., Sakata, T., Fujiwara, S., Sakakura, A., Sugai, T., Tago, K., et al. (2018). Hydroxytyrosol butyrate inhibits 6-OHDA-induced apoptosis through activation of the Nrf2/HO-1 axis in SH-SY5Y cells. *Eur. J. Pharmacol.* 834, 246–256. doi: 10.1016/j.ejphar.2018.07.043

Gad, H. I. (2012). Effects of pravastatin or 12/15 lipoxygenase pathway inhibitors on indices of diabetic nephropathy in an experimental model of diabetic renal disease. *Saudi Med. J.* 33, 608–616.

Gao, X., Grignon, D. J., Chbihi, T., Zacharek, A., Chen, Y. Q., Sakr, W., et al. (1995). Elevated 12-lipoxygenase mRNA expression correlates with advanced stage and poor differentiation of human prostate cancer. *Urology* 46, 227–237. doi: 10.1016/S0090-4295(99)80198-8

Gao, P., Zhai, F., Guan, L., and Zheng, J. (2011). Nordihydroguaiaretic acid inhibits growth of cervical cancer SiHa cells by up-regulating p21. *Oncol. Lett.* 2, 123–128. doi: 10.3892/ol.2010.205

Gold, L. S., and Slone, T. H. (2003). Aristolochic acid, an herbal carcinogen, sold on the Web after FDA alert. *N Engl. J. Med.* 349, 1576–1577. doi: 10.1056/NEJM200310163491619

Goldfarb, D., Hast, B. E., Wang, W., and Major, M. B. (2014). Spotlite: web application and augmented algorithms for predicting co-complexed proteins from affinity purification–mass spectrometry data. *J. Proteome Res.* 13, 5944–5955. doi: 10.1021/pr5008416

Goodman, T., Grice, H. C., Becking, G. C., and Salem, F. A. (1970). A cystic nephropathy induced by nordihydroguaiaretic acid in the rat. Light and electron microscopic investigations. *Lab. Invest.* 23, 93–107.

Goodman, Y., Steiner, M. R., Steiner, S. M., and Mattson, M. P. (1994). Nordihydroguaiaretic acid protects hippocampal neurons against amyloid beta-peptide toxicity, and attenuates free radical and calcium accumulation. *Brain Res.* 654, 171–176. doi: 10.1016/0006-8993(94)91586-5

Gordon, D. W., Rosenthal, G., Hart, J., Sirota, R., and Baker, A. L. (1995). Chaparral ingestion. The broadening spectrum of liver injury caused by herbal medications. *JAMA* 273, 489–490. doi: 10.1001/jama.1995.03520300063038

Grossman, S. A., Ye, X., Peereboom, D., Rosenfeld, M. R., Mikkelsen, T., Supko, J. G., et al. (2012). Phase I study of terameprocol in patients with recurrent high-grade glioma. *Neuro Oncol.* 14, 511–517. doi: 10.1093/neuonc/nor230

Guzman-Beltran, S., Espada, S., Orozco-Ibarra, M., Pedraza-Chaverri, J., and Cuadrado, A. (2008). Nordihydroguaiaretic acid activates the antioxidant pathway Nrf2/HO-1 and protects cerebellar granule neurons against oxidative stress. *Neurosci. Lett.* 447, 167–171. doi: 10.1016/j.neulet.2008.09.079

Guzman-Beltran, S., Rubio-Badillo, M. A., Juarez, E., Hernandez-Sanchez, F., and Torres, M. (2016). Nordihydroguaiaretic acid (NDGA) and alpha-mangostin inhibit the growth of mycobacterium tuberculosis by inducing autophagy. *Int. Immunopharmacol.* 31, 149–157. doi: 10.1016/j.intimp.2015.12.027

Han, L., Bittner, S., Dong, D., Cortez, Y., Dulay, H., Arshad, S., et al. (2019). Creosote bush-derived NDGA attenuates molecular and pathological changes in a novel mouse model of non-alcoholic steatohepatitis (NASH). *Mol. Cell Endocrinol.* 498, 110538. doi: 10.1016/j.mce.2019.110538

Haney, C. M., Cleveland, C. L., Wissner, R. F., Owei, L., Robustelli, J., Daniels, M. J., et al. (2017). Site-specific fluorescence polarization for studying the disaggregation of alpha-synuclein fibrils by small molecules. *Biochemistry* 56, 683–691. doi: 10.1021/acs.biochem.6b01060

Hayes, J. D., and Dinkova-Kostova, A. T. (2014). The Nrf2 regulatory network provides an interface between redox and intermediary metabolism. *Trends Biochem. Sci.* 39, 199–218. doi: 10.1016/j.tibs.2014.02.002

Heller, J. D., Kuo, J., Wu, T. C., Kast, W. M., and Huang, R. C. (2001). Tetra-O-methyl nordihydroguaiaretic acid induces G2 arrest in mammalian cells and exhibits tumoricidal activity *in vivo*. *Cancer Res.* 61, 5499–5504.

Hernandez-Damian, J., Anderica-Romero, A. C., and Pedraza-Chaverri, J. (2014). Paradoxical cellular effects and biological role of the multifaceted compound nordihydroguaiaretic acid. *Arch. Pharm. (Weinheim)* 347, 685–697. doi: 10.1002/ardp.201400159

Hope, W. C., Welton, A. F., Fiedler-Nagy, C., Batula-Bernardo, C., and Coffey, J. W. (1983). In vitro inhibition of the biosynthesis of slow reacting substance of anaphylaxis (SRS-A) and lipoxygenase activity by quercetin. *Biochem. Pharmacol.* 32, 367–371. doi: 10.1016/0006-2952(83)90569-5

Huang, J. K., Chen, W. C., Huang, C. J., Hsu, S. S., Chen, J. S., Cheng, H. H., et al. (2004). Nordihydroguaiaretic acid-induced Ca2+ handling and cytotoxicity in human prostate cancer cells. *Life Sci.* 75, 2341–2351. doi: 10.1016/j.lfs.2004.04.043

Huang, L., Wang, J., Chen, L., Zhu, M., Wu, S., Chu, S., et al. (2018). Design, synthesis, and evaluation of NDGA analogues as potential anti-ischemic stroke agents. *Eur. J. Med. Chem.* 143, 1165–1173. doi: 10.1016/j.ejmech.2017.09.028

Ibanez, P., Bonnet, A. M., Debarges, B., Lohmann, E., Tison, F., Pollak, P., et al. (2004). Causal relation between alpha-synuclein gene duplication and familial Parkinson's disease. *Lancet* 364, 1169–1171. doi: 10.1016/S0140-6736(04)17104-3

Ibrahim, N. H., Gregoire, M., Devassy, J. G., Wu, Y., Yoshihara, D., Yamaguchi, T., et al. (2015). Cyclooxygenase product inhibition with acetylsalicylic acid slows disease progression in the Han : SPRD-Cy rat model of polycystic kidney disease. *Prostaglandins Other Lipid Mediat.*, 116–117, 19–25. doi: 10.1016/j.prostaglandins.2014.10.005

Il Lee, S., Zuo, X., and Shureiqi, I. (2011). 15-Lipoxygenase-1 as a tumor suppressor gene in colon cancer: is the verdict in? *Cancer Metastasis Rev.* 30, 481–491.

Im, J. Y., and Han, P. L. (2007). Nordihydroguaiaretic acid induces astroglial death *via* glutathione depletion. *J. Neurosci. Res.* 85, 3127–3134. doi: 10.1002/jnr.21431

Jeon, S. B., Ji, K. A., You, H. J., Kim, J. H., Jou, I., and Joe, E. H. (2005). Nordihydroguaiaretic acid inhibits IFN-gamma-induced STAT tyrosine phosphorylation in rat brain astrocytes. *Biochem. Biophys. Res. Commun.* 328, 595–600. doi: 10.1016/j.bbrc.2005.01.025

Jeong, H., Kim, S., Lee, J., Park, J. Y., Zhou, W., Liu, X., et al. (2017). Characterization of phase i and phase ii hepatic metabolism and reactive intermediates of larrea nitida cav. and its lignan compounds. *Phytother. Res.* 31, 140–151. doi: 10.1002/ptr.5742

Kang, I., Park, M., Yang, S. J., and Lee, M. (2019). lipoprotein lipase inhibitor, nordihydroguaiaretic acid, aggravates metabolic phenotypes and alters hdl particle size in the western diet-fed db/db mice. *Int. J. Mol. Sci.* 20. doi: 10.3390/ijms20123057

Katsuoka, F., and Yamamoto, M. (2016). Small Maf proteins (MafF, MafG, MafK): History, structure and function. *Gene* 586, 197–205. doi: 10.1016/j.gene.2016.03.058

Kim, D., Choi, B. H., Ryoo, I. G., and Kwak, M. K. (2018). High NRF2 level mediates cancer stem cell-like properties of aldehyde dehydrogenase (ALDH)-high ovarian cancer cells: inhibitory role of all-trans retinoic acid in ALDH/NRF2 signaling. *Cell Death Dis.* 9, 896. doi: 10.1038/s41419-018-0903-4

Kitamura, H., and Motohashi, H. (2018). NRF2 addiction in cancer cells. *Cancer Sci.* 109, 900–911. doi: 10.1111/cas.13537

Klil-Drori, A. J., and Ariel, A. (2013). 15-Lipoxygenases in cancer: a double-edged sword? *Prostaglandins Other Lipid Mediat.* 106, 16–22.

Kobayashi, A., Kang, M. I., Okawa, H., Ohtsuji, M., Zenke, Y., Chiba, T., et al. (2004). Oxidative stress sensor Keap1 functions as an adaptor for Cul3-based E3 ligase to regulate proteasomal degradation of Nrf2. *Mol. Cell Biol.* 24, 7130–7139. doi: 10.1128/MCB.24.16.7130-7139.2004

Komatsu, M., Kurokawa, H., Waguri, S., Taguchi, K., Kobayashi, A., Ichimura, Y., et al. (2010). The selective autophagy substrate p62 activates the stress responsive transcription factor Nrf2 through inactivation of Keap1. *Nat. Cell Biol.* 12, 213–223. doi: 10.1038/ncb2021

Lambert, J. D., Zhao, D., Meyers, R. O., Kuester, R. K., Timmermann, B. N., and Dorr, R. T. (2002). Nordihydroguaiaretic acid: hepatotoxicity and detoxification in the mouse. *Toxicon* 40, 1701–1708. doi: 10.1016/S0041-0101(02)00203-9

Lee, D. W., Kwak, I. S., Lee, S. B., Song, S. H., Seong, E. Y., Chung, H. C., et al. (2009). Effects of celecoxib and nordihydroguaiaretic acid on puromycin aminonucleoside-induced nephrosis in the rat. *J. Korean Med. Sci.* 24 Suppl, S183–S188. doi: 10.3346/jkms.2009.24.S1.S183

Lee, M. S., Kim, D., Jo, K., and Hwang, J. K. (2010). Nordihydroguaiaretic acid protects against high-fat diet-induced fatty liver by activating AMP-activated protein kinase in obese mice. *Biochem. Biophys. Res. Commun.* 401, 92–97. doi: 10.1016/j.bbrc.2010.09.016

Lee, J., Kosaras, B., Del Signore, S. J., Cormier, K., Mckee, A., Ratan, R. R., et al. (2011). Modulation of lipid peroxidation and mitochondrial function improves neuropathology in Huntington's disease mice. *Acta Neuropathol.* 121, 487–498. doi: 10.1007/s00401-010-0788-5

Leon, D., Parada, D., Vargas-Uribe, M., Perez, A. A., Ojeda, L., Zambrano, A., et al. (2016). Effect of nordihydroguaiaretic acid on cell viability and glucose transport in human leukemic cell lines. *FEBS Open Bio* 6, 1000–1007. doi: 10.1002/2211-5463.12106

Li, F., Pham, J. D., Anderson, M. O., and Youngren, J. F. (2009). Nordihydroguaiaretic acid inhibits transforming growth factor beta type 1 receptor activity and downstream signaling. *Eur. J. Pharmacol.* 616, 31–37. doi: 10.1016/j.ejphar.2009.06.012

Li, Q., Mao, M., Qiu, Y., Liu, G., Sheng, T., Yu, X., et al. (2016). Key role of ROS in the process of 15-Lipoxygenase/15-hydroxyeicosatetraenoiccid-induced pulmonary vascular remodeling in hypoxia pulmonary hypertension. *PloS One* 11, e0149164. doi: 10.1371/journal.pone.0149164

Li, X., Fan, S., Pan, X., Xiaokaiti, Y., Duan, J., Shi, Y., et al. (2016). Nordihydroguaiaretic acid impairs prostate cancer cell migration and tumor metastasis by suppressing neuropilin 1. *Oncotarget* 7, 86225–86238. doi: 10.18632/oncotarget.13368

Li, Q. Q., Li, Q., Jia, J. N., Liu, Z. Q., Zhou, H. H., and Mao, X. Y. (2018). 12/15 lipoxygenase: a crucial enzyme in diverse types of cell death. *Neurochem. Int.* 118, 34–41. doi: 10.1016/j.neuint.2018.04.002

Limanaqi, F., Biagioni, F., Ryskalin, L., Busceti, C. L., and Fornai, F. (2019). Molecular mechanisms linking ALS/FTD and psychiatric disorders, the potential effects of lithium. *Front. Cell Neurosci.* 13, 450. doi: 10.3389/fncel.2019.00450

Liu, Y., Wang, H., Zhu, Y., Chen, L., and Qu, Y. (2012). The protective effect of nordihydroguaiaretic acid on cerebral ischemia/reperfusion injury is mediated by the JNK pathway. *Brain Res.* 1445, 73–81. doi: 10.1016/j.brainres.2012.01.031

Lo, S. C., and Hannink, M. (2006). PGAM5, a Bcl-XL-interacting protein, is a novel substrate for the redox-regulated Keap1-dependent ubiquitin ligase complex. *J. Biol. Chem.* 281, 37893–37903. doi: 10.1074/jbc.M606539200

Lu, J. M., Nurko, J., Weakley, S. M., Jiang, J., Kougias, P., Lin, P. H., et al. (2010). Molecular mechanisms and clinical applications of nordihydroguaiaretic acid (NDGA) and its derivatives: an update. *Med. Sci. Monit.* 16, RA93–R100.

Lynch, M. A., Errington, M. L., and Bliss, T. V. (1989). Nordihydroguaiaretic acid blocks the synaptic component of long-term potentiation and the associated increases in release of glutamate and arachidonate: an *in vivo* study in the dentate gyrus of the rat. *Neuroscience* 30, 693–701. doi: 10.1016/0306-4522(89)90162-0

Ma, Q. (2013). Role of nrf2 in oxidative stress and toxicity. *Annu. Rev. Pharmacol. Toxicol.* 53, 401–426. doi: 10.1146/annurev-pharmtox-011112-140320

Mak, D. H., Schober, W. D., Chen, W., Heller, J., Andreeff, M., and Carter, B. Z. (2007). Tetra-O-methyl nordihydroguaiaretic acid inhibits growth and induces death of leukemia cells independent of Cdc2 and survivin. *Leuk Lymphoma* 48, 774–785. doi: 10.1080/10428190601186143

Manda, G., Isvoranu, G., Comanescu, M. V., Manea, A., Debelec Butuner, B., and Korkmaz, K. S. (2015). The redox biology network in cancer pathophysiology and therapeutics. *Redox Biol.* 5, 347–357. doi: 10.1016/j.redox.2015.06.014

Mariani, F., Sena, P., and Roncucci, L. (2014). Inflammatory pathways in the early steps of colorectal cancer development. *World J. Gastroenterol.* 20, 9716–9731. doi: 10.3748/wjg.v20.i29.9716

Martin, D., Salinas, M., Fujita, N., Tsuruo, T., and Cuadrado, A. (2002). Ceramide and reactive oxygen species generated by H2O2 induce caspase-3-independent degradation of Akt/protein kinase B. *J. Biol. Chem.* 277, 42943–42952. doi: 10.1074/jbc.M201070200

Mashima, R., and Okuyama, T. (2015). The role of lipoxygenases in pathophysiology; new insights and future perspectives. *Redox Biol.* 6, 297–310. doi: 10.1016/j.redox.2015.08.006

Mcmahon, M., Thomas, N., Itoh, K., Yamamoto, M., and Hayes, J. D. (2004). Redox-regulated turnover of Nrf2 is determined by at least two separate protein domains, the redox-sensitive Neh2 degron and the redox-insensitive Neh6 degron. *J. Biol. Chem.* 279, 31556–31567. doi: 10.1074/jbc.M403061200

Mcmahon, M., Thomas, N., Itoh, K., Yamamoto, M., and Hayes, J. D. (2006). Dimerization of substrate adaptors can facilitate cullin-mediated ubiquitylation of proteins by a "tethering". *Mech.: A Two-site Interact. Model Nrf2-Keap1 Complex J. Biol. Chem.* 281, 24756–24768. doi: 10.1074/jbc.M601119200

Meldrum, B., and Garthwaite, J. (1990). Excitatory amino acid neurotoxicity and neurodegenerative disease. *Trends Pharmacol. Sci.* 11, 379–387. doi: 10.1016/0165-6147(90)90184-A

Meyer, G. E., Chesler, L., Liu, D., Gable, K., Maddux, B. A., Goldenberg, D. D., et al. (2007). Nordihydroguaiaretic acid inhibits insulin-like growth factor signaling, growth, and survival in human neuroblastoma cells. *J. Cell Biochem.* 102, 1529–1541. doi: 10.1002/jcb.21373

Meyer, A. N., Mcandrew, C. W., and Donoghue, D. J. (2008). Nordihydroguaiaretic acid inhibits an activated fibroblast growth factor receptor 3 mutant and blocks downstream signaling in multiple myeloma cells. *Cancer Res.* 68, 7362–7370. doi: 10.1158/0008-5472.CAN-08-0575

Milkovic, L., Zarkovic, N., and Saso, L. (2017). Controversy about pharmacological modulation of Nrf2 for cancer therapy. *Redox Biol.* 12, 727–732. doi: 10.1016/j.redox.2017.04.013

Monks, T. J., Hanzlik, R. P., Cohen, G. M., Ross, D., and Graham, D. G. (1992). Quinone chemistry and toxicity. *Toxicol. Appl. Pharmacol.* 112, 2–16. doi: 10.1016/0041-008X(92)90273-U

Moody, T. W., Leyton, J., Martinez, A., Hong, S., Malkinson, A., and Mulshine, J. L. (1998). Lipoxygenase inhibitors prevent lung carcinogenesis and inhibit non-small cell lung cancer growth. *Exp. Lung Res.* 24, 617–628. doi: 10.3109/01902149809087390

Moss, M. A., Varvel, N. H., Nichols, M. R., Reed, D. K., and Rosenberry, T. L. (2004). Nordihydroguaiaretic acid does not disaggregate beta-amyloid(1-40) protofibrils but does inhibit growth arising from direct protofibril association. *Mol. Pharmacol.* 66, 592–600.

Muir, J. L. (1997). Acetylcholine, aging, and Alzheimer's disease. *Pharmacol. Biochem. Behav.* 56, 687–696. doi: 10.1016/S0091-3057(96)00431-5

Mundhe, N. A., Kumar, P., Ahmed, S., Jamdade, V., Mundhe, S., and Lahkar, M. (2015). Nordihydroguaiaretic acid ameliorates cisplatin induced nephrotoxicity and potentiates its anti-tumor activity in DMBA induced breast cancer in female Sprague-Dawley rats. *Int. Immunopharmacol.* 28, 634–642. doi: 10.1016/j.intimp.2015.07.016

Mundhe, N., Kumar, P., Arora, I., Ahmed, S., and Lahkar, M. (2019). Differential effect of NDGA on cisplatin-induced nephrotoxicity in Spargue-Dawley rats. *Immunopharmacol. Immunotoxicol.* 41, 68–75. doi: 10.1080/08923973.2018.1547741

Nagahora, N., Yamada, H., Kikuchi, S., Hakozaki, M., and Yano, A. (2017). Nrf2 Activation by 5-lipoxygenase metabolites in human umbilical vascular endothelial cells. *Nutrients* 9. doi: 10.3390/nu9091001

Naiki, H., Hasegawa, K., Yamaguchi, I., Nakamura, H., Gejyo, F., and Nakakuki, K. (1998). Apolipoprotein E and antioxidants have different mechanisms of inhibiting Alzheimer's beta-amyloid fibril formation *in vitro*. *Biochemistry* 37, 17882–17889. doi: 10.1021/bi980550y

Nelson, M. J., Batt, D. G., Thompson, J. S., and Wright, S. W. (1991). Reduction of the active-site iron by potent inhibitors of lipoxygenases. *J. Biol. Chem.* 266, 8225–8229.

Nie, D., Tang, K., Diglio, C., and Honn, K. V. (2000). Eicosanoid regulation of angiogenesis: role of endothelial arachidonate 12-lipoxygenase. *Blood* 95, 2304–2311. doi: 10.1182/blood.V95.7.2304

Nie, D., Krishnamoorthy, S., Jin, R., Tang, K., Chen, Y., Qiao, Y., et al. (2006). Mechanisms regulating tumor angiogenesis by 12-lipoxygenase in prostate cancer cells. *J. Biol. Chem.* 281, 18601–18609. doi: 10.1074/jbc.M601887200

Nusrat, S., Zaidi, N., Zaman, M., Islam, S., Ajmal, M. R., Siddiqi, M. K., et al. (2016). Repositioning nordihydroguaiaretic acid as a potent inhibitor of systemic amyloidosis and associated cellular toxicity. *Arch. Biochem. Biophys.* 612, 78–90. doi: 10.1016/j.abb.2016.10.014

O'brien, P. J. (1991). Molecular mechanisms of quinone cytotoxicity. *Chem. Biol. Interact.* 80, 1–41. doi: 10.1016/0009-2797(91)90029-7

Ono, K., Hasegawa, K., Yoshiike, Y., Takashima, A., Yamada, M., and Naiki, H. (2002). Nordihydroguaiaretic acid potently breaks down pre-formed Alzheimer's beta-amyloid fibrils *in vitro*. *J. Neurochem.* 81, 434–440. doi: 10.1046/j.1471-4159.2002.00904.x

Ono, K., Hasegawa, K., Naiki, H., and Yamada, M. (2004). Curcumin has potent anti-amyloidogenic effects for Alzheimer's beta-amyloid fibrils *in vitro*. *J. Neurosci. Res.* 75, 742–750. doi: 10.1002/jnr.20025

Orthwein, A., Noordermeer, S. M., Wilson, M. D., Landry, S., Enchev, R. I., Sherker, A., et al. (2015). A mechanism for the suppression of homologous recombination in G1 cells. *Nature* 528, 422–426. doi: 10.1038/nature16142

Ostman, A., Frijhoff, J., Sandin, A., and Bohmer, F. D. (2011). Regulation of protein tyrosine phosphatases by reversible oxidation. *J. Biochem.* 150, 345–356. doi: 10.1093/jb/mvr104

Pajares, M., Jimenez-Moreno, N., Garcia-Yague, A. J., Escoll, M., De Ceballos, M. L., Van Leuven, F., et al. (2016). Transcription factor NFE2L2/NRF2 is a regulator of macroautophagy genes. *Autophagy* 12, 1902–1916. doi: 10.1080/15548627.2016.1208889

Pajares, M., Rojo, A. I., Arias, E., Diaz-Carretero, A., Cuervo, A. M., and Cuadrado, A. (2018). Transcription factor NFE2L2/NRF2 modulates chaperone-mediated autophagy through the regulation of LAMP2A. *Autophagy* 14, 1310–1322. doi: 10.1080/15548627.2018.1474992

Park, R., Chang, C. C., Liang, Y. C., Chung, Y., Henry, R. A., Lin, E., et al. (2005). Systemic treatment with tetra-O-methyl nordihydroguaiaretic acid suppresses the growth of human xenograft tumors. *Clin. Cancer Res.* 11, 4601–4609. doi: 10.1158/1078-0432.CCR-04-2188

Pavani, M., Fones, E., Oksenberg, D., Garcia, M., Hernandez, C., Cordano, G., et al. (1994). Inhibition of tumoral cell respiration and growth by nordihydroguaiaretic acid. *Biochem. Pharmacol.* 48, 1935–1942. doi: 10.1016/0006-2952(94)90592-4

Peralta, I., Marrassini, C., Filip, R., Alonso, M. R., and Anesini, C. (2018). Food preservation by Larrea divaricata extract: participation of polyphenols. *Food Sci. Nutr.* 6, 1269–1275. doi: 10.1002/fsn3.640

Powis, G. (1987). Metabolism and reactions of quinoid anticancer agents. *Pharmacol. Ther.* 35, 57–162. doi: 10.1016/0163-7258(87)90105-7

Probst, L., Dachert, J., Schenk, B., and Fulda, S. (2017). Lipoxygenase inhibitors protect acute lymphoblastic leukemia cells from ferroptotic cell death. *Biochem. Pharmacol.* 140, 41–52. doi: 10.1016/j.bcp.2017.06.112

Rada, P., Rojo, A. I., Chowdhry, S., Mcmahon, M., Hayes, J. D., and Cuadrado, A. (2011). SCF/{beta}-TrCP promotes glycogen synthase kinase 3-dependent degradation of the Nrf2 transcription factor in a Keap1-independent manner. *Mol. Cell Biol.* 31, 1121–1133. doi: 10.1128/MCB.01204-10

Rada, P., Rojo, A. I., Evrard-Todeschi, N., Innamorato, N. G., Cotte, A., Jaworski, T., et al. (2012). Structural and functional characterization of Nrf2 degradation by the glycogen synthase kinase 3/beta-TrCP axis. *Mol. Cell Biol.* 32, 3486–3499. doi: 10.1128/MCB.00180-12

Randall, M. J., Spiess, P. C., Hristova, M., Hondal, R. J., and Van Der Vliet, A. (2013). Acrolein-induced activation of mitogen-activated protein kinase signaling is mediated by alkylation of thioredoxin reductase and thioredoxin 1. *Redox Biol.* 1, 265–275. doi: 10.1016/j.redox.2013.02.001

Remya, C., Dileep, K. V., Tintu, I., Variyar, E. J., and Sadasivan, C. (2013). In vitro inhibitory profile of NDGA against AChE and its in silico structural modifications based on ADME profile. *J. Mol. Model* 19, 1179–1194. doi: 10.1007/s00894-012-1656-0

Rieckmann, P., Traboulsee, A., Devonshire, V., and Oger, J. (2008). Escalating immunotherapy of multiple sclerosis. *Ther. Adv. Neurol. Disord.* 1, 181–192. doi: 10.1177/1756285608098359

Rios, P., Nunes-Xavier, C. E., Tabernero, L., Kohn, M., and Pulido, R. (2014). Dual-specificity phosphatases as molecular targets for inhibition in human disease. *Antioxid. Redox Signal* 20, 2251–2273. doi: 10.1089/ars.2013.5709

Rizzolio, S., and Tamagnone, L. (2011). Multifaceted role of neuropilins in cancer. *Curr. Med. Chem.* 18, 3563–3575. doi: 10.2174/092986711796642544

Robison, T. W., Sevanian, A., and Forman, H. J. (1990). Inhibition of arachidonic acid release by nordihydroguaiaretic acid and its antioxidant action in rat alveolar macrophages and Chinese hamster lung fibroblasts. *Toxicol. Appl. Pharmacol.* 105, 113–122. doi: 10.1016/0041-008X(90)90363-Y

Rojo, A. I., Medina-Campos, O. N., Rada, P., Zuniga-Toala, A., Lopez-Gazcon, A., Espada, S., et al. (2012). Signaling pathways activated by the phytochemical nordihydroguaiaretic acid contribute to a Keap1-independent regulation of

Nrf2 stability: role of glycogen synthase kinase-3. *Free Radic. Biol. Med.* 52, 473–487. doi: 10.1016/j.freeradbiomed.2011.11.003

Rojo, A. I., Rada, P., Mendiola, M., Ortega-Molina, A., Wojdyla, K., Rogowska-Wrzesinska, A., et al. (2014). The PTEN/NRF2 axis promotes human carcinogenesis. *Antioxid. Redox Signal* 21, 2498–2514. doi: 10.1089/ars.2014.5843

Roskar, I., Strukelj, B., and Lunder, M. (2016). Screening of phenolic compounds reveals inhibitory activity of nordihydroguaiaretic acid against three enzymes involved in the regulation of blood glucose level. *Plant Foods Hum. Nutr.* 71, 88–89. doi: 10.1007/s11130-016-0530-0

Rowe, D. L., Ozbay, T., Bender, L. M., and Nahta, R. (2008). Nordihydroguaiaretic acid, a cytotoxic insulin-like growth factor-I receptor/HER2 inhibitor in trastuzumab-resistant breast cancer. *Mol. Cancer Ther.* 7, 1900–1908. doi: 10.1158/1535-7163.MCT-08-0012

Sadagurski, M., Cady, G., and Miller, R. A. (2017). Anti-aging drugs reduce hypothalamic inflammation in a sex-specific manner. *Aging Cell* 16, 652–660. doi: 10.1111/acel.12590

Sahu, S. C., Ruggles, D. I., and O'donnell, M. W. (2006). Prooxidant activity and toxicity of nordihydroguaiaretic acid in clone-9 rat hepatocyte cultures. *Food Chem. Toxicol.* 44, 1751–1757. doi: 10.1016/j.fct.2006.05.016

Sarveswaran, S., Chakraborty, D., Chitale, D., Sears, R., and Ghosh, J. (2015). Inhibition of 5-lipoxygenase selectively triggers disruption of c-Myc signaling in prostate cancer cells. *J. Biol. Chem.* 290, 4994–5006. doi: 10.1074/jbc.M114.599035

Satoh, T., Kosaka, K., Itoh, K., Kobayashi, A., Yamamoto, M., Shimojo, Y., et al. (2008). Carnosic acid, a catechol-type electrophilic compound, protects neurons both *in vitro* and *in vivo* through activation of the Keap1/Nrf2 pathway *via* S-alkylation of targeted cysteines on Keap1. *J. Neurochem.* 104, 1116–1131. doi: 10.1111/j.1471-4159.2007.05039.x

Satoh, T., Mckercher, S. R., and Lipton, S. A. (2013). Nrf2/ARE-mediated antioxidant actions of pro-electrophilic drugs. *Free Radic. Biol. Med.* 65, 645–657. doi: 10.1016/j.freeradbiomed.2013.07.022

Seufferlein, T., Seckl, M. J., Schwarz, E., Beil, M., V Wichert, G., Baust, H., et al. (2002). Mechanisms of nordihydroguaiaretic acid-induced growth inhibition and apoptosis in human cancer cells. *Br. J. Cancer* 86, 1188–1196. doi: 10.1038/sj.bjc.6600186

Shaposhnikova, V. V., Kublik, L. N., Narimanov, A. A., Levitman, M., Orlova, O. E., Kudriavtsev, A. A., et al. (2001). [Growth inhibition and induction of tumor cell death by phospholipase A2 and lipoxygenase inhibitors]. *Izv Akad Nauk Ser. Biol.*, 249–252.

Shishido, Y., Furushiro, M., Hashimoto, S., and Yokokura, T. (2001). Effect of nordihydroguaiaretic acid on behavioral impairment and neuronal cell death after forebrain ischemia. *Pharmacol. Biochem. Behav.* 69, 469–474. doi: 10.1016/S0091-3057(01)00572-X

Siddique, Y. H., Ara, G., Jyoti, S., and Afzal, M. (2012). The dietary supplementation of nordihydroguaiaretic acid (NDGA) delayed the loss of climbing ability in Drosophila model of Parkinson's disease. *J. Diet Suppl.* 9, 1–8. doi: 10.3109/19390211.2011.630716

Singh, M., Bittner, S., Li, Y., Bittner, A., Han, L., Cortez, Y., et al. (2019). Anti-hyperlipidaemic effects of synthetic analogues of nordihydroguaiaretic acid in dyslipidaemic rats. *Br. J. Pharmacol.* 176, 369–385.

Smith, A. Y., Feddersen, R. M., Gardner, K. D.Jr., and Davis, C. J.Jr. (1994). Cystic renal cell carcinoma and acquired renal cystic disease associated with consumption of chaparral tea: a case report. *J. Urol* 152, 2089–2091. doi: 10.1016/S0022-5347(17)32317-0

Stefani, M. (2010). Protein aggregation diseases: toxicity of soluble prefibrillar aggregates and their clinical significance. *Methods Mol. Biol.* 648, 25–41. doi: 10.1007/978-1-60761-756-3_2

Takahashi, R., Ono, K., Takamura, Y., Mizuguchi, M., Ikeda, T., Nishijo, H., et al. (2015). Phenolic compounds prevent the oligomerization of alpha-synuclein and reduce synaptic toxicity. *J. Neurochem.* 134, 943–955. doi: 10.1111/jnc.13180

Talalay, P., De Long, M. J., and Prochaska, H. J. (1988). Identification of a common chemical signal regulating the induction of enzymes that protect against chemical carcinogenesis. *Proc. Natl. Acad. Sci. U. S. A* 85, 8261–8265. doi: 10.1073/pnas.85.21.8261

Tang, D. G., and Honn, K. V. (1997). Apoptosis of W256 carcinosarcoma cells of the monocytoid origin induced by NDGA involves lipid peroxidation and depletion of GSH: role of 12-lipoxygenase in regulating tumor cell survival. *J. Cell Physiol.* 172, 155–170. doi: 10.1002/(SICI)1097-4652(199708)172:2<155::AID-JCP3>3.0.CO;2-N

Tang, K., and Honn, K. V. (1999). 12(S)-HETE in cancer metastasis. *Adv. Exp. Med. Biol.* 447, 181–191. doi: 10.1007/978-1-4615-4861-4_17

Tang, D. G., Chen, Y. Q., and Honn, K. V. (1996). Arachidonate lipoxygenases as essential regulators of cell survival and apoptosis. *Proc. Natl. Acad. Sci. U. S. A* 93, 5241–5246. doi: 10.1073/pnas.93.11.5241

Tateson, J. E., Randall, R. W., Reynolds, C. H., Jackson, W. P., Bhattacherjee, P., Salmon, J. A., et al. (1988). Selective inhibition of arachidonate 5-lipoxygenase by novel acetohydroxamic acids: biochemical assessment *in vitro* and ex vivo. *Br. J. Pharmacol.* 94, 528–539. doi: 10.1111/j.1476-5381.1988.tb11557.x

Thornton, T. M., Pedraza-Alva, G., Deng, B., Wood, C. D., Aronshtam, A., Clements, J. L., et al. (2008). Phosphorylation by p38 MAPK as an alternative pathway for GSK3beta inactivation. *Science* 320, 667–670. doi: 10.1126/science.1156037

Tibes, R., Mcdonagh, K. T., Lekakis, L., Bogenberger, J. M., Kim, S., Frazer, N., et al. (2015). Phase I study of the novel Cdc2/CDK1 and AKT inhibitor terameprocol in patients with advanced leukemias. *Invest. New Drugs* 33, 389–396. doi: 10.1007/s10637-014-0198-y

Tong, W. G., Ding, X. Z., and Adrian, T. E. (2002). The mechanisms of lipoxygenase inhibitor-induced apoptosis in human breast cancer cells. *Biochem. Biophys. Res. Commun.* 296, 942–948. doi: 10.1016/S0006-291X(02)02014-4

Tong, K. I., Kobayashi, A., Katsuoka, F., and Yamamoto, M. (2006). Two-site substrate recognition model for the Keap1-Nrf2 system: a hinge and latch mechanism. *Biol. Chem.* 387, 1311–1320. doi: 10.1515/BC.2006.164

Truty, M. J., and Urrutia, R. (2007). Basics of TGF-beta and pancreatic cancer. *Pancreatology* 7, 423–435. doi: 10.1159/000108959

Van Weeren, P. C., De Bruyn, K. M., De Vries-Smits, A. M., Van Lint, J., and Burgering, B. M. (1998). Essential role for protein kinase B (PKB) in insulin-induced glycogen synthase kinase 3 inactivation. Characterization of dominant-negative mutant of PKB. *J. Biol. Chem.* 273, 13150–13156. doi: 10.1074/jbc.273.21.13150

Vasquez-Martinez, Y., Ohri, R. V., Kenyon, V., Holman, T. R., and Sepulveda-Boza, S. (2007). Structure-activity relationship studies of flavonoids as potent inhibitors of human platelet 12-hLO, reticulocyte 15-hLO-1, and prostate epithelial 15-hLO-2. *Bioorg. Med. Chem.* 15, 7408–7425. doi: 10.1016/j.bmc.2007.07.036

Wagenknecht, B., Schulz, J. B., Gulbins, E., and Weller, M. (1998). Crm-A, bcl-2 and NDGA inhibit CD95L-induced apoptosis of malignant glioma cells at the level of caspase 8 processing. *Cell Death Differ* 5, 894–900. doi: 10.1038/sj.cdd.4400435

Wang, B., Yu, S. C., Jiang, J. Y., Porter, G. W., Zhao, L. T., Wang, Z., et al. (2011). An inhibitor of arachidonate 5-lipoxygenase, Nordy, induces differentiation and inhibits self-renewal of glioma stem-like cells. *Stem Cell Rev. Rep.* 7, 458–470. doi: 10.1007/s12015-010-9175-9

West, M., Mhatre, M., Ceballos, A., Floyd, R. A., Grammas, P., Gabbita, S. P., et al. (2004). The arachidonic acid 5-lipoxygenase inhibitor nordihydroguaiaretic acid inhibits tumor necrosis factor alpha activation of microglia and extends survival of G93A-SOD1 transgenic mice. *J. Neurochem.* 91, 133–143. doi: 10.1111/j.1471-4159.2004.02700.x

Whitman, S., Gezginci, M., Timmermann, B. N., and Holman, T. R. (2002). Structure-activity relationship studies of nordihydroguaiaretic acid inhibitors toward soybean, 12-human, and 15-human lipoxygenase. *J. Med. Chem.* 45, 2659–2661. doi: 10.1021/jm0201262

Wilcock, G. K., Esiri, M. M., Bowen, D. M., and Smith, C. C. (1982). Alzheimer's disease. Correlation of cortical choline acetyltransferase activity with the severity of dementia and histological abnormalities. *J. Neurol. Sci.* 57, 407–417. doi: 10.1016/0022-510X(82)90045-4

Woodgett, J. R. (2005). Recent advances in the protein kinase B signaling pathway. *Curr. Opin. Cell Biol.* 17, 150–157. doi: 10.1016/j.ceb.2005.02.010

Xue, H., Zhang, X. Y., Liu, J. M., Song, Y., Liu, T. T., and Chen, D. (2013). NDGA reduces secondary damage after spinal cord injury in rats *via* anti-inflammatory effects. *Brain Res.* 1516, 83–92. doi: 10.1016/j.brainres.2013.04.016

Yamamoto, T., Suzuki, T., Kobayashi, A., Wakabayashi, J., Maher, J., Motohashi, H., et al. (2008). Physiological significance of reactive cysteine residues of

Keap1 in determining Nrf2 activity. *Mol. Cell Biol.* 28, 2758–2770. doi: 10.1128/MCB.01704-07

Yamamura, H., Sakamoto, K., Ohya, S., Muraki, K., and Imaizumi, Y. (2002). Mechanisms underlying the activation of large conductance Ca2+-activated K + channels by nordihydroguaiaretic acid. *Jpn. J. Pharmacol.* 89, 53–63. doi: 10.1254/jjp.89.53

Yam-Canul, P., Chirino, Y. I., Sanchez-Gonzalez, D. J., Martinez-Martinez, C. M., Cruz, C., Villanueva, C., et al. (2008). Nordihydroguaiaretic acid attenuates potassium dichromate-induced oxidative stress and nephrotoxicity. *Food Chem. Toxicol.* 46, 1089–1096. doi: 10.1016/j.fct.2007.11.003

Yang, P., Cartwright, C. A., Li, J., Wen, S., Prokhorova, I. N., Shureiqi, I., et al. (2012). Arachidonic acid metabolism in human prostate cancer. *Int. J. Oncol.* 41, 1495–1503. doi: 10.3892/ijo.2012.1588

Yin, B., Yang, Y., Zhao, Z., Zeng, Y., Mooney, S. M., Li, M., et al. (2011). Arachidonate 12-lipoxygenase may serve as a potential marker and therapeutic target for prostate cancer stem cells. *Int. J. Oncol.* 38, 1041–1046. doi: 10.3892/ijo.2011.901

Yoshida, T., Shiraishi, T., Horinaka, M., Nakata, S., Yasuda, T., Goda, A. E., et al. (2007). Lipoxygenase inhibitors induce death receptor 5/TRAIL-R2 expression and sensitize malignant tumor cells to TRAIL-induced apoptosis. *Cancer Sci.* 98, 1417–1423. doi: 10.1111/j.1349-7006.2007.00559.x

Youngren, J. F., Gable, K., Penaranda, C., Maddux, B. A., Zavodovskaya, M., Lobo, M., et al. (2005). Nordihydroguaiaretic acid (NDGA) inhibits the IGF-1 and c-erbB2/HER2/neu receptors and suppresses growth in breast cancer cells. *Breast Cancer Res. Treat* 94, 37–46. doi: 10.1007/s10549-005-6939-z

Zhang, D. D., and Hannink, M. (2003). Distinct cysteine residues in Keap1 are required for Keap1-dependent ubiquitination of Nrf2 and for stabilization of Nrf2 by chemopreventive agents and oxidative stress. *Mol. Cell Biol.* 23, 8137–8151. doi: 10.1128/MCB.23.22.8137-8151.2003

Zhang, Y., Xu, S., Lin, J., Yao, G., Han, Z., Liang, B., et al. (2012). mTORC1 is a target of nordihydroguaiaretic acid to prevent breast tumor growth *in vitro* and *in vivo*. *Breast Cancer Res. Treat* 136, 379–388. doi: 10.1007/s10549-012-2270-7

Zhang, H., Shen, W. J., Cortez, Y., Kraemer, F. B., and Azhar, S. (2013). Nordihydroguaiaretic acid improves metabolic dysregulation and aberrant hepatic lipid metabolism in mice by both PPARalpha-dependent and -independent pathways. *Am. J. Physiol. Gastrointest Liver Physiol.* 304, G72–G86.

Zhang, H., Li, Y., Hu, J., Shen, W. J., Singh, M., Hou, X., et al. (2015). Effect of creosote bush-derived NDGA on expression of genes involved in lipid metabolism in liver of high-fructose fed rats: relevance to NDGA amelioration of hypertriglyceridemia and hepatic steatosis. *PloS One* 10, e0138203. doi: 10.1371/journal.pone.0138203

Zhang, H., Shen, W. J., Li, Y., Bittner, A., Bittner, S., Tabassum, J., et al. (2016). Microarray analysis of gene expression in liver, adipose tissue and skeletal muscle in response to chronic dietary administration of NDGA to high-fructose fed dyslipidemic rats. *Nutr. Metab. (Lond)* 13, 63. doi: 10.1186/s12986-016-0121-y

Zhao, Q. W., Lin, Y., Xu, C. R., Yao, Y. L., Cui, Y. H., Zhang, X., et al. (2017). NDGA-P21, a novel derivative of nordihydroguaiaretic acid, inhibits glioma cell proliferation and stemness. *Lab. Invest.* 97, 1180–1187. doi: 10.1038/labinvest.2017.46

Zuniga-Toala, A., Zatarain-Barron, Z. L., Hernandez-Pando, R., Negrette-Guzman, M., Huerta-Yepez, S., Torres, I., et al. (2013). Nordihydroguaiaretic acid induces Nrf2 nuclear translocation *in vivo* and attenuates renal damage and apoptosis in the ischemia and reperfusion model. *Phytomedicine* 20, 775–779. doi: 10.1016/j.phymed.2013.03.020

Conflict of Interest: The authors declare that the research was conducted in the absence of any commercial or financial relationships that could be construed as a potential conflict of interest.

frontiers in Plant Science

ORIGINAL RESEARCH
published: 23 September 2020
doi: 10.3389/fpls.2020.508658

UPLC-HRMS Analysis Revealed the Differential Accumulation of Antioxidant and Anti-Aging Lignans and Neolignans in *In Vitro* Cultures of *Linum usitatissimum* L

Shankhamala Bose[1], Thibaut Munsch[1], Arnaud Lanoue[1], Laurine Garros[2,3], Duangjai Tungmunnithum[3,4], Souhila Messaili[2], Emilie Destandau[2], Kévin Billet[1], Benoit St-Pierre[1], Marc Clastre[1], Bilal Haider Abbasi[1,3,5], Christophe Hano[3] and Nathalie Giglioli-Guivarc'h[1]*

[1] EA2106 Biomolécules et Biotechnologies Végétales, Université de Tours, Tours, France, [2] UMR7311, Institut de Chimie Organique et Analytique, Université d'Orléans, CNRS, Orléans, France, [3] USC1328 Laboratoire de Biologie des Ligneux et des Grandes Cultures, Université d'Orléans, INRA, Orléans, France, [4] Department of Pharmaceutical Botany, Mahidol University, Bangkok, Thailand, [5] Department of Biotechnology, Quaid-i-Azam University, Islamabad, Pakistan

OPEN ACCESS

Edited by:
Jens Rohloff,
Norwegian University of Science and Technology, Norway

Reviewed by:
Ericsson Coy-Barrera,
Universidad Militar Nueva Granada, Colombia
Adeyemi Oladapo Aremu,
North-West University, South Africa

***Correspondence:**
Nathalie Giglioli-Guivarc'h
nathalie.guivarch@univ-tours.fr
Bilal Haider Abbasi
bhabbasi@qau.edu.pk

Specialty section:
This article was submitted to Plant Metabolism and Chemodiversity, a section of the journal Frontiers in Plant Science

Received: 30 October 2019
Accepted: 28 August 2020
Published: 23 September 2020

Citation:
Bose S, Munsch T, Lanoue A, Garros L, Tungmunnithum D, Messaili S, Destandau E, Billet K, St-Pierre B, Clastre M, Abbasi BH, Hano C and Giglioli-Guivarc'h N (2020) UPLC-HRMS Analysis Revealed the Differential Accumulation of Antioxidant and Anti-Aging Lignans and Neolignans in In Vitro Cultures of Linum usitatissimum L. Front. Plant Sci. 11:508658. doi: 10.3389/fpls.2020.508658

Over the last few decades, methods relating to plant tissue culture have become prevalent within the cosmetic industry. Forecasts predict the cosmetic industry to grow to an annual turnover of around a few hundred billion US dollars. Here we focused on *Linum usitatissimum* L., a plant that is well-known for its potent cosmetic properties. Following the a) establishment of cell cultures from three distinct initial explant origins (root, hypocotyl, and cotyledon) and b) selection of optimal hormonal concentrations, two *in vitro* systems (callus *vs* cell suspensions) were subjected to different light conditions. Phytochemical analysis by UPLC-HRMS not only confirmed high (neo)lignan accumulation capacity of this species with high concentrations of seven newly described (neo)lignans. Evaluation over 30 days revealed strong variations between the two different *in vitro* systems cultivated under light or dark, in terms of their growth kinetics and phytochemical composition. Additionally, antioxidant (*i.e.* four different *in vitro* assays based on hydrogen-atom transfer or electron transfer mechanism) and anti-aging (*i.e.* four *in vitro* inhibition potential of the skin remodeling enzymes: elastase, hyaluronidase, collagenase and tyrosinase) properties were evaluated for the two different *in vitro* systems cultivated under light or dark. A prominent hydrogen-atom transfer antioxidant mechanism was illustrated by the DPPH and ABTS assays. Potent tyrosinase and elastase inhibitory activities were also observed, which was strongly influenced by the *in vitro* system and light conditions. Statistical treatments of the data showed relationship of some (neo)lignans with these biological activities. These results confirmed the accumulation of flax (neo)lignans in different *in vitro* systems that were subjected to distinct light conditions. Furthermore, we showed the importance of optimizing these parameters for specific applications within the cosmetic industry.

Keywords: lignans, neolignans, callus, cell culture, antioxidant activity, anti-aging activity

INTRODUCTION

Records on the cosmetic usage of natural plant products date back to ancient times as described in famous texts, including 1) Ayurvedic books on traditional Indian medicine (3,000–2,000 BC), 2) Chinese pharmacopoeia, 3) "The Divine Farmer's Herb-Root Classic", by Shen Nong (3,494 BC), and 4) the ancient Greek book "De Materia Medica", written by Pedanius Dioscorids (Ota and Yokoyama, 2010). However, regardless of a vast and well-established ethnobotanical knowledge base, very few plants have been thoroughly investigated in modern times for their potential use within the cosmetic industry (Fongnzossie et al., 2017).

Within this modern era of technology and globalization, it is quite surprising to find a shift in consumer preference from chemical based synthetic products to more natural or "green" products. This could perhaps be explained by the increasing concerns of side effects that are associated with chemical products (Hazra and Panda, 2013). However, due to a recent increase in the global demand for active plant ingredients within the medical and cosmetic industries, medicinal plant species are now experiencing severe mass exploitation which may ultimately lead to their extinction. *In vitro* plant tissue culture technology can aid in supplying the growing global demand for active biomolecules, without over exploitation of plant biomes (Barbulova et al., 2014).

Moreover, the use of plant cell cultures instead of cultivated plants for active biomolecule production may help to overcome limitations of inconsistent quality due to seasonal changes, cultivation methods and geographic variations. Batch to batch inconsistencies can also be avoided by creating an environment that is free of pathogens and contamination (Barbulova et al., 2014). Furthermore, due to the controlled conditions associated with this technology, it can also be successfully applied to increase the amount of active biomolecule production by using biotransformation techniques and/or elicitation of stress (biotic and abiotic) conditions.

Linum usitatissimum L., often referred to as flax, is a commercially important plant, belonging to the Linaceae family. Its literature dates back to 5,000 BC when it was primarily cultivated for fiber and oil in Western Europe, Mediterranean region, North Africa and South-West Asia (Oomah, 2001; Zohary et al., 2012). Recent studies of *L. usitatisimum* have elucidated several useful properties of the plant, including anticancer (Shim et al., 2014), anti-diarrhea (Palla et al., 2015) anti-microbial (Bakht et al., 2011), anti-inflammatory (Oomah, 2001), antioxidant and prevention against cardiovascular diseases (Zanwar et al., 2011). Part of these health benefits has been associated with the presence of (neo)lignans in flax. Following their consumption, plant lignans are converted to enterolignans (enterolactone and enterodiol) by intestinal microbes in the gut which have been reported to reduce the occurrence of different cancers (Lainé et al., 2009; Zanwar et al., 2011).

There are many reports describing *in vitro* tissue culture systems used for propagating *L. usitatisimum* from hypocotyl (Cunha and Ferreira, 1999; Dedičová et al., 2000; Salaj et al., 2005) and anther (Nichterlein et al., 1991; Rutkowska-Krause et al., 2003) explants. Additionally, callus (Anjum et al., 2017a; Zahir et al., 2018) and cell suspension cultures (Attoumbré et al., 2006a; Attoumbré et al., 2006b; Hano et al., 2006; Beejmohun et al., 2007; Hano et al., 2008; Corbin et al., 2013a; Corbin et al., 2013b; Gabr et al., 2016; Anjum et al., 2017b; Nadeem et al., 2018; Nadeem et al., 2019; Ahmad et al., 2019; Markulin et al., 2019) producing higher amounts of industrially important lignans and neolignans have also been described.

Flax is considered to be a potential cosmetic ingredient all over the world, including China (China Food & Drug Administration, 2015). It is therefore surprising that this multifunction and economically important crop has hardly been exploited within the cosmetic industry. Thus, the main objective of this study was to establish cell lines (solid and liquid) of *L. usitatissimum*, producing valuable specialized metabolites of great importance for cosmetics.

MATERIALS AND METHODS

Chemicals and Reagents

The extraction solvents used in this experiment were of analytical grade, supplied by Thermo Scientific (Courtaboeuf, France), while all other standards and reagents were purchased from Sigma-Aldrich (Saint-Quentin Fallavier, France).

Plant Material and Establishment of Callus

The selection of explants (hypocotyls, cotyledons, and roots) and callus formation was achieved following the protocol described by Hano et al. (2006), with slight modifications. Briefly, hypocotyl explants were chosen, and the best growing callus was found to be in Murashige and Skoog (1962) media containing 2 $mg.L^{-1}$ BAP and 0.5 $mg.L^{-1}$ NAA. Cultures were maintained under two illumination conditions: 1) one with 12 h light with 25 $\mu E\ m^{-2}\ s^{-1}$ light intensity/ 12 h dark and 2) the other in total darkness (24 h per day). Light intensity was measured by using Luxmeter under the light source. Illumination was ensured by dark red/white LED (18 W, Green Power TLED DR/W, Philips). The growth room temperature was maintained at 24°C for both conditions. The callus was subcultured after every 30 days for both conditions.

Establishment of Suspension Culture

For initiation of cell suspension culture, approximately 1 g of fresh weight (FW) callus was added to a 125 ml Erlenmeyer flask containing 25 ml of MS media fortified with 2 $mg.L^{-1}$ benzylaminopurine (BAP) and 0.5 $mg.L^{-1}$ 1-Naphthaleneacetic acid (NAA). The suspension cultures were kept on a gyratory shaker at 120 rpm, at 24°C. Then suspension cultures were maintained either in 12 h light/12 h dark or 24 h darkness and subcultured every 14 days.

Study of Growth Kinetics

For analysis of growth kinetics (callus and cell suspension culture), 10 sampling points were studied over a period of 30 days with 3 interval days.

For the determination of the FW of the suspension culture, the cells were harvested by filtration using a 0.45 µm stainless steel sieve, then washed twice with distilled water to remove any trace of medium. In order to remove the excess adhering water, the cells are manually pressed between two filter papers several times until no more traces of liquid are visible on the papers. The cells are then weighed. For dry weight (DW) estimation, cells were frozen and lyophylized 48 h (lyophilizator CHRIST Alpha 1-5) and then weighed.

Plant Extract Preparation

Dried cells were ground to a fine powder with a mortar and pestle. Fifty milligrams of the powder was extracted in 1 ml ethanol/water solution (75%, v/v) in a sonication bath for 1 h. The extracts were then centrifuged at 18,000 g for 10 min. Supernatant (500 µl) was collected and stored at −20°C for performing bioassays and metabolic profiling.

UPLC-MS Analyses

For detection of phenolics, lignans, and neolignans, UPLC-MS analyses were performed according to Billet et al. (2018). Briefly, the analysis was performed on an ACQUITY^{TM} Ultra Performance Liquid Chromatography system coupled to a photo diode array detector (PDA) and a Xevo TQD mass spectrometer (Waters, Milford, MA). The Xevo TQD was controlled by MassLynx 4.1 software (Waters, Milford, MA) and equipped with an electrospray ionization (ESI) source. Sample separation was accomplished by Waters Acquity HSST3 C18 column (150 × 2.1 mm, 1.8 µm) with a flow rate of 0.4 ml.min^{-1} at 55°C. The injection volume was 5 µl. The mobile phase consisted of solvent A (0.1% formic acid (FA) in water) and solvent B (0.1% formic acid in acetonitrile). Chromatographic separation was accomplished using a 19-min linear gradient from 5 to 60% mobile phase B. Mass spectrometry (MS) detection was performed in both positive and negative ionization modes, the source temperature being 120°C and the desolvation temperature 350°C. The capillary voltage was 3,000 V, and sample cone voltages were 30 and 50 V in full scan mode. The cone and desolvation gas flow rates were 60 and 800 L.h^{-1} respectively. Analytes were annotated according to their retention time, UV, and mass spectra by comparison with pure commercial standards and data from the literature (**Table S1**). Integration of the peaks was done using TargetLynx software. Targeted data collection was carried in selected ion monitoring (SIM) mode for (1) *erythro*-guaiacylglycerol-*β*-coniferyl alcohol ether glucoside ([M+H-2H$_2$O]$^+$; *m/z* 521; RT = 5.66 min), (2) *threo*-guaiacylglycerol-*β*-coniferyl alcohol ether glucoside ([M+H-2H$_2$O]$^+$; *m/z* 521; RT = 5.79 min), (3) *p*-coumaric ([M-H]$^-$; *m/z* 163; RT = 6.49 min), (4) dehydrodiconiferyl alcohol-4-*β*-D-glucoside isomer 1([M+H-H$_2$O]$^+$; *m/z* 503; RT = 7.3 min), (5) *erythro*-guaiacylglycerol-*β*-coniferyl alcohol ether ([M+H-2H$_2$O]$^+$; *m/z* 341; RT = 7.69 min), (6) *threo*-guaiacylglycerol-*β*-coniferyl alcohol ether ([M+H-2H$_2$O]$^+$; *m/z* 341; RT = 7.85 min), (7) dehydrodiconiferyl alcohol-4-*β*-D-glucoside isomer 2 ([M+H-H$_2$O]$^+$; *m/z* 503; RT = 8.3 min), (8) secoisolariciresinol ([M+H-2H$_2$O]$^+$; *m/z* 327; RT = 9.42 min), (9) lariciresinol ([2M+H]$^+$; *m/z* 721; RT = 9.77 min), (10) epipinoresinol ([M+H-H$_2$O]$^+$ *m/z* 341; RT = 9.9 min), (11) pinoresinol ([M+H-H2O]+; *m/z* 165; RT = 10.48 min), (12) pluviatolide ([M+H]$^+$; *m/z* 357; RT = 11.36 min), (13) guaiacylglycerol-*β*-coniferyl aldehyde ether hexoside ([M+H-2H$_2$O]$^+$; *m/z* 519; RT = 11.74 min), (14) phillygenin ([M-H]$^-$; *m/z* 371; RT = 13.23 min). Peak integration was performed using the ApexTrack algorithm with a mass window of 0.1 Da and relative retention time window of 1 min followed by Savitzky–Golay smoothing (iteration = 1 and width = 1). The resulting pairs of m/z values and retention times were also manually examined.

As there are limited reference mass spectra available for lignan and neolignan identification, high-resolution mass spectrometry was further employed for confirmation of UPLC-DAD-MS identification. Chromatographic analyses were performed using an Ultimate 3000 RSLC system equipped with a binary pump, an autosampler and a thermostated column compartment (Dionex, Germering, Germany). Analytes were separated on a Luna omega C18 column (150 × 2.1 mm; 1.6 µm, Phenomenex) at 40°C. The mobile phase at a flow rate of 500 µl.min^{-1} was composed of solvent A (0.1% formic acid in water) and solvent B (0.08% formic acid in acetonitrile); the gradient program was as follows: 97% A and 3% B from 0 to 3 min, 55% A and 45% B at 12 min, 10% A and 90% B from 14 to 15 min, 97% A and 3% B at 15.5 min, then the column was re-equilibrated under initial conditions during 3 min. The injection volume was 2 µl. MS experiments were performed on a maXis UHR-Q-TOF mass spectrometer (Bruker, Bremen, Germany) in positive and negative electrospray ionization (ESI) modes. Capillary voltage was set at 4.5 kV in positive mode and 4.0 kV in negative mode. The flow rates of nebulizing and drying gas (nitrogen) were respectively set at 2 bars and 9 L.min^{-1}, and drying gas was heated at 200°C. The analysis was made with an acquisition frequency of 0.6 Hz for MS and MS/MS; the mass scan range was set from *m/z* 50 to 1,550. MS/MS experiments were carried out using data dependent acquisition (DDA) mode. Two collision energies were applied according to *m/z*, and the spectra were averaged to obtain MS/MS spectra from 20 and 45 eV at *m/z* 140 to 35 and 78 eV at *m/z* 1,000. Data were processed using DataAnalysis 4.4. The molecular formula was calculated using the following parameters: elemental composition ^{12}C, ^{1}H, ^{16}O, ^{14}N$_{0\text{-}5}$ and mass accuracy ≤2 ppm. The HRMS data for the 14 identified metabolites are presented in **Table 1**.

All the 14 metabolites identified were followed during growth kinetic in callus and cell suspensions, and the relative abundance of each metabolite is estimated according Arbitrary Unit (AU) by mg of DW.

Antioxidant Activity

DPPH Radical Scavenging Assay

To determine the antioxidant activity in the cell culture extracts, the 2,2-Diphenyl-1-picrylhydrazyl (DPPH) antioxidant free radical scavenging assay was performed according to the method described by Lee et al. (1998). Briefly, 20 µl of cell extract was mixed with 180 µl of DPPH reagent and kept for 30 min in the dark at room temperature, after which the absorbance was noted using a microplate reader at 517 nm. Trolox C was used as positive control. The assay was performed in triplicate and results expressed in µM of Trolox C Equivalent

TABLE 1 | UHPLC-HR-ESI-MS data of *Linum usitatissimum* cell suspension extracts.

Peak	RT (min)	Compound class	CompoundAssignement	Molecular formula	m/z measured	m/z calculated	Error [ppm]
1	5.68	neolignan	*erythro*-guaiacylglycerol-*β*-coniferyl alcohol ether glucoside	C26H33O11	521.202052 $[M+H-H2O]^+$	521.201738	–0.6
2	5.80	neolignan	*threo*-guaiacylglycerol-*β*-coniferyl alcohol ether glucoside	C26H33O11	521.201547 $[M+H-H2O]^+$	521.201738	0.4
3	4.26	phenolic acid	*p*-coumaric acid	C9H9O3	165.054376 $[M+H]^+$	165.054621	1.5
4	7.19	neolignan	dehydrodiconiferyl alcohol-4-*β*-D-glucoside isomer1	C26H31O10	503.1909 $[M+H-H2O]^+$	503.191174	1.6
5	7.35	neolignan	*erythro*-guaiacylglycerol-*β*-coniferyl alcohol ether	C20H24NaO7	399.14164 $[M+Na]^+$	399.14142	–0.5
6	7.52	neolignan	*threo*-guaiacylglycerol-*β*-coniferyl alcohol ether	C20H24NaO7	399.14150 $[M+Na]^+$	399.14142	–0.2
7	7.80	neolignan	dehydrodiconiferyl alcohol-4-*β*-D-glucoside isomer2	C26H33O11	521.201475 $[M+H]^+$	521.201738	1.6
8	6.78	dibenzylbutane	secoisolariciresinol	C20H27O6	363.180449 $[M+H]^+$	363.180215	–0.6
9	9.31	furan	lariciresinol	C20H24NaO6	383.146804 $[M+Na]^+$	383.146509	–0.8
10	9.37	furofuran	epipinoresinol	C20H23O6 C20H22NaO6	359.148467 $[M+H]^+$ 381.131 $[M+Na]^+$	359.148915 381.130859	1.2 –0.4
11	9.74	furofuran	pinoresinol	C20H22NaO6	381.131389 $[M+Na]^+$	381.130859	–1.4
12	10.68	dibenzylbutyrolactone	pluviatolide	C20H21O6	357.133699 $[M+H]^+$	357.133265	–1.2
13	10.93	neolignan	guaiacylglycerol-*β*-coniferyl aldehyde ether hexoside	C30H33O9	537.211577 $[M+H]^+$	537.211909	0.6
14	12.09	furofuran	Phillygenin	C21H24NaO6	395.146532 $[M+Na]^+$	395.146509	–0.1

Antioxidant Capacity (TEAC) using a 6-point calibration curve (R^2 = 0.9994).

ABTS Radical Scavenging Assay

This assay, also known as Trolox equivalent antioxidant capacity assay, was performed with the 2,2′-azinobis-(3-ethylbenzothiazoline-6-sulfonate) (ABTS) radical as described by Tagliazucchi et al. (2010) with slight modifications. Briefly, equal volumes of 7 mM ABTS solution were added to 2.45 mM potassium persulphate solution and incubated in the dark for 16 h at room temperature. Next, the absorbance was recorded at 734 nm and adjusted to 0.7, after which the extracts were added. The reaction was then kept in the dark for 15 min at 25°C, and the absorbance was measured again at 734 nm by the use of BioTek ELX800 absorbance microplate reader (BioTek Instruments, Colmar, France). Trolox C was used as positive control. The assay was performed in triplicate and results expressed in µM of Trolox C Equivalent Antioxidant Capacity (TEAC) using a 6-point calibration curve (R^2 = 0.9977).

FRAP Assay

Ferric reducing antioxidant power assay (FRAP) was carried out according to the protocol described by Benzie and Strain (1996) with small modifications. Briefly, 10 µl of sample plant extract was added to 190 µl of FRAP solution, which was composed of 20 mM $FeCl_3$ 10 mM TPTZ, $6H_2O$, along with 300 mM acetate buffer (pH 3.6) in 1:1:10 (v/v/v) ratio. The reaction mix was incubated for 15 min at 25°C. The absorbance was then measured at 630 nm using a BioTek ELX800 absorbance microplate reader (BioTek Instruments, Colmar, France). Trolox C was used as positive control. The assay was performed in triplicate and results expressed in µM of Trolox C Equivalent Antioxidant Capacity (TEAC) using a 6-point calibration curve (R^2 = 0.9941).

CUPRAC Assay

A modified method of Apak et al. (2004) was used to determine the cupric ion reducing antioxidant capacity (CUPRAC) of the samples. Briefly, 10 µl of sample plant extract was mixed with 190 µl of CUPRAC solution, containing 10 mM Cu(II), 7.5 mM neocuproine, and 1 M acetate buffer (pH 7.0) in a 1:1:1 (v/v/v) ratio. The mixture was then incubated for 15 min at 25°C and the absorbance recorded at 450 nm using the BioTek ELX800 absorbance microplate reader (BioTek Instruments, Colmar, France). Trolox C was used as positive control. The assay was performed in triplicate and results expressed in µM of Trolox C Equivalent Antioxidant Capacity (TEAC) using a 6-points calibration curve (R^2 = 0.9997).

Anti-Aging Activity

Collagenase Assay

The collagenase assay was performed according to Wittenauer et al. (2015). Collagenase from *Clostridium histolyticum* (Sigma Aldrich) was used with the substrate N-[3-(2-furyl)acryloyl]-Leu-Gly-Pro-Ala (FALGPA; Sigma Aldrich) and the decrease in absorbance of FALGPA was monitored at 335 nm over a period of 20 min, using a BioTek ELX800 absorbance microplate reader (BioTek Instruments, Colmar, France). All the reactions were performed in triplicate, and the anti-collagenase activity was detected as a percentage of inhibition relative to the control (by adding the same volume of extraction solvent) for each extract. 1,10-Phenantroline (100 µM) was used as the specific inhibitor of collagenase leading to an inhibition of 33.6 ± 2.2%.

Elastase Assay

For this assay, porcine pancreatic elastase (Sigma Aldrich) was used according to the protocol described by Wittenauer et al. (2015). Here, N-Succ-Ala-Ala-Ala-*p*-nitroanilide (AAAVPN; Sigma Aldrich) was used as a substrate, and the release of *p*-nitroaniline was measured at 410 nm using an absorbance microplate reader (BioTek ELX800; BioTek Instruments). All the experiments were performed in triplicate, and the anti-elastase activity was expressed as a percentage of inhibition relative to the control which consisted of the same volume of extraction solvent. Oleanolic acid (10 µM) was used as the specific inhibitor of elastase leading to an inhibition of 47.8 ± 1.4%.

Hyaluronidase Assay

The assay for hyaluronidase inhibitory action was carried out as described by Kolakul and Sripanidkulchai (2017). For the reaction, 1.5 units of hyaluronidase (Sigma Aldrich) was added to the substrate *i.e.* 0.03% (w/v) hyaluronic acid solution, after which, acid albumin solution [0.1% (w/v) BSA] was used to precipitate undigested form of hyaluronic acid. The absorbance was recorded at 600 nm using an absorbance microplate reader (BioTek ELX800; BioTek Instruments, Colmar, France). All the experiments were performed in triplicate, and the hyaluronidase inhibitory action was expressed as a percentage of inhibition relative to the control which consisted of the same volume of extraction solvent. Oleanolic acid (10 μM) was used as the specific inhibitor of hyaluronidase leading to an inhibition of 33.5 ± 2.8%.

Tyrosinase Assay

Tyrosinase inhibitory assay was carried out as described by Chai et al. (2018). Briefly, the diphenolase substrate L-DOPA (5 mM; Sigma Aldrich) was mixed in sodium phosphate buffer (50 mM, pH 6.8) with 10 μl of *L. usitatissimum* extract after which, 0.2 $mg.ml^{-1}$ of mushroom tyrosinase solution (Sigma Aldrich) was added to the reaction mixture to make a final volume of 200 μl. A control experiment was performed in parallel using an equal amount of extraction solvent. The absorbance of the reaction was measured using an absorbance microplate reader (BioTek ELX800; BioTek Instruments) at 475 nm. All the experiments were performed in triplicate, and the hyaluronidase inhibitory action was expressed as a percentage of inhibition relative to the control for each extract. Kojic acid (10 μM) was used as the specific inhibitor of tyrosinase leading to an inhibition of 51.2 ± 0.9%.

Statistical Analysis

Visualization of the data and data analysis were carried out with MeV 4.9.0 software (Saeed et al., 2003). Every experiment was carried out in triplicate. Statistical significance from different treatments was revealed after one-way analysis of variance (ANOVA) followed by Tukey's test. Partial Least Square (PLS) models were performed using SIMCAP+ version 13.0 (Umetrics AB, Umeå, Sweden) with 14 metabolites as X variables and eight biological activities as Y variables. All variables were mean-centered and unit-variance (UV) scaled prior to PLS. Correlation analysis was performed using Past 3.0 (Øyvind Hammer, Natural History Museum, University of Oslo, Oslo, Norway) using the Pearson parametric correlation test and visualized using Heatmapper (Babicki et al., 2016). Significant thresholds at $p < 0.05$ with significant differences represented by different letters or $p < 0.05$, <0.01, and <0.001 were used for all statistical tests and represented by different letters or by *, **, and ***, respectively.

RESULTS

Establishment of Callus Culture

The most optimal callus induction frequency was established by testing different hormonal combinations of auxins and cytokinins, either alone or in combination (**Table 2**). Media containing cytokinin in combination with auxin resulted in the highest accumulation of callus biomass. Murashige and Skoog (MS) (1962) media supplemented with 2 $mg.L^{-1}$ BAP and 0.5 $mg.L^{-1}$ NAA gave the maximum growth index (**Table 2**).

Next, we evaluated the influence of the explant origin on callus formation using root, cotyledon, or hypocotyl starting explants. Callus formation was observed for each of these initial explants. Growth index as the ratio between final biomass and initial biomass (*i.e.*, 1 g FW per petri dish for 5 micro-callus) has been deduced for each case for determination at day 20 of cultivation on MS media containing 2 $mg.L^{-1}$ BAP and 0.5 $mg.L^{-1}$ NAA. The present results showed that hypocotyls constituted the best initial explants for the establishment of calli in terms of biomass accumulation (**Table 3**).

Study of Growth Kinetics

The growth kinetics of cell suspension (**Figure 1A**) and callus (**Figure 1B**) under light or dark were studied in *L. usitatissimum* over a period of 30 days. We decided to focus on dry weight (DW) measurements, as fresh weight (FW) cannot provide an accurate evaluation of biomass production (Park and Kim, 1993). In flax callus cultures the maximum biomass accumulation (DW) was observed on day 30 of culture (**Figure 1B**). In light grown cultures (**Figure 2A**), 1.176 g DW/flask was recorded, while 0.702 g DW/flask was measured for cultures growing in the dark (**Figure 2B**). In both conditions *i.e.* dark and light, the exponential-growth phase started from day 9 of culture, after an initial lag phase. Whereas in cell suspension cultures, the exponential-growth phase

TABLE 2 | Growth indices of *L. usitatissimum* calli grown *in vitro* on Murashige and Skoog media containing different 1-naphthaleneacetic acid (NAA) and 6-benzylaminopurine (BAP) hormonal concentrations after 20 days of culture.

NAA(mg/L)	BAP(mg/L)	Growth index[1]
0.1	1	1.36 ± 0.07^{d}
0.5	1	1.43 ± 0.06^{d}
1	1	1.76 ± 0.05^{c}
0.1	2	2.07 ± 0.10^{b}
0.5	2	2.79 ± 0.03^{a}
1	2	2.67 ± 0.09^{a}

[1]Growth index represents the ratio of final biomass (in dry weight (DW)) divided by the initial biomass (in DW) determined at day 20 of cultivation. No callus induction was observed on Murashige and Skoog medium without addition of any phytohormone. Values are means ± SD of 3 independent experiments; superscript letters indicate significant differences ($p < 0.05$).

TABLE 3 | Growth indices in *L. usitatissimum* calli as a function of the initial explant grown on Murashige and Skoog media containing 2 $mg.L^{-1}$ 6-benzylaminopurine (BAP) and 0.5 $mg.L^{-1}$ 1-naphthaleneacetic acid (NAA).

Initial explant origin	Growth index[1]
Root	2.55 ± 0.06^{b}
Hypocotyl	2.79 ± 0.03^{a}
Cotyledon	2.24 ± 0.07^{c}

[1]Growth index represents the ratio of final biomass [in dry weight (DW)] divided by the initial biomass (in DW) determined at day 20 of cultivation. Values are means ± SD of three independent experiments; superscript letters indicate significant differences ($p < 0.05$).

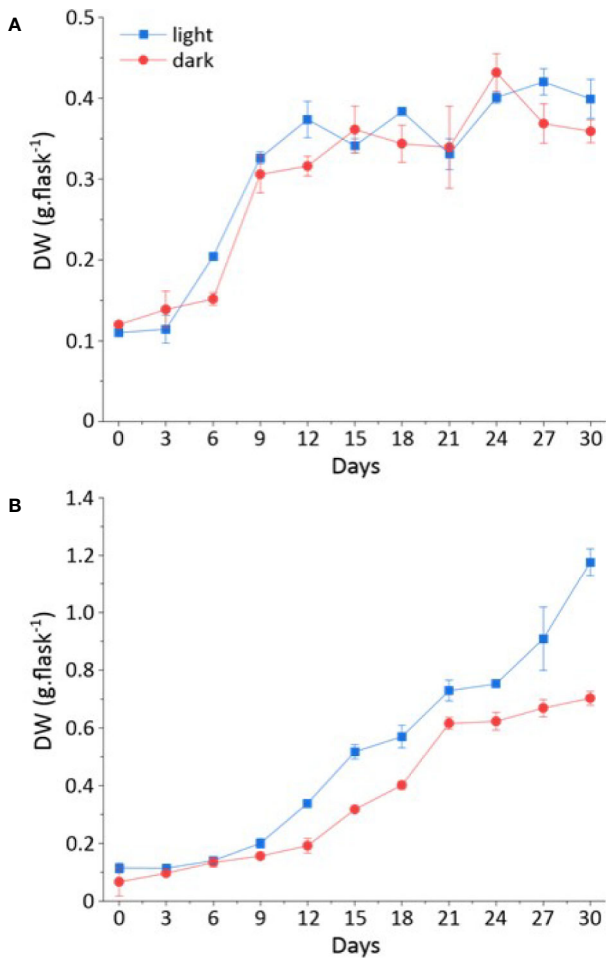

FIGURE 1 | Growth kinetics of callus and cell suspension cultures in light and dark represented in dry weight (in g/flask) on a time period of 30 days. **(A)** Dry weight (DW) of callus grown in the light (Blue); dry weight of callus grown in the dark (Red) **(B)** Dry weight (DW) of cell suspension culture grown in the light (Blue); dry weight of cell suspension culture grown in the dark (Red).

was activated earlier on day 3 in the light condition and on day 6 in the dark condition (**Figure 1A**). The highest suspension cell culture DW in the light was recorded on day 27 (0.399 g/flask) whereas in the dark the highest biomass was recorded on day 24 (0.359 g/flask). These two opposing conditions, *i.e.* light (**Figure 2C**) and dark (**Figure 2D**), were studied to see if there was any effect of the photoperiod on biomass accumulation. Light did not have an effect on the growth of suspension cell cultures.

Identification of Metabolites by UPLC-DAD-MS

To identify the phenolic compounds in cell extracts of *L. usitatissimum*, qualitative UPLC-DAD-MS/MS analysis in both ES^+ and ES^- modes were carried out, and major peaks were annotated according to their MS and UV features (**Table 1**, **Figure S1**, and **Table S1**). The 14 major analytes were assigned by comparison with pure standards or data from the literature. Peaks 3, 8, 9, and 11 were undoubtedly identified as *p*-coumaric acid, secoisolariciresinol, lariciresinol, and pinoresinol respectively, by comparison with pure standards. Peaks 1 and 2 show similar MS and UV spectra. In ES^+ mode the following ions are produced; $[M+H-H_2O]^+$ at *m/z* 521, $[M+H\text{-glucose}]^+$at *m/z* 377.0, and $[M+H\text{-glucose-}2H_2O]^+$ at *m/z* 341.1. In ES^- mode, an $[M+FA-H]^-$ ion at *m/z* 583.2 and an $[M-H\text{-glucose}]^-$ ion at *m/z* 375.2 were detected. These spectral features corresponded to the two isomers previously reported in flax cell extracts (Beejmohun et al., 2007) as *erythro* (peak 1) and *threo* (peak 2) forms of the guaiacylglycerol-β-coniferyl alcohol ether glucosides (GGCG). Peaks 4 and 7 showed similar MS and UV spectra. In ES^+ mode they produce the following ions: $[M+H-H_2O]^+$ at *m/z* 503, $[M+H-H_2O\text{-glucose}]^+$ at *m/z* 341. In ES^- mode, $[M+FA-H]^-$ ions at *m/z* 565, $[M-H-H_2O\text{-glucose}]^-$ ions at *m/z* 339.1 and $[2M-H]^-$ ions at *m/z* 1039 were detected. These chemical features corresponded to dehydrodiconiferyl alcohol-4-β-D-glucosides in agreement with Beejmohun et al. (2007). Our analyses enabled the detection of two isomers provisionally assigned as dehydrodiconiferyl alcohol-4-β-D-glucoside (DCG) isomer 1 (peak 4) and isomer 2 (peak 7), whereas previous studies reported only one isomer (Attoumbre et al., 2006a; Beejmohun et al., 2007). Peaks 5 and 6 produced similar MS and UV spectra. In ES^+ mode they produced $[M+H-2H_2O]^+$ ions at *m/z* 341.0, $[M+Na]^+$ ions at *m/z* 398.9, and $[2M-2H_2O+H]^+$ ions at *m/z* 717.1. In ES^- mode, $[M-H]^-$ ions at *m/z* 375, $[2M-H]^-$ ions at *m/z* 751.5, $[M-H-H_2O-CH_2O]^-$ ions at *m/z* 327.1, and $[M-H-H_2O-CH_2O-CH_3]^-$ ions at *m/z* 312. 3 were detected. The structures of these two isomers were tentatively identified as *erythro* (peak 5) and *threo* (peak 6) forms of the guaiacylglycerol-β-coniferyl alcohol ether (GGC), whereas only their glucoside forms have been previously reported in flax cell extracts (Beejmohun et al., 2007). In ES^+ mode, peak 10 produced the following ions: $[M+H-H_2O]^+$ at *m/z* 341.1, $[M+H-2H_2O]^+$ at *m/z* 323.0, and $[M+H-H_2O-2CH_3]^+$ at *m/z* 311.1. In ES^- mode an $[2M-H]^-$ ion at *m/z* 715.2, $[M+FA-H]^-$ ion at *m/z* 403.1, $[M-H-H_2O]^-$ ion at *m/z* 339.1 and $[M-H-2CH_3]^-$ ion at *m/z* 327.2 were detected. These chemical features were similar to those observed for pinoresinol (peak 11) and might be assigned to its enantiomer epipinoresinol. The compound has been previously reported in *Forsythia intermedia* cell suspension cultures (Schmitt and Petersen, 2002) and now, for the first time, in flax cells. In ES^+ mode, peak 12 produces an $[M+H-H_2O]^+$ ion at *m/z* 339.1, and an $[M+H-2H_2O]^+$ ion at *m/z* 321.0. In ES^- mode, the same peak produces an $[M-H-H_2O]^-$ ion at *m/z* 337.1 and an $[M+FA-H]^-$ ion at *m/z* 400.9. The formation of the two characteristic fragments $[A]^+$ ion at *m/z* 137 and $[B]^+$ ion at *m/z* 161 allowed for unambiguously assigning these compounds as pluviatolide as previously described from aerial parts of *L. usitatissimum* (Schmidt et al., 2008). The presence of pluviatolide in *L. usitatissimum* cell suspension cultures is described for the first time in this study. In ES^+ mode, peak 13 produces an $[M+H-H_2O]^+$ ion at *m/z* 519.2, an $[M+H-H_2O\text{-hexoside}]^+$ ion at *m/z* 357.0 (hexose neutral loss: −162 Da). In ES^- mode, peak 13 produces an $[M-H+FA]^-$ ion at *m/z* 581.1, an $[M-H-H_2O]^-$ ion at *m/z* 517 and an $[M-H-H_2O\text{-hexose}]^-$ ion at *m/z* 355 (hexose neutral loss: −162 Da), with the UV spectrum showing a λmax at

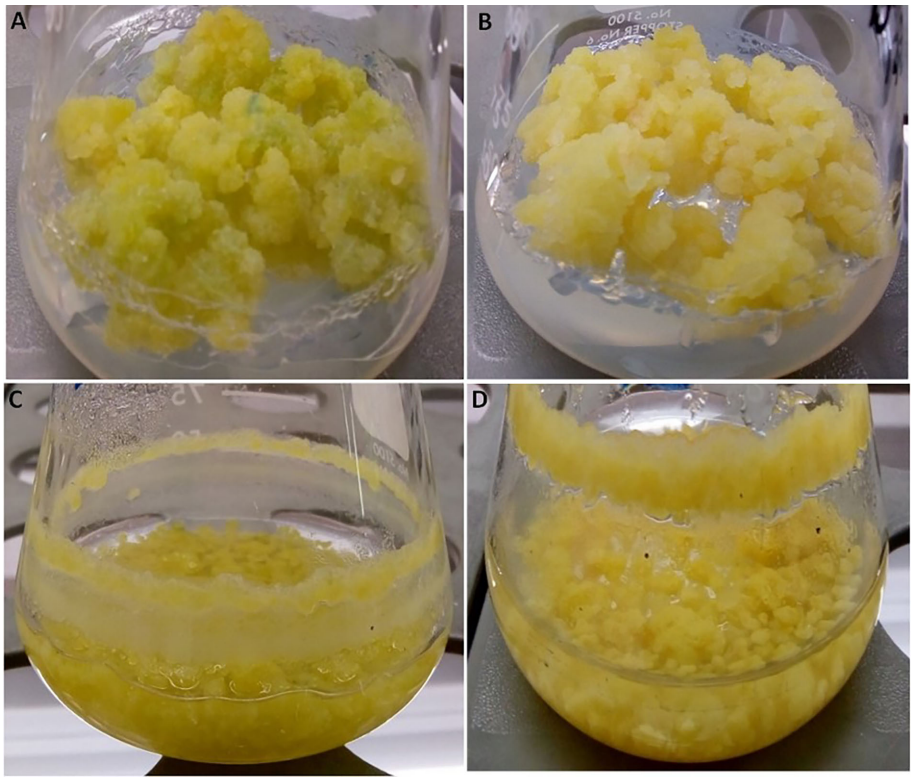

FIGURE 2 | Pictures of representative *L. usitatissimum* cultures. **(A)** Callus culture in the light after 30 days. **(B)** Callus culture in the dark after 30 days. **(C)** Suspension culture in the light after 27 days of culture. Suspension culture in the dark after 24 days of culture **(D)**.

277 and 344 nm. These MS and UV characteristics corresponded to the hexoside form of guaiacylglycerol-β-coniferyl aldehyde ether described by Yao et al. (2018). Consequently, this compound was tentatively assigned as guaiacylglycerol-β-coniferyl aldehyde ether hexoside. To our knowledge, we are the first to report its presence in flax cells. In ES^+ mode peak 14 produces an$[M+Na]^+$ ion at *m/z* 394.9, an $[M+H\text{-}H_2O\text{-}CH_3]^+$ ion at *m/z* 341.0, and in ES^- mode an $[M\text{-}H\text{-}H_2O]^-$ ion at *m/z* 352.9 and an $[M\text{-}H\text{-}2CH_3]^-$ ion at *m/z* 341. These MS spectral features enabled us to provisionally assign this compound as phillygenin, as previously described in sesame seed extracts (Eklund et al., 2008).

Accumulation of Specialized Metabolites

The accumulation of these compounds in the cell cultures was measured over a period of 30 days. We observed the accumulation of 14 different specialized metabolites in *L. usitatissimum* callus and cell suspension cultures, following UPLC-HRMS analysis (**Figures 3**, **S2**).

The analysis of specialized metabolite accumulation in callus grown under light *versus* dark conditions showed a higher accumulation of these metabolites on day 18 of cultivation under light conditions (**Figures 3A**, **S2A**). Similar results were obtained for cell suspension cultures propagated under light conditions, where the production of specialized metabolites was comparatively higher than under dark conditions (**Figures 3B**, **S2B**).

Epipinoresinol and pluviatolide were the major lignans of flax callus and cell suspension cultures. Their biosynthesis appeared to be growth associated with maximum accumulation at the end of the exponential growth phase. No significant difference was observed between the accumulations in callus *vs.* cell suspension. However, a stimulation of the light on their accumulation has been observed. For the accumulation of other lignans, phillygenin was higher in the dark-grown callus, while secoisolariciresinol and lariciresinol contents were higher in the cell suspension under light conditions. Under these conditions, pinoresinol accumulation did not show any marked variation.

DCG (isomer 1) was the main neolignan produced in both culture and cell suspension conditions. The DCG (isomer 1) accumulation was twofold more important in cell suspension (day 6) than in callus (day 3), with an observed stimulating effect of light. In both types of *in vitro* culture, its maximum accumulation was observed both at the beginning and at the end of the culture cycle. With the exception of *erythro*-guaiacylglycerol-β-coniferyl alcohol ether glucoside, *erythro*-guaiacylglycerol-β-coniferyl alcohol ether, and *threo*-guaiacylglycerol-β-coniferyl alcohol ether, all of which peaked at day 18 in flax cell suspension under light conditions, the accumulation of other neolignans under other conditions remained relatively stable throughout the culture cycle.

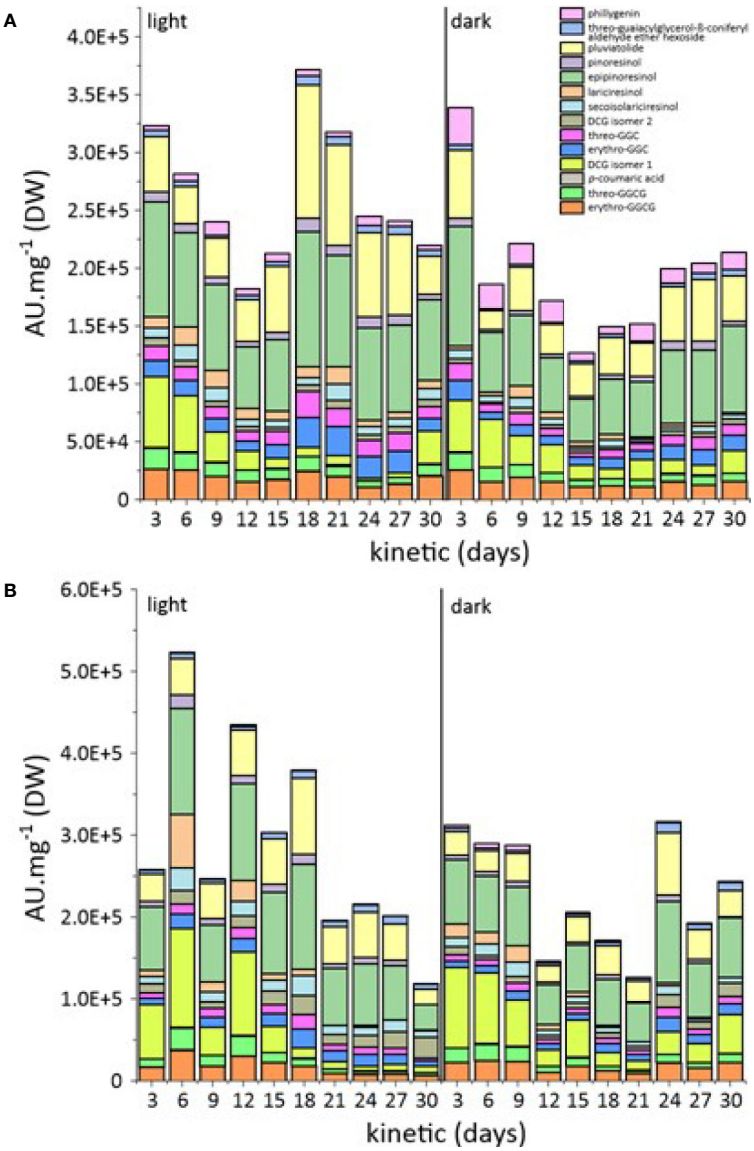

FIGURE 3 | **(A)** Comparison of metabolic variations in *L. usitatissimum* callus cultures in the light and dark. **(B)** Comparison of metabolic variations in *L. usitatissimum* cell suspension cultures in the light and dark. A.U. mg^{-1} refers to the sum of arbitrary unit of each compound per mg of DW.

Antioxidant and Anti-Aging Activities

A complete evaluation of antioxidant and anti-aging activities of all the cell extracts of *L. usitatissimum* was performed. In total, four different types of assays were performed in order to provide a complete view on the antioxidant capacities of the extracts: two assays (DPPH and ABTS) to detect antioxidants acting through a hydrogen-atom transfer (HAT) mechanism, and two other assays (CUPRAC and FRAP) acting through a single electron transfer (ET) mechanism (Prior et al., 1998 and Apak et al., 2007).

It is clear from **Figure 4** and **Table S2** that ABTS and DPPH activities were higher in comparison to the CUPRAC and FRAP activities. Nonetheless, cell suspension extracts grown under light conditions showed the best result, with the highest antioxidant activity observed on day 18 of culture for all *in vitro* assays (with TEAC of 558.5 μM (ABTS), 334.7 μM (DPPH), 142.8 μM (CUPRAC), and 108.5 μM (FRAP)).

Next, we examined the anti-aging capacity of all *L. usitatissimum* cell extracts by performing four different assays. Tyrosinase, elastase, collagenase, and hyaluronidase inhibitors are of great interest to the cosmetics industry. From heat maps (**Figure 5**), it can be interpreted that anti-tyrosinase and anti-elastase activities displayed a comparatively higher propensity in the dark than in the light. But in more details, cell suspension, in particular SL18 extract (*i.e.* cell suspension grown under light conditions on day 18 of culture) presented the maximum inhibitory action for tyrosinase and elastase enzymes with observed inhibitions of 50.6 and 34.9%,

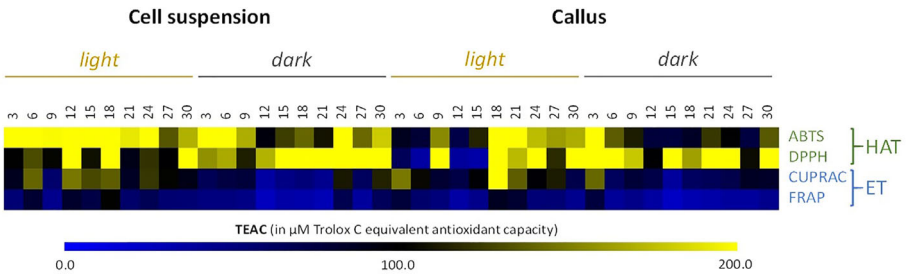

FIGURE 4 | Heat map showing *in vitro* antioxidant activity in all the cell cultures of cell suspensions and callus extracts of *L. usitatissimum* over a time period of 30 days. Antioxidant activities are expressed in µM of Trolox C Equivalent Antioxidant Capacity (TEAC). Values are presented in **Table S2** . DPPH, 1,1-Diphenyl-2-picryl-hydrazyl; ABTS, 2,2-azinobis-(3-ethyl-benzothiazoline-6-sulfonic acid); FRAP, ferric reducing antioxidant power; CUPRAC, cupric reducing antioxidant capacity; HAT, hydrogen atom transfer antioxidant mechanism; ET, electron transfer antioxidant mechanism.

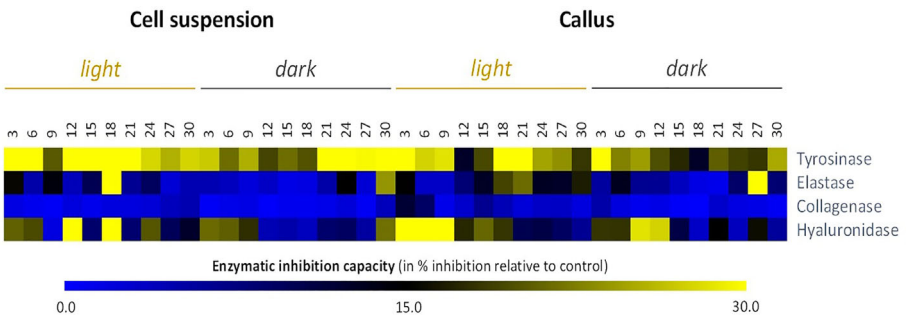

FIGURE 5 | Heat map showing relative *in vitro* anti-aging activity inhibitory activity against skin remodeling enzymes) of cell suspensions and callus extracts of *L. usitatissimum* over a time period of 30 days. *In vitro* anti-aging activities are expressed in inhibition % relative to the control (same volume of extraction solvent). Values are presented in **Table S3**.

respectively (**Figure 5**, **Table S3**). Better results have been achieved with collagenase and hyaluronidase inhibition of callus cultures. Nevertheless, *L. usitatissimum* extracts did not have major inhibitory effects on collagenase enzyme activity, with a maximum inhibition of 11.9% observed for CL3 extract (*i.e.*, callus grown under light conditions on day 3 of culture). On the contrary, the same CL3 extract showed the maximum inhibitory potential for the hyaluronidase enzyme with a 52.8% inhibition observed.

Multivariate Statistical Analyses

Partial Least Square models were performed on the data sets from cell suspensions and callus cultures to extract relevant changes of metabolic composition and biological activities under light or dark treatments, as well as over time. For cell suspension cultures, the PLS score plot of the two first components shown in **Figure 6A** explained 72.3% of the variation and revealed a slight effect of the light/dark treatment along component 1 axis. The loading plot (**Figure 6B**) showed the variables potentially responsible for the discriminations observed in **Figure 6A**.

As an example, the projection on component 1 positive values of the neolignans (*erythro*-guaiacylglycerol-β-coniferyl alcohol ether, *threo*-guaiacylglycerol-β-coniferyl alcohol ether, dehydrodiconiferyl alcohol-4-β-D-glucoside isomer2, guaiacylglycerol-β-coniferyl aldehyde ether hexoside), the lignans (secoisolariciresinol, epipinoresinol, pinoresinol) and the anti-oxidant tests (ABTS, FRAP and CUPRAC) suggested that under light treatment these metabolites are induced resulting in higher antioxidant activities. It is noteworthy that biomass accumulation (DW and FW) was not associated with the variables corresponding to metabolic composition and biological activities. For callus cultures, the PLS score plot of the two first components shown in **Figure 6C** explained 77% of the variation and a slight effect of light/dark treatment was observed similarly to cell suspension cultures. Interestingly, the variables associated with the light treatment were the same in the cell suspension and callus cultures (**Figures 6B, D**) suggesting that in both callus and cell suspension cultures of *L. usitattissimum* light treatment induced the production of several lignans and neolignans.

To evaluate the connection between phytochemicals and biological activities of the extracts, Pearson coefficient correlations (PCCs) were calculated (**Figure 7**; **Table S4**). From this analysis, according to their high and significant PCC values, the lignans epipinoresinol, secoisolariciresinol, and pinoresinol and the neolignans dehydrodiconiferyl alcohol-4-β-D-glucoside (isomer 2) appeared as the main potential contributors toward the ABTS antioxidant assay. In addition to these compounds, the two neolignans *erythro*- and *threo*-

guaiacylglycerol-β-coniferyl alcohol ether and guaiacylglycerol-β-coniferyl aldehyde ether hexoside were highly correlated to the FRAP antioxidant assay. The same compounds were strongly associated with the CUPRAC antioxidant assay, except for DCG (isomer 2) and secoisolariciresinol. No significant correlation was noted for DPPH radical scavenging assay.

The lignan epipinoresinol and the neolignans dehydrodiconiferyl alcohol-4-β-D-glucoside (isomer 2) and guaiacylglycerol-β-coniferyl aldehyde ether hexoside emerged as the main possible contributors to tyrosinase enzyme inhibition. A high and significant correlation pointed to the possible implication of pluviatolide in the inhibition of elastase enzyme. A moderate but highly significant correlation between inhibition of hyaluronidase enzyme and neolignans erythro-guaiacylglycerol-β-coniferyl alcohol ether glucoside and dehydrodiconiferyl alcohol-4-β-D-glucoside (isomer 1) and lignan epipinoresinol was measured.

DISCUSSION

Flax extract is considered to be a potential cosmetic ingredient all over the world, including China (China Food & Drug Administration, 2015). Therefore, our objective was to characterize cell suspension extracts that could be used within this field. An undoubted advantage of using cell cultures as opposed to whole plants is that they can be used efficiently for a continuous production of bioactive metabolites (Eibl et al., 2018; Georgiev et al., 2018). This in turn guarantees more reproducible production of economically important extracts and under controlled sanitary conditions. Most importantly, the production of these extracts can be adjusted to the demand at any time.

Flax cell suspensions have been proposed as a useful system for the production of plant biomass able to produce and accumulate bioactive compounds (Attoumbre et al., 2006b). *L. usitatissimum* callus-derived cell suspension has been previously initiated from various starting materials: root explants (Attoumbre et al., 2006a; Attoumbre et al., 2006b), hypocotyls (Hano et al., 2006; Corbin et al., 2013a), or shoots (Gabr et al., 2016). Efficiency in obtaining higher biomass was assessed starting with different tissues. Unsurprisingly, considering the high organogenesis competency of hypocotyl epidermal and sub-epidermal cells (Lamblin et al., 2007), these tissues gave the best results. In the present study, the most optimal callus induction frequency was established by testing different hormonal combinations of auxins and cytokinins. Murashige and

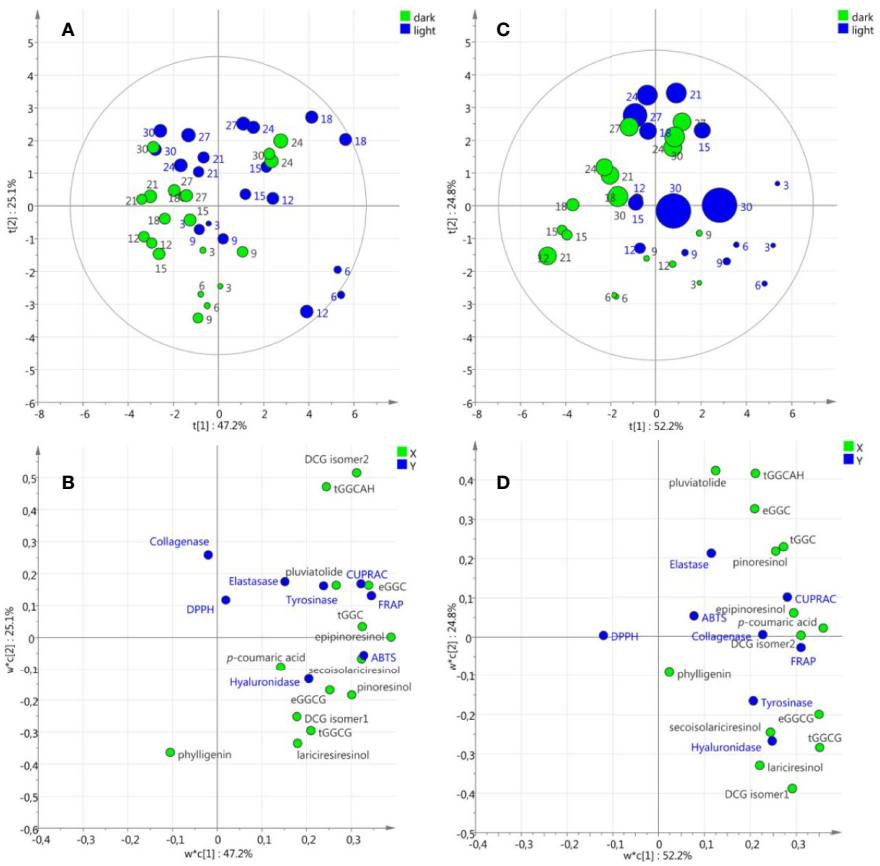

FIGURE 6 | Partial Least Square models of metabolic composition and biological activities of cell suspension **(A, B)** and callus **(C, D)** cultures under light/dark treatment. Score plots **(A, C)** with round size relative to the biomass expressed as dry weight and numbered with the corresponding days of culture. Loading plots **(B, D)** with X variables in green and Y variables in blue.

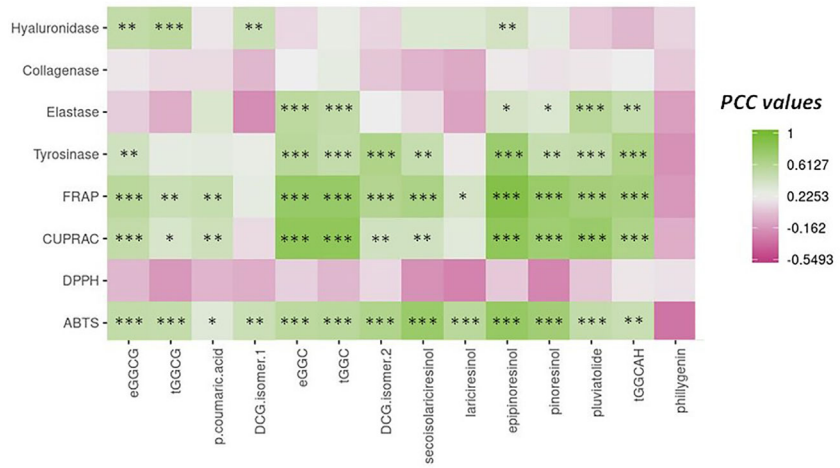

FIGURE 7 | Pearson correlation analysis (PCC) of the relation between the main phytochemicals from flax *in vitro* culture extracts and the different antioxidant (ABTS, DPPH, CUPRAC, and TBARS) and anti-aging (tyrosinase, hyaluronidase, elastase, and collagenase) activities. *** significant $p < 0.001$; ** significant $p < 0.01$; * significant $p < 0.05$; actual PCC values are indicated in **Table S4**.

Skoog media containing cytokinin in combination with auxin (*i.e.*, 2 $mg.L^{-1}$ BAP and 0.5 $mg.L^{-1}$ NAA) resulted in the highest biomass accumulation. Attoumbre et al. (2006b) also reported higher biomass production of *L. usitatissimum* cell suspension in LS medium (Linsmaier and Skoog, 1965) supplemented with NAA at 1 $mg.L^{-1}$, whereas Gabr et al. (2016) reported higher biomass production with B5 medium (Gamborg et al., 1968) supplemented with 2,4D at 1.0 $mg.L^{-1}$ and GA_3 at 0.5 $mg.L^{-1}$. Here, the optimal hormonal concentrations are in good agreement with our previous results (Hano et al., 2006; Beejmohun et al., 2007; Hano et al., 2008; Corbin et al., 2013a; Corbin et al., 2013b; Markulin et al., 2019). The presence of two lignans (secoisolariciresinol diglucoside [SDG] and lariciresinol diglucoside [LDG]) and two neolignans (dehydrodiconiferyl alcohol glucoside [DCG] and guaiacylglycerol-β-coniferyl alcohol ether glucoside [GGCG]) in *in vitro* cultured cells has already been reported in *L. usitatissimum* (Attoumbre et al., 2006a; Attoumbre et al., 2006b; Hano et al., 2006; Hano et al., 2008; Corbin et al., 2013a; Corbin et al., 2013b; Gabr et al., 2016; Anjum et al., 2017a; Anjum et al., 2017b; Zahir et al., 2018; Nadeem et al., 2018; Nadeem et al., 2019; Ahmad et al., 2019; Markulin et al., 2019). In this study, using a high resolving chromatographic method (UPLC), we show for the first time that our newly established flax callus and their corresponding derived cell suspension lines are able to accumulate at least 14 lignans, neolignans, and derivatives. These compounds include the four compounds already described and 10 metabolites never found before in flax cell suspension systems. This shows the versatility of these cell systems and the usefulness of developing new *L usitatissimum* cell lines to enhance specific metabolic development according to targeted applications. Callus and cell suspension of flax of our study presented a similar qualitative metabolic profile. However, stress from the status modification (from callus to the suspension), physiological and/or chronological conditions (*e.g.*, growth) or light conditions may alter the accumulation of each component in the extracts. Light has already been mentioned as a stress inducer in several plant species, which triggers specialized metabolite biosynthesis (Shohael et al., 2006; Younas et al., 2018; Zahir et al., 2018; Shah et al., 2019). In our study, all the 14 annotated metabolites were followed in callus and cell suspensions at light or dark for 30 days in order to estimate the effect of the culture parameters on their accumulation. The sum of lignans and neolignans in both callus and cell suspensions is nearly the same, except for two lignans (epipinoresinol and pluviatolide) and one neolignan (DCG isomer 1). A beneficial influence of light on this accumulation was presumably observed considering their relative higher accumulation. The initial high level of DCG isomer 1 could be due to the osmotic stress during the subculture as it has already been observed with other phenylpropanoids and lignans (Seidel et al., 2002). Interestingly, phillygenin is the only lignan produced in the same amount in callus, whatever the light condition, while the accumulation of phillygenin in the cell suspension was stimulated in the dark.

In a final step, we were interested in the biological activities of interest for cosmetic application by using antioxidant and enzymatic anti-aging tests. We observed that light condition produced cell extracts with higher antioxidant activity, whereas dark condition was linked with a higher anti-aging activity. Therefore, light not only activates biosynthesis of lignans and neolignans in *L. usitatissimum* cells, but also plays a significant role in the biological properties of extracts which have been suggested by Arias et al. (2016) for cell suspension of *Thevenia peruviana*. The correlation analysis of phytochemicals and biological activities contributed to the identification of metabolites correlated with antioxidant or anti-aging activity. Some metabolites are commons for both activity such as epipinoresinol, DCG (isomer 2) and guaiacylglycerol-β-coniferyl aldehyde ether hexoside, while others are more directly related to antioxidant activity, such as secoisolariresinol, as it was previously showed for some of its derivatives (Prassad, 1999; Kitts et al., 1999; Hano et al., 2017;

Socrier et al., 2019) or anti-aging, such as pluviatolide. Surprisingly, phillygenin was not associated with anti-aging activity, probably due to its narrow accumulation profile, because it was primarily present in dark cultured cells. It is also difficult to conclude that the activity of the extract is attributable to a specific metabolite, although some accumulation patterns of similar metabolites tend to be closely related to certain biological activities. To explore further the properties of each molecule, analysis with purified molecules will be necessary. In fact, the variability in the relative abundance of the extract may also be the key to the possible biological activities of the extract. It is commonly agreed that the biological activities of plant extracts may result in the synergistic action of several metabolites, which can be almost inactive on their own in their purified form. Therefore, the study of a specific combination of such molecules may be interesting. Finally, it is also important to bear in mind that our analysis was centered on lignans and neolignans, but extracts contained several other unidentified compounds that may be part of their biological activity. Nevertheless, our findings reinforced and further strengthened the interest in the cosmetic applications of flax lignans and neolignans produced in plant cell culture grown in *in vitro* systems under distinct light conditions.

DATA AVAILABILITY STATEMENT

All datasets generated for this study are included in the article/ **Supplementary Material**.

AUTHOR CONTRIBUTIONS

SB did the research work, data analyses and manuscript write-up. TM, NG-G'H, BA, LG, DT, and BS-P contributed to the experimental design and the analysis of the *in vitro* culture experiments. AL, KB, TM, SM, ED, and MC helped with phytochemical and multivariate statistical analyses. BA and CH have supervised the biological assays. CH, BA, and NG-G'H have contributed to the conception of the project, analyses of results and critically reviewed the manuscript.

FUNDING

This research was supported by Cosmetosciences, a global training and research program dedicated to the cosmetic industry. Located in the heart of the Cosmetic Valley, this program led by University of Orleans is funded by the Region Centre-Val de Loire (VALBIOCOSM 17019UNI).

ACKNOWLEDGMENTS

SB, TM, LG and SM acknowledge Cosmetosciences for their fellowship. BHA acknowledges the research fellowship of Le Studium-Institute for Advanced Studies, Loire Valley, Orleans, France.

The authors would like to acknowledge networking support by the CNRS GDR3711 COSM'ACTIFS.

SUPPLEMENTARY MATERIAL

The Supplementary Material for this article can be found online at: https://www.frontiersin.org/articles/10.3389/fpls.2020.508658/full#supplementary-material

SUPPLEMENTARY FIGURE 1 | (A) UPLC-MS chromatogram of 30 days *L. usitatissimum* cell suspension extract using photo-diode array detection. (1) *erythro*-guaiacylglycerol-*β*-coniferyl alcohol ether glucoside, (2) *threo*-guaiacylglycerol-*β*-coniferyl alcohol ether glucoside, (3) *p*-coumaric acid, (4) dehydrodiconiferyl alcohol-4-*β*-D-glucoside isomer 1, (5) *erythro*-guaiacylglycerol-β-coniferyl alcohol ether, (6) *threo*-guaiacylglycerol-*β*-coniferyl alcohol ether, (7) dehydrodiconiferyl alcohol-4-*β*-D-glucoside isomer 2, (8) secoisolariciresinol, (9) lariciresinol, (10) epipinoresinol, (11) pinoresinol, (12) pluviatolide, (13) guaiacylglycerol-*β*-coniferyl aldehyde ether hexoside, (14) phillygenin. Chemical structures of main specialized metabolites accumulated in the callus and suspension cell cultures of *L. usitatissimum*. **(B)** Chemical structures of some of the main specialized metabolites accumulated in the callus and suspension cell cultures of *L. usitatissimum*.

SUPPLEMENTARY FIGURE 2 | Heat map showing relative cell suspensions and callus extracts of *L. usitatissimum* cultivated in the light and dark for 30 days.

REFERENCES

Ahmad, W., Zahir, A., Nadeem, M., Garros, L., Drouet, S., Renouard, S., et al. (2019). Enhanced production of lignans and neolignans in chitosan-treated flax (*Linum usitatissimum* L.) cell cultures. *Process Biochem.* 79, 155–165. doi: 10.1016/j.procbio.2018.12.025

Anjum, S., Abbasi, B. H., and Hano, C. (2017a). Trends in accumulation of pharmacologically important antioxidant-secondary metabolites in callus cultures of *Linum usitatissimum* L. *Plant Cell Tissue Organ Cult.* 129, 73–87. doi: 10.1007/s11240-016-1158-3

Anjum, S., Abbasi, B. H., Doussot, J., Favre-Réguillon, A., and Hano, C. (2017b). Effects of photoperiod regimes and ultraviolet-C radiations on biosynthesis of industrially important lignans and neolignans in cell cultures of *Linum usitatissimum* L. (Flax). *J. Photochem. Photobiol. B. Biol.* 167, 216–227. doi: 10.1016/j.jphotobiol.2017.01.006

Apak, R., Güçlü, K., Özyürek, M., and Karademir, S. E. (2004). Novel total antioxidant capacity index for dietary polyphenols and vitamins C and E, using their cupric ion reducing capability in the presence of neocuproine: CUPRAC method. *J. Agric. Food Chem.* 52, 7970–7981. doi: 10.1021/jf048741x

Apak, R., Güçlü, K., Demirata, B., Özyürek, M., Celik, S., Bektaşoğlu, B., et al. (2007). Comparative evaluation of various total antioxidant capacity assays applied to phenolic compounds with the CUPRAC assay. *Molecules* 12, 1496–1547. doi: 10.3390/12071496

Arias, J. P., Zapata, K., Rojano, B., and Arias, M. (2016). Effect of light wavelength on cell growth, content of phenolic compounds and antioxidant activity in cell suspension cultures of Thevetia peruviana. *J. Photochem. Photobiol. B. Biol.* 163, 87–91. doi: 10.1016/j.jphotobiol.2016.08.014

Attoumbre, J., Hano, C., Mesnard, F., Lamblin, F., Bensaddek, L., Raynaud-Le Grandic, S., et al. (2006a). Identification by NMR and accumulation of a neolignan, the dehydrodiconiferyl alcohol-4-b-D-glucoside, in *Linum usitatissimum* cell cultures. *C. R. Chim.* 9, 420–425. doi: 10.1016/j.crci.2005.06.012

Attoumbre, J., Charlet, S., Baltora-Rosset, S., Hano, C., Raynaud-Le Grandic, S., Gillet, F., et al. (2006b). High accumulation of dehydrodiconiferyl alcohol-4-β-d-glucoside in free and immobilized *Linum usitatissimum* cell cultures. *Plant Cell Rep.* 25, 859–864. doi: 10.1007/s00299-006-0137-2

Babicki, S., Arndt, D., Marcu, A., Liang, Y., Grant, J. R., Maciejewski, A., et al. (2016). Heatmapper: Web-enabled heat mapping for all. *Nucleic Acids Res.* 44, W147–W153. doi: 10.1093/nar/gkw419

Bakht, J., Ali, H., Khan, M. A., Khan, A., Saeed, M., Shafi, M., et al. (2011). Antimicrobial activities of different solvents extracted samples of *Linum usitatissimum* by disc diffusion method. *Afr. J. Biotechnol.* 10, 19825–19835. doi: 10.5897/AJB11.229

Barbulova, A., Apone, F., and Colucci, G. (2014). Plant cell cultures as source of cosmetic active ingredients. *Cosmetics* 1, 94–104. doi: 10.3390/cosmetics1020094

Beejmohun, V., Fliniaux, O., Hano, C., Pilard, S., Grand, E., Lesur, D., et al. (2007). Coniferin dimerisation in lignan biosynthesis in flax cells. *Phytochemistry* 68, 2744–2752. doi: 10.1016/j.phytochem.2007.09.016

Benzie, I. F., and Strain, J. J. (1996). The ferric reducing ability of plasma (FRAP) as a measure of "antioxidant power": the FRAP assay. *Anal. Biochem.* 239, 70–76. doi: 10.1006/abio.1996.0292

Billet, K., Houillé, B., de Bernonville, T. D., Besseau, S., Oudin, A., Courdavault, V., et al. (2018). Field-based metabolomics of *Vitis vinifera* l. Stems provides new insights for genotype discrimination and polyphenol metabolism structuring. *Front. Plant Sci.* 9:798:798. doi: 10.3389/fpls.2018.00798

Chai, W. M., Huang, Q., Lin, M. Z., Ou-Yang, C., Huang, W. Y., Wang, Y. X., et al. (2018). Condensed tannins from longan bark as inhibitor of tyrosinase: structure, activity, and mechanism. *J. Agric. Food Chem.* 66, 908–917. doi: 10.1021/acs.jafc.7b05481

China Food & Drug Administration (2015). *China IECIC - Inventory of Existing Cosmetic Ingredients in China*. Available at: https://www.chemsafetypro.com/Topics/Cosmetics/China_IECIC_Finder.html.

Corbin, C., Decourtil, C., Marosevic, D., Bailly, M., Lopez, T., Renouard, S., et al. (2013a). Role of protein farnesylation events in the ABA-mediated regulation of the pinoresinol–lariciresinol Reductase 1 (*LuPLR1*) gene expression and lignan biosynthesis in flax (*Linum usitatissimum* L.). *Plant Physiol. Biochem.* 72, 96–111. doi: 10.1016/j.plaphy.2013.06.001

Corbin, C., Renouard, S., Lopez, T., Lamblin, F., Lainé, E., and Hano, C. (2013b). Identification and characterization of *cis*-acting elements involved in the regulation of ABA- and/or GA-mediated *LuPLR1* gene expression and lignan biosynthesis in flax (*Linum usitatissimum* L.) cell cultures. *J. Plant Physiol.* 170, 516–522. doi: 10.1016/j.jplph.2012.11.003

Cunha, A., and Ferreira, M. F. (1999). Influence of medium parameters on somatic embryogenesis from hypocotyl explants of flax (*Linum usitatissimum* L.): effect of carbon source, total inorganic nitrogen and balance between ionic forms and interaction between calcium and zeatin. *J. Plant Physiol.* 155, 591–597. doi: 10.1016/S0176-1617(99)80059-5

Dedičová, B., Hricova, A., Šamaj, J., Obert, B., Bobák, M., and Pret'ová, A. (2000). Shoots and embryo-like structures regenerated from cultured flax (*Linum usitatissimum* L.) hypocotyl segments. *J. Plant Physiol.* 157, 327–334. doi: 10.1016/S0176-1617(00)80055-3

Eibl, R., Meier, P., Stutz, I., Schildberger, D., Hühn, T., and Eibl, D. (2018). Plant cell culture technology in the cosmetics and food industries: current state and future trends. *Appl. Microbiol. Biotechnol.* 102 (20), 8661–8675. doi: 10.1007/s00253-018-9279-8

Eklund, P. C., Backman, M. J., Kronberg, L.Å., Smeds, A. I., and Sjöholm, R. E. (2008). Identification of lignans by Liquid Chromatography-electrospray ionization Ion-Trap Mass Spectrometry. *J. Mass Spectrom.* 43, 97–107. doi: 10.1002/jms.1276

Fongnzossie, E. F., Tize, Z., Nde, P. F., Biyegue, C. N., Ntsama, I. B., Dibong, S. D., et al. (2017). Ethnobotany and pharmacognostic perspective of plant species used as traditional cosmetics and cosmeceuticals among the Gbaya ethnic group in Eastern Cameroon. *South Afr. J. Bot.* 112, 29–39. doi: 10.1016/j.sajb.2017.05.013

Gabr, A. M., Mabrok, H. B., Ghanem, K. Z., Blaut, M., and Smetanska, I. (2016). Lignan accumulation in callus and agrobacterium rhizogenes-mediated hairy root cultures of flax (*Linum usitatissimum*). *Plant Cell Tissue Organ Cult.* 126, 255–267. doi: 10.1007/s11240-016-0995-4

Gamborg, O. L., Miller, R. A., and Ojima, K. (1968). Nutrient requirements of suspension cultures of soybean root cells. *Exp. Cell Res.* 50, 151–158. doi: 10.1016/0014-4827(68)90403-5

Georgiev, V., Slavov, A., Vasileva, I., and Pavlov, A. (2018). Plant cell culture as emerging technology for production of active cosmetic ingredients. *Eng. Life Sci.* 18 (11), 779–798. doi: 10.1002/elsc.201800066

Hano, C., Addi, M., Bensaddek, L., Crônier, D., Baltora-Rosset, S., Doussot, J., et al. (2006). Differential accumulation of monolignol-derived compounds in elicited flax (*Linum usitatissimum*) cell suspension cultures. *Planta* 223, 975–989. doi: 10.1007/s00425-005-0156-1

Hano, C., Addi, M., Fliniaux, O., Bensaddek, L., Duverger, E., Mesnard, F., et al. (2008). Molecular characterization of cell death induced by a compatible interaction between *Fusarium oxysporum* f. sp. linii and flax (*Linum usitatissimum*) cells. *Plant Physiol. Biochem.* 46, 590–600. doi: 10.1016/j.plaphy.2008.02.004

Hano, C., Corbin, C., Drouet, D., Quéro, A., Rombaut, N., Savoire, R., et al. (2017). The lignan +–secoisolariciresinol extracted from flax hulls is an effective protectant of linseed oil and its emulsion against oxidative damage. *Eur. J. Lipid Sci. Technol.* 119, 1600219. doi: 10.1002/ejlt.201600219

Hazra, J., and Panda, A. K. (2013). Concept of beauty and ayurveda medicine. *J. Clin. Exp. Dermatol. Res.* 4:2. doi: 10.4172/2155-9554.1000178

Kitts, D. D., Yuan, Y. V., Wijewickreme, N., and Thompson, L. U. (1999). Antioxidant activity of the flaxseed lignan secoisolariciresinol diglycoside and its mammalian lignan metabolites enterodiol and enterolactone. *Mol. Cell Biochem.* 202, 91–100. doi: 10.1023/A:1007022329660

Kolakul, P., and Sripanidkulchai, B. (2017). Phytochemicals and anti-aging potentials of the extracts from *Lagerstroemia speciosa* and *Lagerstroemia floribunda*. *Ind. Crops Prod.* 109, 707–716. doi: 10.1016/j.indcrop.2017.09.026

Lainé, E., Hano, C., and Lamblin, F. (2009). "Phytoestrogens: Lignans," in *Chemoprevention of Cancer and DNA Damage by Dietary Factors*. Eds. S. Knasmüller, D. M. DeMarini, I. Johnson and C. Gerhäuser (Weinheim: WILEY-VCH), 555–577. doi: 10.1002/9783527626588.ch31

Lamblin, F., Aimé, A., Hano, C., Roussy, I., Domon, J. M., Van Droogenbroeck, B., et al. (2007). The use of the phosphomannose isomerase gene as alternative selectable marker for Agrobacterium-mediated transformation of flax (*Linum usitatissimum*). *Plant Cell Rep.* 26, 765–772. doi: 10.1007/s00299-006-0280-9

Lee, S. K., Mbwambo, Z. H., Chung, H., Luyengi, L., Gamez, E. J., Mehta, R. G., et al. (1998). Evaluation of the antioxidant potential of natural products. *Comb. Chem. High Throughput Screen.* 1, 35–46.

Linsmaier, E. M., and Skoog, F. (1965). Organic Growth Factor Requirements of Tobacco Tissue Cultures. *Physiol. Plant* 18, 100–127. doi: 10.1111/j.1399-3054.1965.tb06874.x

Markulin, L., Drouet, S., Corbin, C., Decourtil, C., Garros, L., Renouard, S., et al. (2019). The control exerted by ABA on lignan biosynthesis in flax (*Linum usitatissimum* L.) is modulated by a Ca2+ signal transduction involving the calmodulin-like LuCML15b. *J. Plant Physiol.* 236, 74–87. doi: 10.1016/j.jplph.2019.03.005

Murashige, T., and Skoog, F. (1962). A revised medium for rapid growth and bioassay with tobacco tissue culture. *Physiol. Plant* 15, 473–497. doi: 10.1111/j.1399-3054.1962.tb08052.x

Nadeem, M., Abbasi, B. H., Garros, L., Drouet, S., Zahir, A., Ahmad, W., et al. (2018). Yeast-extract improved biosynthesis of lignans and neolignans in cell suspension cultures of *Linum usitatissimum* L. *Plant Cell Tissue Organ Cult.* 135, 347–355. doi: 10.1007/s11240-018-1468-8

Nadeem, M., Ahmad, W., Zahir, A., Hano, C., and Abbasi, B. H. (2019). Salicylic acid-enhanced biosynthesis of pharmacologically important lignans and neo lignans in cell suspension culture of *Linum ussitatsimum* L. *Eng. Life Sci.* 19, 168–174. doi: 10.1002/elsc.201800095

Nichterlein, K., Umbach, H., and Friedt, W. (1991). Genotypic and exogenous factors affecting shoot regeneration from anther callus of linseed (*Linum usitatissimum* L.). *Euphytica* 58, 157–164. doi: 10.1007/BF00022816

Oomah, B. D. (2001). Flaxseed as a functional food source. *J. Sci. Food Agric.* 81, 889–894. doi: 10.1002/jsfa.898

Ota, M., and Yokoyama, M. (2010). "Chemistry of cosmetics," in *Comprehensive natural products II: Chemistry and Biology*, vol. 3 . Eds. L. Mander and H. W. Liu (Amsterdam, Netherlands: Elsevier), 317–349. doi: 10.1016/B978-008045382-8.00728-0

Palla, A. H., Khan, N. A., Bashir, S., Iqbal, J., and Gilani, A. H. (2015). Pharmacological basis for the medicinal use of *Linum usitatissimum* (Flaxseed) in infectious and non-infectious diarrhea. *J. Ethnopharmacol.* 160, 61–68. doi: 10.1016/j.jep.2014.11.030

Park, I. S., and Kim, D. II (1993). Significance of fresh weight to dry cell weight ratio in plant cell suspension cultures. *Biotechnol. Tech.* 7, 627–630. doi: 10.1007/BF00151859

Prassad, K. (1999). Antioxidant activity of secoisolariciresinol diglucoside-derived metabolites, secoisolariciresinol, Enterodiol, and enterolactone. *Int. J. Angiol.* 9, 220–225. doi: 10.1007/BF01623898

Prior, R. L., Cao, G., Martin, A., Sofic, E., McEwen, J., O'Brien, C., et al. (1998). Antioxidant capacity as influenced by total phenolic and anthocyanin content, maturity, and variety of *Vaccinium* species. *J. Agric. Food Chem.* 46, 2686–2693. doi: 10.1021/jf980145d

Rutkowska-Krause, I., Mankowska, G., Lukaszewicz, M., and Szopa, J. (2003). Regeneration of flax (*Linum usitatissimum* L.) plants from anther culture and somatic tissue with increased resistance to. *Fusarium oxysporum. Plant Cell Rep.* 22, 110–116. doi: 10.1007/s00299-003-0662-1

Saeed, A., Sharov, V., White, J., Li, J., Liang, W., and Bhagabati, N. (2003). TM4: a free, open-source system for microarray data management and analysis *Biotechniques* 34(2), 374–378. doi: 10.2144/03342mt01

Salaj, J., Petrovská, B., Obert, B., and Pret'ová, A. (2005). Histological study of embryo-like structures initiated from hypocotyl segments of flax (*Linum usitatissimum* L.). *Plant Cell Rep*. 24, 590–595. doi: 10.1007/s00299-005-0029-x

Schmidt, T. J., Alfermann, A. W., and Fuss, E. (2008). High-performance liquid chromatography/mass spectrometric identification of dibenzylbutyrolactone-type lignans: insights into electrospray ionization tandem mass spectrometric fragmentation of lign-7-eno-9,9′-lactones and application to the lignans of *Linum usitatissimum* L. (Common Flax). *Rapid Commun. Mass Spectrom.* 22, 3642–3650. doi: 10.1002/rcm.3783

Schmitt, J., and Petersen, M. (2002). Pinoresinol and matairesinol accumulation in a Forsythia× intermedia cell suspension culture. *Plant Cell Tissue Organ Cult.* 68, 91–98. doi: 10.1023/A:1012909131741

Seidel, V., Windhövel, J., Eaton, G., Alfermann, W. A., Arroo, R. R., Medarde, M., et al. (2002). Biosynthesis of podophyllotoxin in Linum album cell cultures. *Planta* 215 (6), 1031–1039. doi: 10.1007/s00425-002-0834-1

Shah, M., Ullah, M. A., Drouet, S., Younas, M., Tungmunnithum, D., Giglioli-Guivarc'h, N., et al. (2019). Interactive Effects of Light and Melatonin on Biosynthesis of Silymarin and Anti-Inflammatory Potential in Callus Cultures of *Silybum marianum* (L.) Gaertn. *Molecules* 24:1207. doi: 10.3390/molecules24071207

Shim, Y. Y., Gui, B., Arnison, P. G., Wang, Y., and Reaney, M. J. (2014). Flaxseed (*Linum usitatissimum* L.) bioactive compounds and peptide nomenclature: a review. *Trends Food Sci. Technol.* 38, 5–20. doi: 10.1016/j.tifs.2014.03.011

Shohael, A. M., Ali, M. B., Yu, K. W., Hahn, E. J., Islam, R., and Paek, K. Y. (2006). Effect of light on oxidative stress, secondary metabolites and induction of antioxidant enzymes in *Eleutherococcus senticosus* somatic embryos in bioreactor. *Process Biochem.* 41, 1179–1185. doi: 10.1016/j.procbio.2005.12.015

Socrier, L., Quéro, L., Verdu, M., Song, Y., Molinié, R., Mathiron, D., et al. (2019). Flax phenolic compounds as inhibitors of lipid oxidation: Elucidation of their mechanisms of action. *Food Chem.* 274, 651–658. doi: 10.1016/j.foodchem.2018.08.126

Tagliazucchi, D., Verzelloni, E., Bertolini, D., and Conte, A. (2010). In vitro bio-accessibility and antioxidant activity of grape polyphenols. *Food Chem.* 120, 599–606. doi: 10.1016/j.foodchem.2009.10.030

Wittenauer, J., Mäckle, S., Sußmann, D., Schweiggert-Weisz, U., and Carle, R. (2015). Inhibitory effects of polyphenols from grape pomace extract on collagenase and elastase activity. *Fitoterapia* 101, 179–187. doi: 10.1016/j.fitote.2015.01.005

Yao, G. D., Wang, J., Song, X. Y., Zhou, L., Lou, L. L., Zhao, W. Y., et al. (2018). Stereoisomeric guaiacylglycerol-β-coniferyl aldehyde ether induces distinctive apoptosis by downregulation of MEK/ERK pathway in hepatocellular carcinoma cells. *Bioorg. Chem.* 81, 382–388. doi: 10.1016/j.bioorg.2018.08.033

Younas, M., Drouet, S., Nadeem, M., Giglioli-Guivarc'h, N., Hano, C., and Abbasi, B. H. (2018). Differential accumulation of silymarin induced by exposure of *Silybum marianum* L. callus cultures to several spectres of monochromatic lights. *J. Photochem. Photobiol. B. Biol.* 184, 61–70. doi: 10.1016/j.jphotobiol.2018.05.018

Zahir, A., Ahmad, W., Nadeem, M., Giglioli-Guivarc'h, N., Hano, C., and Abbasi, B. H. (2018). *In vitro* cultures of *Linum usitatissimum* L.: Synergistic effects of mineral nutrients and photoperiod regimes on growth and biosynthesis of lignans and neolignans. *J. Photochem. Photobiol. B. Biol.* 187, 141–150. doi: 10.1016/j.jphotobiol.2018.08.009

Zanwar, A., Hegde, M., and Bodhankar, S. (2011). Cardioprotective activity of flax lignan concentrate extracted from seeds of *Linum usitatissimum* in isoprenalin induced myocardial necrosis in rats. *Interdiscip. Toxicol.* 4, 90–97. doi: 10.2478/v10102-011-0016-8

Zohary, D., Hopf, M., and Weiss, E. (2012). *Domestication of Plants in the Old World. 4th ed* (New York, United States: Oxford University Press), 101–103.

Conflict of Interest: The authors declare that the research was conducted in the absence of any commercial or financial relationships that could be construed as a potential conflict of interest.

Advantages of publishing in Frontiers

OPEN ACCESS
Articles are free to read for greatest visibility and readership

FAST PUBLICATION
Around 90 days from submission to decision

HIGH QUALITY PEER-REVIEW
Rigorous, collaborative, and constructive peer-review

TRANSPARENT PEER-REVIEW
Editors and reviewers acknowledged by name on published articles

Frontiers
Avenue du Tribunal-Fédéral 34
1005 Lausanne | Switzerland

Visit us: www.frontiersin.org
Contact us: frontiersin.org/about/contact

REPRODUCIBILITY OF RESEARCH
Support open data and methods to enhance research reproducibility

DIGITAL PUBLISHING
Articles designed for optimal readership across devices

FOLLOW US
@frontiersin

IMPACT METRICS
Advanced article metrics track visibility across digital media

EXTENSIVE PROMOTION
Marketing and promotion of impactful research

LOOP RESEARCH NETWORK
Our network increases your article's readership